Universidad de Huelva

**Departamento de Ingeniería Química,
Química Física y Química Orgánica**

Comportamiento electroquímico de nitrocompuestos: síntesis y reducción electroquímica de 4-nitroimidazoles sustituidos y su comparación con 2- y 5-nitroimidazoles

**Memoria para optar al grado de doctor
presentada por:**

Juan Arturo Squella Serrano

Fecha de lectura: 5 de septiembre de 2008

Bajo la dirección de los doctores:

José de la Coronada Carbajo Timoteo
José Joaquín Maraver Puig

Huelva, 2010

ISBN: 978-84-92944-86-6
D.L.: H 66-2010

COMPORTAMIENTO ELECTROQUÍMICO DE NITROCOMPUESTOS: SÍNTESIS Y REDUCCIÓN ELECTROQUÍMICA DE 4-NITROIMIDAZOLES SUSTITUIDOS Y SU COMPARACIÓN CON 2- Y 5- NITROIMIDAZOLES.

Juan Arturo Squella Serrano

ÁREA DE CONOCIMIENTO : **QUÍMICA FÍSICA**

GRUPO DE INVESTIGACIÓN : **ELECTROQUÍMICA APLICADA**

COMPORTAMIENTO ELECTROQUÍMICO DE NITROCOMPUESTOS: SÍNTESIS Y REDUCCIÓN ELECTROQUÍMICA DE 4-NITROIMIDAZOLES SUSTITUIDOS Y SU COMPARACIÓN CON 2- Y 5- NITROIMIDAZOLES.

Tesis Doctoral presentada por

Juan Arturo Squella Serrano

Huelva septiembre de 2008

Trabajo para optar al Grado de
Doctor en Química
(Quimica Fisica)

Programa de Doctorado :

Técnicas Instrumentales en Química

Departamento Responsable :

Química y Ciencia de los materiales. "Profesor José Carlos Vilchez Martín"

Fdo : Juan Arturo Squella Serrano

Director

Fdo. : José de la Coronada Carbajo Timoteo
Catedrático de Escuela Universitaria
del Área de Química Física de la Universidad
de Huelva

Director

Fdo. : José Joaquín Maraver Puig
Catedrático de Escuela Universitaria
del Área de Química Física de la Universidad
de Huelva

JOSÉ DE LA CORONADA CARBAJO TIMOTEO, y JOSÉ JOAQUÍN MARAVER PUIG Catedráticos de Escuela Universitaria del Área de Conocimiento de Química Física en el Departamento de Ingeniería Química, Química Física y Química Orgánica de la Universidad de Huelva

INFORMAN:

Que el trabajo presentado por D. Juan Arturo Squella Serrano, titulado "**COMPORTAMIENTO ELECTROQUÍMICO DE NITROCOMPUESTOS: SÍNTESIS Y REDUCCIÓN ELECTROQUÍMICA DE 4-NITROIMIDAZOLES SUSTITUIDOS Y SU COMPARACIÓN CON 2- Y 5-NITROIMIDAZOLES.**", ha sido realizado en los laboratorios de Electroquímica Aplicada de la Universidad de Huelva y Bioelectroquímica de la Facultad de Química de la Universidad de Chile bajo nuestra dirección, reuniendo las condiciones exigidas para ser presentado como Tesis Doctoral según la legislación vigente.

Y para que conste y surta los efectos oportunos firmamos el presente informe en Huelva a 20 de junio de 2008.

Fdo. J. C. Carbajo Timoteo Fdo. J. J. Maraver Puig

Mi agradecimiento especial a todos los miembros del grupo de Investigación Electroquímica Aplicada de la Universidad de Huelva por su colaboración y orientación que han permitido que el presente trabajo haya podido realizarse en un ambiente muy estimulante de trabajo.

Juan Arturo Squella Serrano

Parte de los resultados mostrados en esta tesis han sido comunicados en las siguientes publicaciones:

Cyclic voltammetric study of the disproportionation reaction of the nitro radical anion from 4-nitroimidazole in protic media.
J.Carbajo, S.Bollo, L.J. Núñez.Vergara, A. Campero y J.A.Squella.
J. Electroanal.Chem. 531(2) (2002) 187-194

Voltammetric behaviour of a new 4-nitroimidazole derivative: Nitro radical anion formation and stability.
C.Yañez, J.Pezoa, M. Rodriguez, L.J.Núñez-Vergara, y J.A.Squella.
J.Electrochem.Soc. 152 (6) (2005) J46-J51

Nitro radical anion formation from some iodo substituted nitroimidazoles.
S. Bollo, L.J. Núñez.Vergara,C. Barrientos, y J.A.Squella.
Electroanalysis 17 (18) (2005) 1665-1673

Electrochemical reduction of 2-nitroimidazole in aprotic médium: Influence of its dissociation equilibrium on the reduction mechanism.
J.A. Squella, A. Campero, J. Maraver, y J. Carbajo.
Electrochimica Acta 52 (2) (2006) 511-518

Electrochemical reduction of 2-nitroimidazole in aqueous mixed medium.
J.A. Squella, L.J.Núñez-Vergara, A. Campero, J. Maraver, P. Jara-Ulloa y J. Carbajo.
J. Electrochem.Soc. 154(4)(2007) F77-F81

Micellar effects on the reduction of 4-nitroimidazole derivative: detection and quantification of the nitro radical anion.
P.Jara-Ulloa, L.J.Núñez-Vergara, y J.A.Squella.
Electroanalysis 19 (14) (2007) 1490-1495

ÍNDICE

1. Introducción 1

2. Experimental 7
   2.1. Equipo instrumental 7
   2.2. Reactivos 8
      2.2.1. Nitroimidazoles 8
      2.2.2. Reactivos para síntesis y preparación de disoluciones 12
   2.3. Disoluciones de trabajo 13

3. Resultados y discusión 16
   3.1. 2-Nitroimidazol 16
      3.1.a. Medio no acuoso 16
      3.1.b. Medio acuoso mixto (60%DMF) 27
   3.2. 5-Nitroimidazoles 35
      3.2.a. Medio no acuoso 35
      3.2.b. Medio acuoso 39
   3.3. 4-Nitroimidazoles 44
      3.3.a. Medio no acuoso 44
      3.3.b. Medio acuoso 52
      3.3.c. Medio micelar 66

4. Conclusiones 69

5. Referencias 71

6.- Publicaciones derivadas del trabajo de investigación de la tesis 75
   J. Electroanal.Chem. 531(2) (2002) 187-194
   J.Electrochem.Soc. 152 (6) (2005) J46-J51
   Electroanalysis 17 (18) (2005) 1665-1673
   Electrochimica Acta 52 (2) (2006) 511-518
   J. Electrochem.Soc. 154(4)(2007) F77-F81
   Electroanalysis 19 (14) (2007) 1490-1495

1. INTRODUCCIÓN

Los compuestos nitroimidazólicos presentan un diverso espectro de actividad biológica donde sobresalen, entre otros, su uso como drogas radiosensibilizadoras y drogas antibacterianas o antiprotozoarias. Su uso como radiosensibilizadores aprovecha su característica de citotoxicidad en células mamíferas hipóxicas, lo que permite aumentar la sensibilidad a la radiación de los tumores cancerígenos (1-4). Su característica antimicrobiana aprovecha su toxicidad selectiva hacia microorganismos anaeróbicos y permite que estos compuestos sean usados extensamente en el tratamiento de enfermedades infecciosas tanto en la terapéutica humana como animal (5-11). No obstante la genotoxicidad mostrada por estos compuestos, que les hace tan útiles en el tratamiento de infecciones microbianas, se puede manifestar también contra las mismas células sanas del organismo; así algunos estudios en animales relacionan el uso de estos compuestos con un descenso en la tasa de fertilidad (12) y otros estudios les achacan propiedades mutagénicas y cancerígenas (13-16).

La acción antimicrobiana de los compuestos nitroimidazólicos es producida dentro de los microorganismos patógenos debido a que algunas formas reducidas del grupo nitro interaccionan con el DNA del microorganismo causándole daño estructural e impidiendo su reproducción. En consecuencia, resulta vital para el mecanismo de acción que los microorganismos tengan un sistema enzimático capaz de reducir el grupo nitro. La reducción de estos compuestos nitroimidazólicos puede ser producida por dos rutas diferentes de acuerdo a si las condiciones del medio son aeróbicas o anaeróbicas (7,12), sin embargo, ambas rutas comparten una primera etapa común que corresponde a la reducción monoelectrónica del grupo nitro para formar el anión radical nitro de acuerdo a:

$$RNO_2 + e^- \rightarrow RNO_2^{\cdot -} \quad (1)$$

Bajo condiciones anaeróbicas, el anión radical nitro ($RNO_2^{\cdot -}$) formado inicialmente puede seguir reduciéndose hasta formar los productos de reducción: derivado nitroso (RNO), derivado hidroxilamina (RNHOH) y derivado amina (RNH_2) de acuerdo a las siguientes reacciones de transferencia electrónica:

$$RNO_2^{\cdot -} + e^- + 2H^+ \rightarrow RNO + H_2O \quad (2)$$

$$RNO + 2e^- + 2H^+ \rightarrow RNHOH \quad (3)$$

$$RNHOH + 2e^- + 2H^+ \rightarrow RNH_2 + H_2O \quad (4)$$

Por otra parte, bajo condiciones aeróbicas, el anión radical nitro formado sería re-oxidado por oxígeno para producir superóxido y regenerar el nitroderivado inicial provocando el llamado "ciclo fútil" (17,18):

$$RNO_2^{\cdot -} + O_2 \rightarrow RNO_2 + O_2^{\cdot -} \quad (5)$$

Posteriormente el anión superóxido podrá generar otras especies reactivas de oxígeno como radical hidroxilo, peróxido de hidrógeno, etc.. .

En definitiva, la reducción del grupo nitro juega un rol crucial en el mecanismo de acción biológico de los compuestos nitroimidazólicos y consecuentemente el conocimiento de su comportamiento REDOX es de trascendental importancia debido a que su química radicalaria es determinante para su uso en medicina.

Las propiedades prototrópicas y los tiempos de vida media de los aniones radicales nitro han sido estudiados principalmente usando técnicas como la resonancia de Spin Electrónico y la Radiólisis de Pulso (8,19-21), sin embargo, técnicas electroquímicas como la Voltamperometría Cíclica han demostrado jugar un rol ventajoso en el estudio de estos radicales (22-32). Bajo condiciones adecuadas del medio, la reducción monoelectrónica de nitro a anión radical nitro produce

Voltamperogramas cíclicos muy bien resueltos debidos al par redox $RNO_2/RNO_2^{\cdot -}$. En consecuencia, usando apropiadamente la versatilidad de la técnica de Voltamperometría Cíclica es posible estudiar la factibilidad de formación del anión radical nitro (22) así como su comportamiento prototrópico (23), sus tiempos de vida media naturales (24,25) y su reactividad con otras moléculas (26,27).

Dentro de los derivados nitroimidazólicos se distinguen los derivados 2, 4 y 5-nitroimidazólicos de acuerdo a la posición del sustituyente nitro en el anillo imidazólico. En el siguiente esquema se muestran sus estructuras.

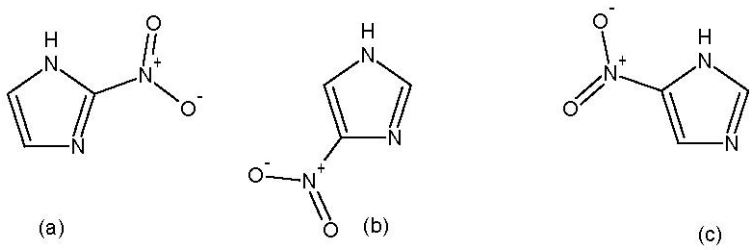

Estructuras de (a) 2-Nitroimidazol, (b) 4-nitroimidazol y (c) 5-nitroimidazol

Desde el punto de vista de su actividad biológica se encuentra descrito que los derivados 2-nitroimidazólicos son empleados preferentemente como radiosensibilizadores, mientras que los derivados 5-nitroimidazólicos son más usados por su toxicidad hacia microorganismos y los derivados 4-nitroimidazólicos son relativamente más inertes biológicamente (33).

Hay numerosos estudios apuntando a aspectos electroquímicos de los compuestos nitroimidazólicos. Sin embargo, en su mayoría, estos trabajos están enfocados a la determinación electroanalítica de algunos 5-nitroimidazoles de importancia en medicina tales como: metronidazol (34), ornidazol (35), secnidazol (36),

tinidazol (37) y megazol (38). Además se ha usado la técnica de Voltamperometría Cíclica en el estudio de los aniones radicales nitro generados desde 5-nitroimidazoles tales como misonidazol, metronidazol y megazol (39-43). Principalmente en estos últimos estudios se demuestra la utilidad de la Voltamperometría Cíclica para el estudio de la formación y estabilidad de los aniones radicales generados. En principio, en medio mixto a pH básico, así como en medio totalmente no acuoso, es posible obtener una respuesta reversible que da cuenta de la transferencia monoelectrónica. En el caso del estudio electroquímico de derivados del 4-nitroimidazol estos son mucho más escasos y el primer trabajo registrado data de los años 80 por el grupo de Vianello (44). En ese trabajo se revisó el comportamiento polarográfico, ciclovoltamétrico y EPC-culombiométrico del 4-nitroimidazol sólo en medio aprótico. Mediante VC se encontró dos picos de reducción. El primer pico fue irreversible hasta una velocidad de 250 V/s mientras que el segundo resultó ser reversible aún a bajas velocidades de barrido. El primer pico irreversible fue atribuido a la siguiente reacción global:

$$5HRNO_2 + 4e^- \rightarrow HRNHOH + 4RNO_2^- + H_2O \quad (6)$$

y el segundo pico reversible se atribuyó a la siguiente reacción de reducción que genera un radical dianión nitro:

$$RNO_2^- + e^- \leftrightarrows RNO_2^{2.-} \quad (7)$$

Además, en ese estudio se informó que el par $RNO_2/RNO_2^{.-}$ no pudo ser aislado debido al rápido decaimiento del $RNO_2^{.-}$ producto de una rápida reacción de protonación por el protón ácido del 4-nitroimidazol inicial (reacción padre-hijo) generando la base conjugada $(RNO_2)^-$ y el radical neutro $RNO_2H^{.}$.

Recientemente y en virtud de la escasez de investigación electroquímica básica sobre 4-nitroimidazol nuestro grupo (45) realizó un exhaustivo estudio acerca del

comportamiento electroquímico de este compuesto en medio prótico en una amplia escala de pH. Nuestros resultados en medio prótico fueron sustancialmente diferentes a los descritos anteriormente por Vianello en medio aprótico, ya que mostraron que la reducción del 4-nitroimidazol, en medio prótico a pH básicos, produjo un anión radical nitro estable dentro de la escala de tiempo de la Voltamperometría cíclica, lo que no había sido posible en medio aprótico. Este resultado resultó sorprendente y paradójico ya que lo esperable es que el anión radical nitro sea mas estable en medio aprótico que en prótico y no como muestran estos resultados. En el medio prótico estudiado el anión radical nitro decayó de acuerdo a una reacción de 2º orden (disproporcionación) de tal manera que la reducción monoelectrónica del 4-nitroimidazol y el posterior decaimiento del anión radical siguieron un esquema EC_2 de acuerdo a:

$$RNO_2 + e^- \rightarrow RNO_2^{\cdot -} \quad (1)$$

$$2\,RNO_2^{\cdot -} + 2H^+ \rightarrow RNO_2 + RNO + H_2O \quad (8)$$

En este trabajo se obtuvo las constantes de velocidad de disproporcionación (k_2) mediante la teoría de Voltamperometría cíclica para reacciones de disproporcionación descrita por Olmstead y Nicholson (46). Se encontró que las constantes de velocidad de disproporcionación dependen fuertemente tanto del pH como del contenido de co-solvente de acuerdo a las siguientes ecuaciones de regresión: $\log k_2 = -0.932\ pH + 12.771$ y $\log (10^{-3} k_2) = -1.998 \log [\%\ EtOH] + 3.873$.

Los estudios electroquímicos acerca del derivado 2-nitroimidazol son aún más escasos y están restringidos casi exclusivamente a un trabajo (47) donde se describe su

reducción electrocatalítica sobre electrodos de oro y de oro modificados. El mecanismo descrito en este trabajo involucró dos rutas distintas en medio ácido, una de tipo electrocatalítica y la otra de intercambio electrónico. En el mecanismo electrocatalítico se asume que la reacción procede a través de la quimisorción del grupo nitro y el rompimiento reductivo de uno de los enlaces N-O. En el mecanismo de intercambio electrónico se propuso que la reacción procedió a través de la reducción inicial a la dihidroxilamina la cual posteriormente pierde agua irreversiblemente para formar el derivado nitroso, el cual se reduce a la correspondiente hidroxilamina. Ninguna referencia se hace en este trabajo a la aparición de intermediarios radicalarios ni a reacciones de protonación involucradas.

Esta escasez de investigación electroquímica en relación a los derivados nitroimidazólicos y la importancia que representa la reducción de estos compuestos en sus aplicaciones médicas nos ha llevado a considerar un estudio electroquímico exhaustivo en medios no acuoso y mixto con el fin de contribuir a su conocimiento REDOX básico.

Específicamente, para el estudio de los mecanismos electroquímicos de los compuestos nitroimidazólicos se utilizará fundamentalmente la técnica de Voltamperometría cíclica que se muestra muy adecuada para el estudio de procesos electroquímicos donde aparecen reacciones químicas acopladas a la transferencia electrónica. En estos casos, la velocidad de barrido será un parámetro importante que influirá en los procesos de electrodo y se utilizará ya sea como criterio de diagnóstico o como variable que permitirá el cálculo de los parámetros cuantitativos que caracterizarán la especie radicalaria.

2. EXPERIMENTAL

2.1. Equipo instrumental

Se utilizó diverso material para la preparación homogénea de las disoluciones y para la realización de las medidas voltamétricas:

• Balanza analítica de precisión: METTLER TOLEDO AB104. Sensibilidad 0.1 mg

• Medidor de pH: pH-metro CRISON BASIC 20 con electrodo de vidrio CRISON 52-01 con resolución de 0.01 y precisión ± 0.01 unidades de pH.

• Agitador magnético: SCHARLAU SCIENCE HI190M.

• Baño ultrasónico: SELECTA.

• Termostato/criostato de recirculación: SELECTA Frigiterm-10. Resolución 0.1 °C.

• Equipo de análisis voltamétrico: El registro de los voltamperogramas se realizó en un equipo analizador electroquímico BAS 100B/W conectado a un PC con el software (BAS 100W 2.3 para Windows) para el control y tratamiento de las experiencias realizadas.

• Electrodos: En todas las experiencias se utilizó como electrodo de trabajo un electrodo de mercurio de crecimiento controlado (BASi EF-1400) dispensando las gotas de mercurio de 0.43 mm^2 de superficie en el modo SMDE (electrodo de mercurio de gota estática). Las medidas de potencial se realizaron tomando como referencia un electrodo de plata/cloruro de plata cuyo electrolito era una disolución de cloruro de sodio 3 M: Ag/AgCl/NaCl (3M) (BASi MF-2052). Como contraelectrodo se empleó uno de platino (BASi MW-1032).

• Para la realización de las medidas espectrofotométricas se utilizó un equipo Varian Cary.

• Los puntos de fusión se determinaron en un aparato Block-Monoscop Werk -

NRZA (50-60 Hz, 220V).

• Los espectros FT-IR se realizaron en un instrumento Bruker FT-IR Paragon 100 PC, con pastilla de KBr para los compuestos sólidos.

• Los espectros 1H-RMN y 13C-RMN se realizaron en un espectrómetro Bruker WM 300. Los desplazamientos químicos se informan en partes por millón (δ) relativo al TMS como estándar interno. Todos los espectros son consistentes con las estructuras asignadas.

• Los análisis elemental (C, H, N) se realizaron en un instrumento Perkin Elmer 2400 y están dentro de los límites aceptables de ± 0,4% de los valores teóricos.

2.2. Reactivos.

2.2.1. Nitroimidazoles:

Los nitroimidazoles estudiados en este trabajo tienen distinta procedencia, tal y como se indica a continuación:

a) Adquiridos en laboratorios comerciales:

- 2-nitroimidazol y 4-nitroimidazol, 97%. Aldrich. Chem. Co.

b) Sintetizados por G. Chauviere del laboratorio de Química Orgánica Biológica de la Universidad Paul Sabatier, Toulousse, Francia.

- 1-metil-5-nitroimidazol
- 1-metil-4-yodo-5-nitroimidazol,
- 1-metil-2,4-diodo-5-nitroimidazol

b) Sintetizados por en los laboratorios de la Universidad de Chile, conforme al procedimiento que se indica para cada uno de ellos:

- **1-metil–2-hidroximetil-4-nitroimidazol (4-MNImOH)**: Se forma una mezcla con 2-hidroximetil-1-metilimidazol y nitrato de potasio, la cual se agrega lentamente sobre ácido sulfúrico sin sobrepasar los 50° C. Luego, se calienta con un baño de agua por 3 horas, se agita a temperatura ambiente por 15 horas. El producto se neutraliza con bicarbonato de sodio hasta pH 7-8. Se extrae con acetato de etilo, se seca con sulfato de sodio anhidro y se evapora al vacío. El sólido se recristaliza en etanol, obteniéndose cristales blancos.

  Rendimiento: 40%;P.F. 180,0 – 181,0 ºC;IR (KBr): νmax. 2982,4. 2800,0. 1253,8,8. 1250,0. 1073,5. 588,2;1HRMN (300 MHz, agua-d): δ 3,2 (s, 1H, OH). 3,8 (s, 3H, -N-CH3). 4,5 (s, 2H, -CH2-). 8,0 (s, 1H, -C=CH-N-CH3);13CRMN (75 MHz, agua-d): 30,0. 55,0. 120,0. (2x149,8).
  Anal. Elem. Cuant. Calculado para C5H7O3N3: C: 38,22; H: 4,46; N: 26,75. Encontrado: C: 37,90; H: 4,58; N: 26,52.

- **1-metil-4-nitroimidazol-2-carboxialdehído** (**4-MNImCHO**): Se disuelve el dicromato de potasio en la mínima cantidad de agua caliente y se adiciona el volumen necesario de ácido sulfúrico, gota a gota. Se enfría a temperatura ambiente. Se disuelve la cantidad calculada de 2-hidroximetil-1-metil-4-nitroimidazol, en la mínima cantidad de agua posible. La solución se enfría entre 5º - 10º C en un baño de hielo-agua, se adiciona la mezcla sulfocrómica gota a gota, muy lentamente y con agitación vigorosa, manteniendo la temperatura entre 5º - 10º C. Luego, se calienta suavemente entre 70º y 80º C

por tres horas; la solución toma un color verde amarillenta. Se agita a temperatura ambiente por 48 horas, la solución toma un color verdosa. Se neutraliza con bicarbonato de sodio hasta pH 7-8, se extrae con acetato de etilo y se evapora al vacío. Se recristaliza en acetona seca, obteniéndose cristales amarillos.

Rendimiento: 90%; P.F. 131,0 – 133,0 ºC; IR (KBr): νmax. 3490,0. 3137,6. 2800,0. 1740,0. 1544,4. 1327,1;1HRMN (300 MHz, agua-d): δ 4,0 (s, 3H, -N-CH3). 8,3 (s, 1H, -C=CH-N-CH3). 9,6 (s, 1H, -CHO);13CRMN (75 MHz, agua-d): 31,5. 119,1. 150,0. 175,2. 180,0.

Anal. Elem. Cuant. Calculado para C5H5O3N3: C: 38,71; H: 3,23; N: 27,10. Encontrado: : 38,38; H: 3,29; N: 26,73.

- **Ácido 1-metil-4-nitroimidazol-2-carboxílico** (**4-MNImCOOH**): Se mezclan 1-metil-4-nitroimidazol-2-carboxialdehído, dicromato de sodio dihidratado y agua; con agitación se agrega ácido sulfúrico durante 30 minutos. Se calienta a reflujo por 1 hora. Se enfría y se vierte la mezcla de reacción en agua. Se filtra al vacío y se lava con agua. Se remueve las sales de cromo con una solución de ácido sulfúrico al 5%, se enfría y se filtra nuevamente. Se lava con abundante agua fría y se seca con sulfato de sodio anhidro. Se recristaliza en acetona, obteniéndose cristales blancos.

  Rendimiento: 85%;P.F. 146,0 – 147,0 ºC;IR (KBr): νmax. 3333,0. 3250,5. 2950,0. 1725,0. 1520,5. 1350,0. 1HRMN (300 MHz, agua-d): δ 4,2 (s, 3H, -N-CH3). 8,6 (s, 1H, -C=CH-N-CH3). 9,8 (s, 1H, -COOH);13CRMN (75 MHz, agua-d): 35,5. 119,9. 145,0. 157,0. 158,0

  Anal. Elem. Cuant. Calculado para C5H5O4N3: C: 35,09; H: 2,94; N: 24,56. Encontrado: : 35,20; H: 2,93; N: 24,50.

- **<u>2-hidroximetil-4-nitroimidazol</u>** (**4-NImOH**): Se forma una mezcla con 2-hidroximetilimidazol y nitrato de potasio, la cual se agrega lentamente sobre ácido sulfúrico sin sobrepasar los 50° C. Luego, se calienta con un baño de agua por 2 horas, se agita a temperatura ambiente por 15 horas. El producto se neutraliza con bicarbonato de sodio hasta pH 7-8. Se extrae con acetato de etilo, se seca con sulfato de sodio anhidro y se evapora al vacío. El líquido viscoso de color amarillo se cristaliza con carbono activado en acetona seca, obteniéndose cristales amarillos.

  Rendimiento: 30%; P.F. 148,0 – 150,0 ºC; IR (KBr): νmax. 3423,7. 2996,9. 1693,3. 1462,9. 1416,2. 1339,8. 1135,3. 769,9. 1HRMN (300 MHz, agua-d): δ 4,5 (s, 2H, -CH2-). 6,9 (s,2H, -NH; OH). 7,3 (s, 1H, -C=CH-NH).13CRMN (75 MHz, agua-d): 55,5. 120,0. 144,5. 150,8.

  Anal. Elem. Cuant. Calculado para C4H5O3N3: C: 33,57; H: 3,50; N: 29,37. Encontrado: C: 33,84; H: 3,58; N: 29,04.

- **<u>4-nitroimidazol-2-carboxialdehído</u>** (**4-NImCHO**): Se disuelve el dicromato de potasio en la mínima cantidad de agua caliente y se adiciona el volumen necesario de ácido sulfúrico, gota a gota. Se enfría a temperatura ambiente. Se disuelve la cantidad calculada de 2-hidroximetil-4-nitroimidazol, en la mínima cantidad de agua posible La solución se enfría entre 5º - 10º C en un baño de hielo-agua, se adiciona la mezcla sulfocrómica, gota a gota, con agitación vigorosa, manteniendo la temperatura entre 5º - 10º C. La solución toma un color café ladrillo. Luego, se calienta suavemente entre 70º y 80º C por una hora; la solución toma un color verde amarillenta y se agita a temperatura ambiente por 48 horas, la solución toma un color verdosa. Se neutraliza con

bicarbonato de sodio hasta pH 7-8, se extrae con acetato de etilo y la fase orgánica de color amarillo claro se evapora al vacío. Se recristaliza con carbón activado en acetona seca, obteniéndose cristales amarillos.

Rendimiento: 80%; P.F. 150,0 – 152,0 ºC;1HRMN (300 MHz, agua-d): δ 6,9 (s, 1H, -C=CH-NH). 7,6 (s, 1H, -NH). 9,6 (s, 1H,-CHO);13CRMN (75 MHz, agua-d): 1214. 150,8. 175,1. 181,0.

Anal. Elem. Cuant. Calculado para C4H3O3N3: C: 34,04; H: 2,13; N: 29,79. Encontrado: C:34,01; H:2,11; N:29,81.

2.2.2. Reactivos para síntesis y preparación de disoluciones :

Para la preparación de las disoluciones y la síntesis de los nitroimidazoles mencionados anteriormente se emplearon los siguientes reactivos con la calidad que se indica para cada uno de ellos :

- Ácido bórico. Sigma Minimum 99.5%
- Ácido cítrico anhidro.
- Ácido clorhídrico 35 %. Panreac
- Ácido perclórico 70-72 % para análisis. Merck
- Cloruro de potasio para análisis. Merck
- Etanol absoluto para análisis. Merck
- Hexafluorofosfato de tetrabutilamonio (HFTBA). Grado electroquímico. Fluka
- Hidróxido de sodio para análisis. Merck
- Hidróxido de tetrabutilamonio (TBAOH) 0.1 M. Merck
- N,N-dimetilformamida (DMF) para análisis. Merck
- 1-metilimidazol
- Formalina 37%, Sigma.

- Metanol, Merck.
- Etanol absoluto, Merck.
- Nitrato de potasio, Merck.
- Ácido sulfúrico, Merck.
- Bicarbonato de sodio, Equilab.
- Hidróxido de potasio, (pellets) Merck.
- Acetato de etilo, Equilab.
- Sulfato de sodio anhidro, (p.a) Merck.
- Dicromato de potasio, Merck.
- Nitrato de potasio, Merck.
- Carbón activado.
- Perclorato de tetrabutilamonio (TBAP). Grado electroquímico. Fluka
- Nitrógeno gaseoso. (impurezas máx: H_2O< 3ppm; O_2< 2 ppm; C_nH_m < 0.5 ppm) ALPHAGAZ-AIR LIQUIDE

2.3. Disoluciones de trabajo:

Todas las experiencias se realizaron tras eliminar el oxígeno disuelto; para ello se hizo pasar una corriente de nitrógeno a través de la disolución en célula durante los diez minutos anteriores a la realización de las medidas.

La temperatura de la disolución de la célula se mantuvo constante a 25 °C, en todas las experiencias.

Disolución buffer Britton-Robinson 0,1 M

Para la preparación de 1 L de disolución de buffer Britton Robinson, se pesa 6,18 g de ácido bórico, se disuelve en un poco de agua Milli-Q, luego se agrega 5,71 mL de ácido acético glacial y 6,75 mL ácido fosfórico, se sonica por diez minutos para eliminar micro burbujas. Se afora en matraz de 1000 mL.

Disolución buffer Citrato 0,15 M + KCl 0,3 M + H_3BO_3 0,03 M

Para la preparación de 1L de disolución de buffer citrato, se pesa y se disuelve 7,21 g de ácido cítrico, 55,91 g de cloruro de potasio y 1,84 g de ácido bórico en agua Milli-Q, luego se afora a 1L.

Soluciones Stock

Se prepararon 2 mL de disolución stock de concentración 1 mM de derivado nitroimidazólico, para esto se pesaron 2 mg de este compuesto en un eppendorf y se agregó con micropipeta 2 mL de disolución madre correspondiente al medio de trabajo que se desea preparar.

Soluciones de Trabajo

Se usaron diferentes soluciones de trabajo para cada medio en el que se realizaron estudios electroquímicos, todas las soluciones fueron de 10 mL.

Medio Acuoso.

La disolución de trabajo en medio acuoso se prepara con buffer 100% Britton Robinson, se toma una alícuota de disolución stock de derivado nitroimidazólico preparada en este buffer y se afora a 10 mL.

Medio Mixto. Britton Robinson – Etanol (70/30).

La disolución de trabajo para este medio se prepara tomando una alícuota de disolución stock de derivado nitroimidazólico preparada en buffer Britton Robinson, se agrega a un matraz de 10 mL, se agregan 3 mL de etanol (p.a.), luego se afora con disolución buffer Britton Robinson. Se ajusta al pH deseado en la celda electroquímica con pequeñas alícuotas de NaOH conc o HCl conc.

Medio buffer citrato – DMF (60/40).

La disolución se prepara tomando una alícuota de disolución stock de derivado nitroimidazólico preparada anteriormente en buffer citrato, se agrega a un matraz de 10

mL, luego se agrega 4 mL de DMF y se afora con buffer Citrato. Se ajusta al pH deseado en la celda electroquímica.

Medio no acuoso. 100% DMF.

Se toma una alícuota de disolución stock de derivado nitroimidazólico preparada en DMF o se disuelve la cantidad apropiada de ácido en DMF, se agrega a un matraz de 10 mL, luego se agrega 0,34192 g de PTBA, y se afora con DMF.

También se realizaron experiencias en un medio DMF (0.1 M HFTBA) para una concentración 1 mM de derivado nitroimidazólico.

Medio no acuoso. 100% DMSO.

Se toma una alícuota de disolución stock de derivado nitroimidazólico preparada en DMSO, se agrega a un matraz de 10 mL, luego se agrega 0,34192 g de PTBA y se afora con DMSO.

El ajuste del pH se llevó a cabo añadiendo pequeñas cantidades de disoluciones, previamente preparadas, de NaOH o HCl concentrados a la disolución componente del medio, según la variación de pH deseada; terminándose con un ajuste fino, justo antes de introducir la disolución en la célula, ya con presencia del derivado nitroimidazólico.

Para estudiar la influencia de procesos ácido-base en el mecanismo electródico en medio no acuoso, se adicionaron alícuotas de hidróxido de tetrabutilamonio comercial 0.1 M y de ácido perclórico 0.2 M en etanol, respectivamente.

3. RESULTADOS Y DISCUSIÓN

3.1.- 2-Nitroimidazol

3.1.a Medio no acuoso

Primeramente se procede al estudio del comportamiento del 2-nitroimidazol (2NMZ) en medio no acuoso, para ello se ha utilizado DMF (dimetilformamida) como disolvente y 0.1 M HFTBA (hexafluoruro de tetrabutilamonio) como electrolito soporte.

En los voltamperogramas obtenidos, para las diferentes velocidades de barrido de potencial, se registran dos picos en el sentido del barrido catódico (Fig. 1).

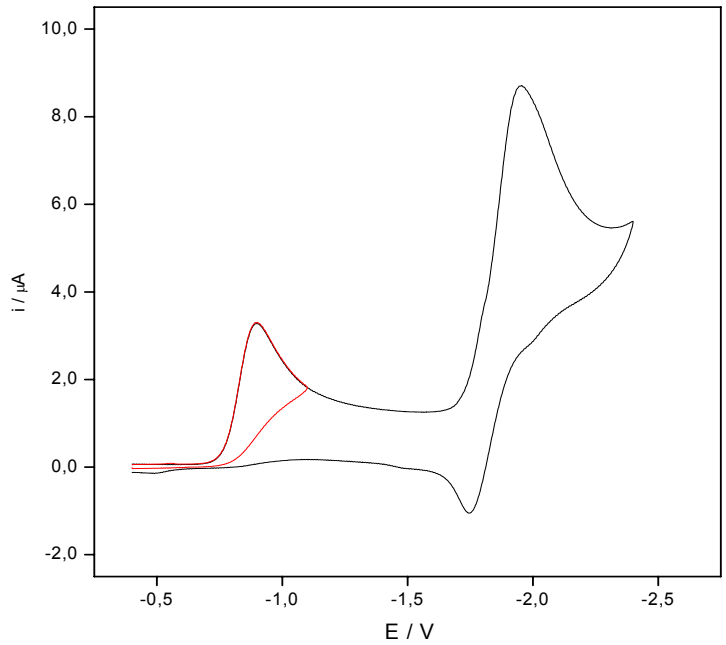

Fig. 1. Voltamperograma cíclico completo y de sólo el primer pico (color rojo) de la reducción del 2NMZ en DMF con 0.1M HFTBA. C°= 1 mM; v= 0.5 V/s.

El primer pico tiene un potencial de pico, $E_{p,c}$, de – 890 mV y el segundo un $E_{p,c}$ de – 1950 mV, a la velocidad de 0.5 V/s. La segunda de estas señales manifiesta un comportamiento aparentemente reversible, ya que se aprecia el correspondiente pico en el barrido anódico ($E_{p,a}$ = -1760 mV). Sin embargo, para la primera señal no se aprecia

ninguna señal cuando se barre en el sentido anódico, lo que indica que corresponde a un proceso irreversible.

A objeto de ver el comportamiento de las respuestas voltamperométricas a diferentes escalas de tiempo del experimento, se realizaron medidas en las que se fue cambiando la velocidad de barrido del potencial. En todas las medidas, los Voltamperogramas obtenidos muestran las mismas señales, cambiando, como es esperado, la intensidad de los diferentes picos. A continuación se recogen las experiencias registradas:

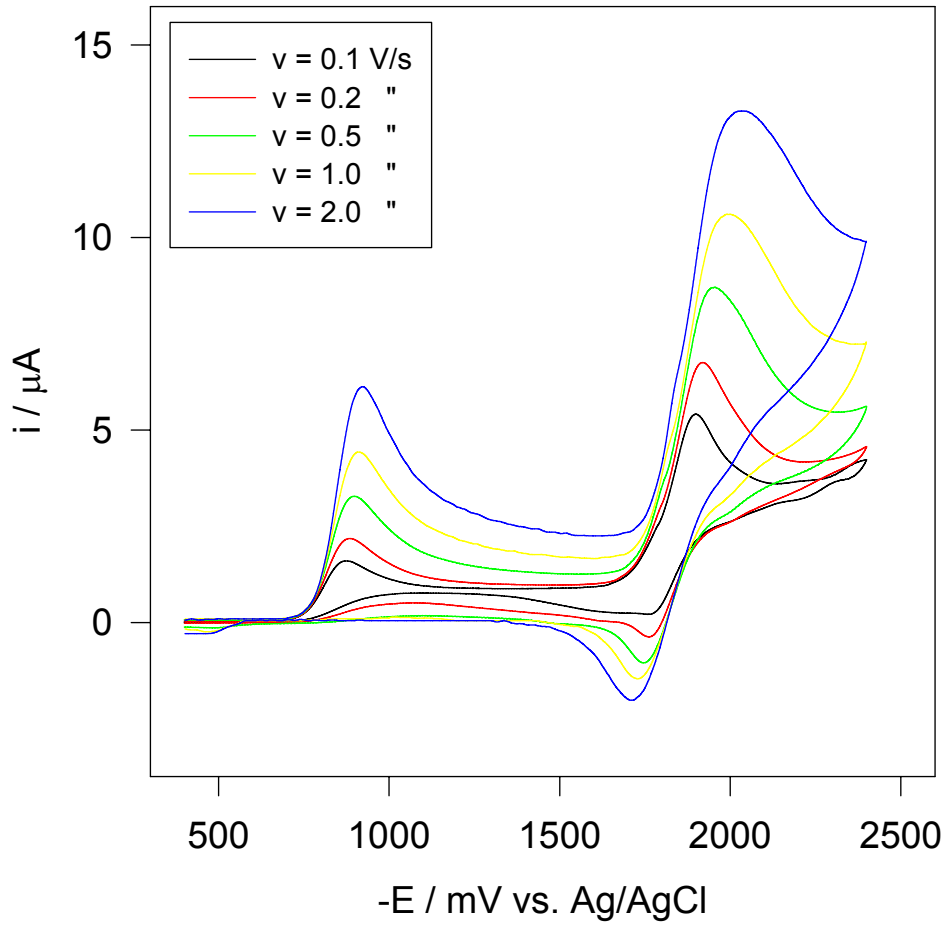

Fig. 2. Voltamogramas cíclicos completos correspondientes a la reducción del 2-nitroimidazol en DMF con 0.1M HFTBA a diferentes velocidades de barrido. C° = 1 mM.

De los voltamperogramas mostrados en la Fig. 2 se aprecia que la diferencia de

los potenciales de pico catódicos y anódicos, ΔE_p, para la onda aparentemente reversible exceden con mucho el valor teórico de 60 mV para un proceso monoelectrónico y más aún, esta diferencia se incrementa considerablemente con la velocidad de barrido pasando de un valor de aproximadamente 120 mV a la velocidad más lenta hasta aproximadamente 380 mV a la velocidad más rápida. Este resultado nos hace descartar la aparente reversibilidad de dicha onda ya que en realidad la transferencia electrónica involucrada obedecería a un proceso cuasi-reversible.

Para analizar el comportamiento del primer pico se realizó barridos cortos que involucraran sólo a dicha señal evitando cualquier otro efecto interferente. Estos resultados están reflejados en los voltamperogramas correspondientes mostrados en la Figura 3:

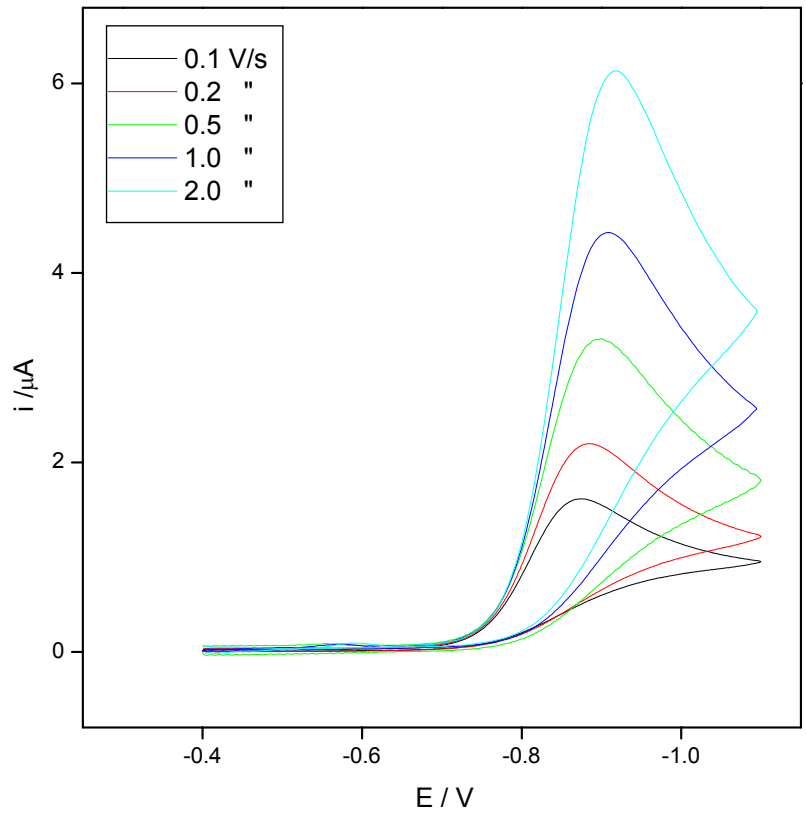

Fig. 3. Voltamogramas cíclicos del primer pico correspondiente a la reducción del 2-nitroimidazol en DMF con 0.1M HFTBA a diferentes velocidades de barrido. C°= 1 mM.

Con los datos de E_{pc} e i_{pc} obtenidos de los anteriores se obtuvieron las representaciones de las Figuras 4 y 5:

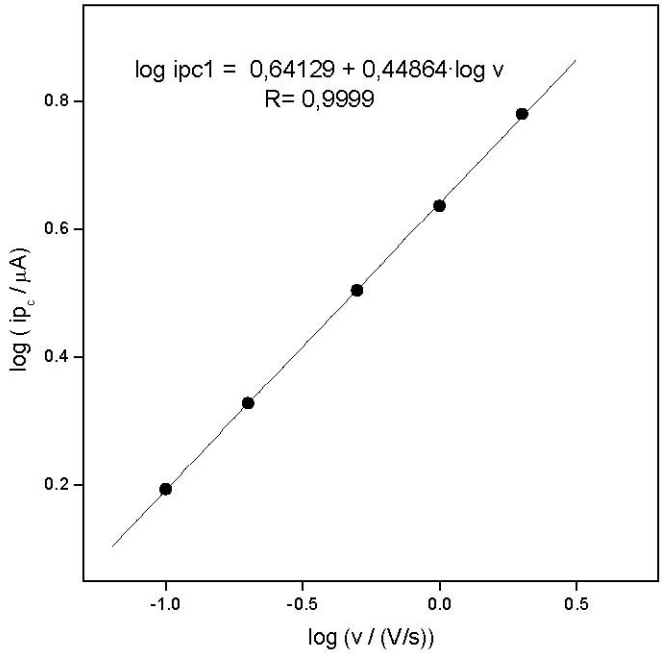

Fig. 4. Log i_{pc} vs log v de la primera onda de la reducción del 2-nitroimidazol en DMF con 0.1M HFTBA. C°= 1 mM.

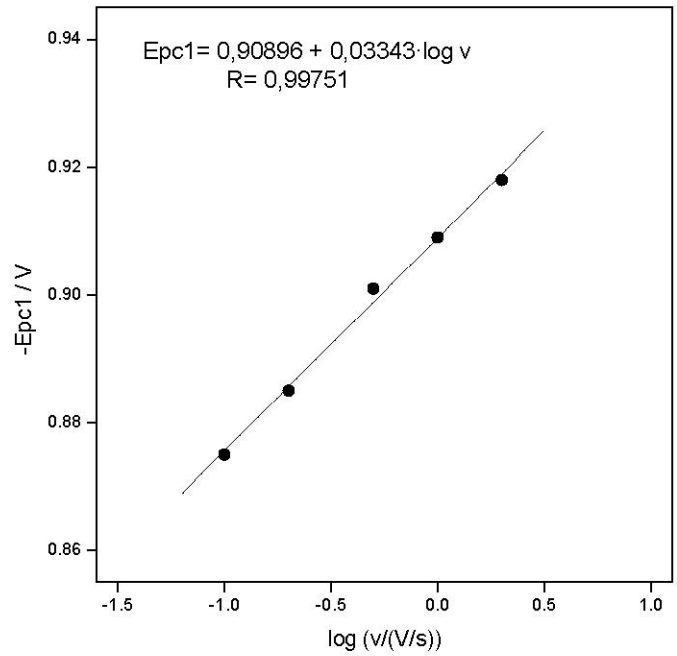

Fig. 5. E_{pc} vs log v de la primera onda de la reducción del 2-nitroimidazol en DMF con 0.1M HFTBA. C°= 1 mM.

En la Figura 4, se observa una dependencia lineal del logaritmo de la intensidad de pico catódico con el logaritmo de la velocidad de barrido de potencial, obteniéndose un valor para la pendiente de 0.44864. Este valor, nos indica que el proceso está regido por difusión; ya que se encuentra próximo al valor teórico de 0.5. Por otra parte, en la Figura 5, se muestra una dependencia lineal entre el potencial del pico y el logaritmo de la velocidad de barrido, siendo en este caso la pendiente de 0.03343 V. Desde ambas representaciones podemos desprender que el primer pico de apariencia irreversible obedecería a un proceso controlado por difusión en el que una reacción de transferencia monoelectrónica lenta es seguida por una reacción química rápida.

En consecuencia, la primera señal obtenida corresponde a un proceso en el que se produce la reducción al tomar un electrón. Como al efectuar el barrido de vuelta, no se registra ninguna señal, se evidencia que la especie reducida en el barrido catódico no es oxidada inmediatamente en el correspondiente barrido anódico, probablemente debido a que se favorece la ocurrencia de una reacción química para dicha especie antes que su oxidación. En consecuencia se trata de un proceso que combina una primera etapa de transferencia de carga seguida de una etapa de tipo químico de acuerdo al siguiente esquema de reacción:

$$HNRNO_2 + e^- \rightarrow HNRNO_2^{\bullet -} \quad (9)$$

$$HNR\text{-}NO_2^{\bullet -} \rightarrow \text{Productos} \quad (10)$$

A partir de esta primera etapa, se plantean varias posibilidades de decaimiento del anión radical formado. Así podría proseguir el proceso mediante algún tipo de reacción ya sea de primer o segundo orden como: protonación con alguna especie que los aporte del medio, dismutación, dimerización o reacción con el reactivo en una

reacción tipo padre-hijo.

Adición de TBAOH

El 2NMZ es un anillo heterocíclico con dos átomos de N de los cuales uno (N1) está enlazado a un átomo de hidrógeno el que puede actuar como dador de protones. El otro N (N3) puede actuar como aceptor de protones. En consecuencia la molécula puede actuar como un ácido y una base de tal manera que este tipo de equilibrios pueden afectar fuertemente su química. Específicamente, con el objeto de considerar este tipo de influencias ácido-base y su incidencia en el mecanismo electródico, se realizaron una serie de experiencias, las primeras de ellas consistieron en adicionar sucesivas cantidades de una base como el hidróxido de tetrabutilamonio (TBA-OH) y estudiar su efecto en los voltamperogramas (Figura 6).

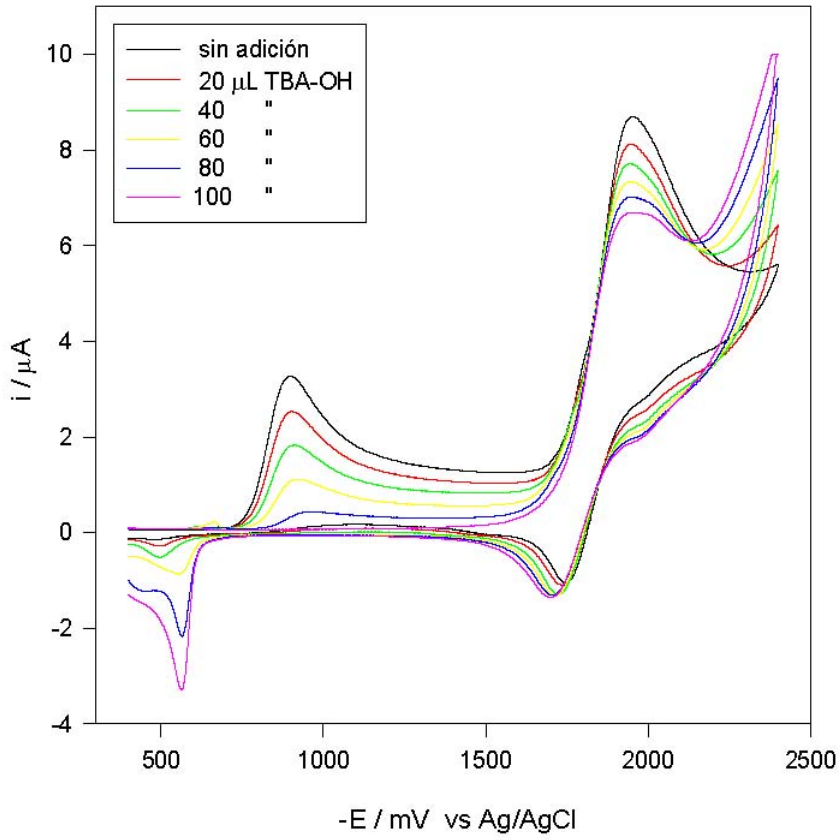

Fig. 6. Voltamperograma cíclico completo de la reducción del 2-nitroimidazol en DMF con 0.1M HFTBA y sucesivas adiciones de TBA-OH. C°= 1 mM ; v= 0.5 V/s.

La evolución de estos voltamperogramas indica que al adicionar la base (TBA-OH) la señal obtenida es menor, lo que significa que la concentración del reactivo inicial disminuye; es decir va desapareciendo la especie que se reduce dando la primera señal. Este resultado nos muestra la existencia de un proceso ácido-base y que probablemente el hidrógeno unido al N1 manifiesta un comportamiento ácido. Además, como se espera para un comportamiento tipo ácido-base, al añadir un ácido al medio alcalinizado se produce la regeneración del compuesto y los picos de los Voltamperogramas del barrido de reducción vuelven a registrarse a valores mayores de intensidad.

Estas experiencias se realizaron para el barrido completo de potencial y consistieron en adiciones sucesivas de $HClO_4$ sobre la solución previamente alcalinizada con el exceso de base, como se muestra en la Fig. 7:

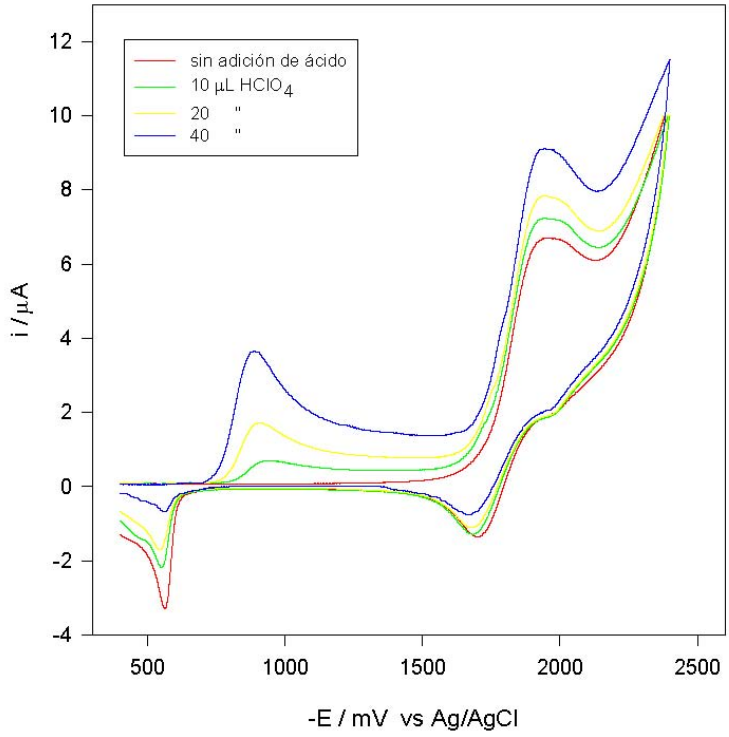

Fig. 7. Voltamperograma cíclico completo de la reducción de 1mM 2-nitroimidazol en DMF + 0.1 M HFTBA. Voltamperogramas dela adición de $HClO_4$ 0.2 M (en etanol) a la disolución con 100 µL de TBA-OH. C°= 1 mM ; v= 0.5 V/s.

De los experimentos anteriores se deduce que el primer pico se debe a la reducción de una especie con carácter ácido la cual desaparece al alcalinizar el medio y que se explica de acuerdo al siguiente equilibrio:

$$HNRNO_2 \quad \leftrightarrows \quad {}^{-}NRNO_2 + H^{+} \quad (11)$$

donde la especie $HNRNO_2$ se refiere al 2NMZ y la especie ${}^{-}NRNO_2$ corresponde al correspondiente nitranión generado como resultado de la cesión del H débilmente ácido unido al N1. En consecuencia la especie que se reduce generando el primer pico corresponde al compuesto 2NMZ en cambio la especie que se reduce generando el segundo pico corresponde a la reducción del nitranión. La generación de este tipo de especies estables tipo nitranión ha sido también recientemente descrita para otro tipo de heterociclos de nitrógeno como derivados dihidropiridínicos (47). En este caso la reducción de la especie nitranión del 2NMZ se reduce a potenciales casi 1000 mV más negativos indicando que el centro de carga negativo del nitranión está muy cercano al sitio de entrada del electrón para la reducción, lo que explica la considerable mayor dificultad que implica la reducción del nitranión.

De esta manera el primer pico se podría representar como causado por la anterior Ecuación 9 y el segundo por la siguiente ecuación:

$$ {}^{-}NRNO_2 + \quad \bar{e} \quad \rightarrow \quad {}^{-}NRNO_2^{\bullet -} \quad (12)$$

donde el nitranión del 2NMZ se reduce al correspondiente dianión radical el cual se oxida en el barrido de vuelta en un proceso cuasireversible, como se mencionó

anteriormente, generando el pico u onda 2.

En el caso del anión radical formado en el primer pico, de acuerdo a la anterior ecuación 9, éste tiene un carácter suficientemente básico como para interaccionar con el 2NMZ original deprotonándolo para generar el radical protonado y el correspondiente nitranión de acuerdo a la siguiente reacción del tipo padre-hijo:

$$HNRNO_2 + HNRNO_2^{\bullet -} \rightarrow HNRNO_2H^{\bullet} + {}^{-}NRNO_2 \quad (13)$$

La ocurrencia de la reacción padre-hijo explica que no se observe un pico de vuelta en la señal 1 ya que la especie generada en vez de oxidarse reacciona más fácil con el reactivo inicial. Además, la ocurrencia de esta reacción es fácilmente verificable, ya que la existencia de ella implica que la generación de la especie $HNRNO_2^{\bullet -}$ lleva asociada el consumo del reactivo inicial $HNRNO_2$. En consecuencia si nosotros producimos la reacción 13 en macroescala (Electrólisis a Potencial controlado) deberíamos observar la desaparición del pico 1 por agotamiento del reactivo inicial.

Electrólisis a Potencial Controlado

Estas experiencias consistieron en la electrólisis de la disolución de 2NMZ para producir exhaustivamente la reducción de 2NMZ. Como se observa en los voltamperogramas realizados antes y después de la electrólisis, según se recoge en la Figura 8, la especie que da lugar al primer pico, se ha consumido prácticamente en su totalidad, comprobando la validez de la anterior ecuación 13.

Además, con el objeto de comprobar que el rol del anión radical generado electroquímicamente en la reacción de tipo padre-hijo es el de una base se comparó los espectros UV-Vis de una solución sometida a electrólisis con una en que se ha agregado base (Figura 9).

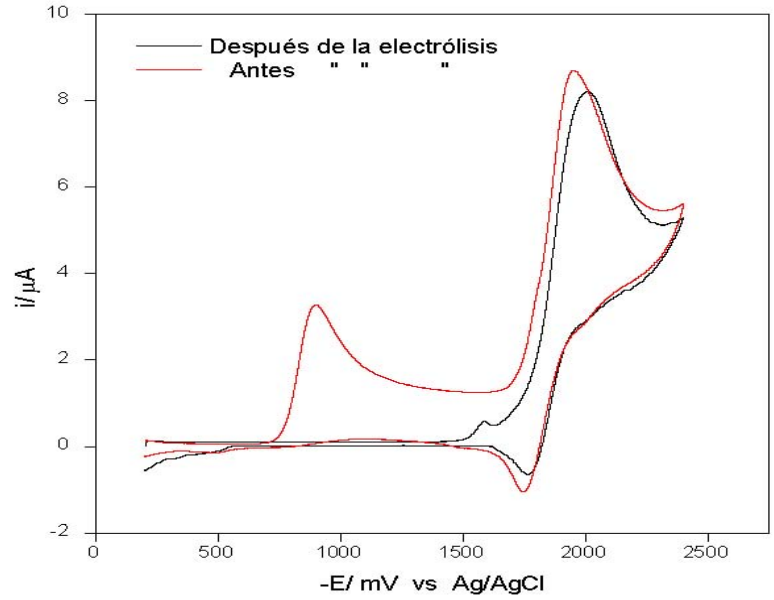

Fig. 8. Voltamperogramas cíclicos completo anterior y posterior a la electrólisis del 2-nitroimidazol en DMF con 0.1M HFTBA. C°= 1 mM ; v= 0.5 V/s.

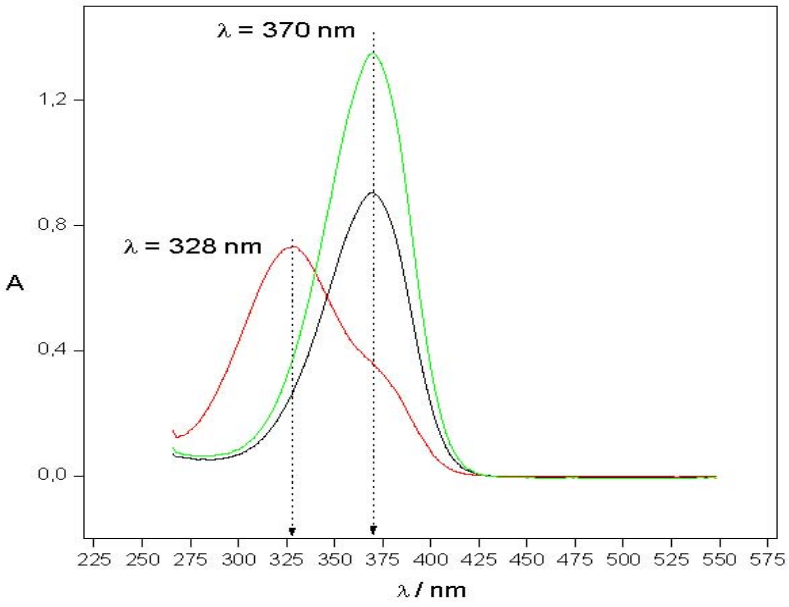

Fig. 9. Espectros comparativos de soluciones de 2-NMZ en DMF (línea roja) con su solución electrolizada (línea negra) o alcalinizada (línea verde).

Al analizar esta Figura 9, se observa una banda (λ = 328 nm) correspondiente al 2NMZ (línea roja). Igualmente se observa que dicha señal desaparece en los espectros

correspondientes a la disolución electrolizada (línea negra) y a la disolución resultante de añadir la base TBAH a la disolución de 2NMZ (línea verde). Además, la señal obtenida en ambos casos presenta un máximo para la misma longitud de onda (λ =370 nm), lo que parece indicar que en ambos procesos se obtiene un mismo compuesto derivado del 2NMZ, el cual correspondería al derivado nitranión de acuerdo a lo indicado en el anterior equilibrio representado por la ecuación 11.

De estos resultados se desprende que la reacción padre-hijo (Ecuación 13) está soportada por los resultados experimentales obtenidos, que comprueban el consumo del reactivo por el anión radical y además la generación del nitranión. No obstante lo anterior, la Ecuación 13 todavía no da cuenta del proceso electroquímico total, ya que considera una especie inestable como el producto de reacción ($HNRNO_2H\bullet$) y no explica la aparición del pico de oxidación que aparece en la zona de potenciales cercanos a -500 mV en medios en que se ha agregado base (ver Figuras 6 y 7). De acuerdo a la evidencia anterior (48), atingente a la reducción de derivados nitro, se puede asegurar que el dicho pico de oxidación corresponde a la oxidación de un derivado hidroxilamínico para producir el derivado nitroso, lo que indicaría que como producto de la reducción se genera el derivado hidroxilamínico correspondiente.

En definitiva, el mecanismo de reducción total, debe dar cuenta de la generación de tanto el derivado hidroxilamínico como del nitranión entre los productos de la reacción total, para lo cual se pueden considerar las siguientes etapas:

$$HNRNO_2 + e^- \rightarrow HNRNO_2^{\bullet -} \quad (9)$$

$$HNRNO_2 + HNRNO_2^{\bullet -} \rightarrow HNRNO_2H\bullet + {}^-NRNO_2 \quad (13)$$

$$HRNO_2H\bullet + HNRNO_2 + e^- \rightarrow HNRNO + {}^-NRNO_2 + H_2O \quad (14)$$

$$HNRNO + 2\,HNRNO_2 + 2\,e^- \rightarrow HNRNHOH + 2\,{}^-NRNO_2 \quad (15)$$

Siendo la reacción global de este proceso la suma de las cuatro etapas anteriores:

$$5\ HNRNO_2 + 4\ e^- \rightarrow 4\ ^-NRNO_2 + HNRNHOH + H_2O \qquad (16)$$

Esta ecuación sí está de acuerdo con la evidencia experimental que implica el consumo del reactivo inicial ($HNRNO_2$) y la generación tanto de un derivado hidroxilamínico (HNRNHOH) como del derivado nitranión ($^-NRNO_2$). Además, un mecanismo en que se describen etapas totalmente análogas ha sido previamente descrito por Vianello y col. (44) para el caso del 4-nitroimidazol.

Una reacción como ésta, implicaría que se debe producir una transferencia global de cuatro electrones por cada cinco moléculas de 2NMZ que participen en el proceso; es decir, el número de electrones transferidos (los equivalentes por mol) debería tender a un valor de (4e) / (5 mol) = 0.8.

Los resultados obtenidos correspondientes a las electrólisis correspondientes a una concentración 4 mM de 2NMZ, indican que la transferencia electrónica por mol de 2NMZ es de 0.801. Con ello se pone de manifiesto la tendencia hacia el valor de 0.8 y que indican que la reacción transcurre a través del mecanismo padre-hijo previsto.

3.1.b - Medio acuoso mixto (60%DMF)

En medio acuoso, como es de esperar, la situación cambia y se encuentra un comportamiento diferente dependiendo del pH. A pH ácidos se encuentra un solo pico irreversible en cambio a pH alcalinos se aprecia una onda reversible seguida por un pico irreversible a potenciales mas catódicos. Este comportamiento está bien reflejado en las siguientes figuras 12 y 13 donde se muestran los voltamperogramas obtenidos en un amplio rango de pHs.

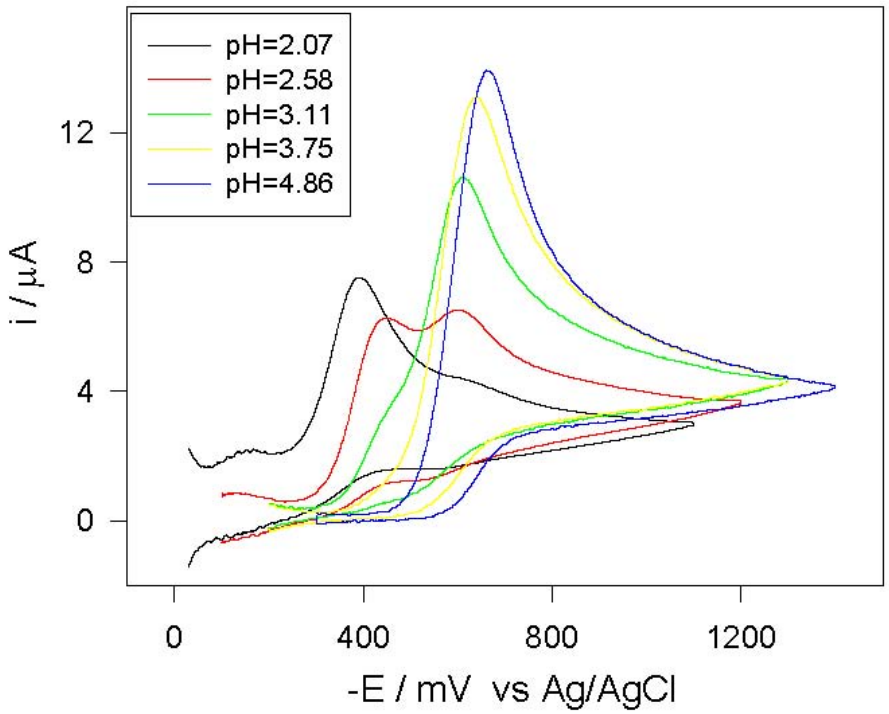

Fig.1 2. Voltamperogramas de soluciones de 1mM 2NMZ en DMFa 1 V/s en función del pH; 60% DMF (0.1 M TBAP)/40%H_2O (0.3M KCl+0.015 M ac. cit.+0.03 M ac. bor.)

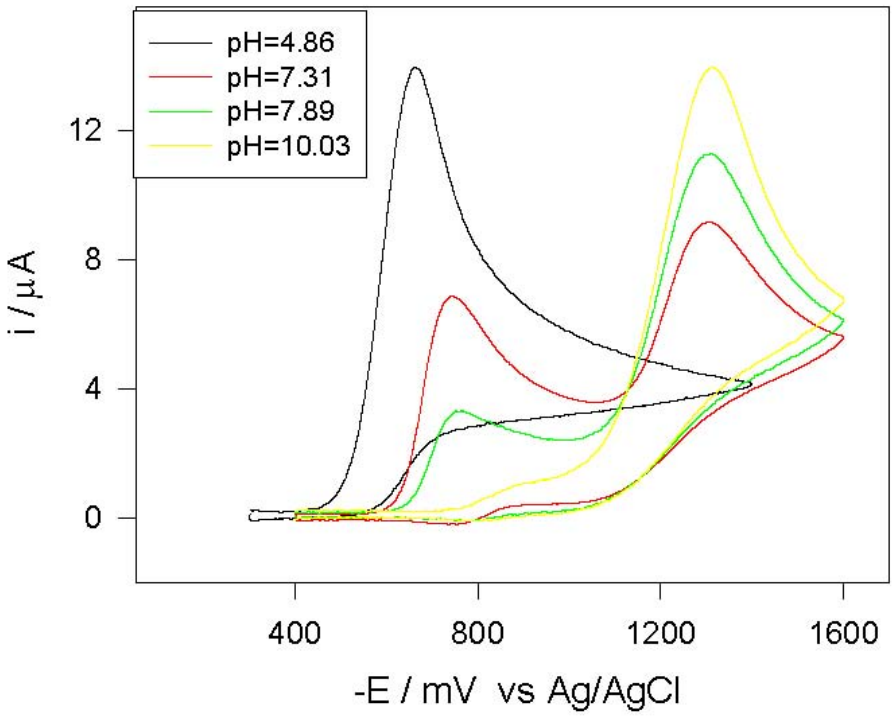

Fig. 13. Voltamperogramas de soluciones de 1mM 2NMZ en DMFa 1 V/s a distintos pH; 60% DMF (0.1 M TBAP)/40% H_2O(0.3M KCl+0.015 M ac. cit.+0.03 M ac. bor.)

El desdoblamiento que se aprecia en el pico irreversible entre pHs 2 y 3 se debe a uno de los pK de la molécula y correspondería al equilibrio que se genera al protonarse el N en la posición 3 del anillo nitroimidazólico. Lo anterior significa que a los pH más ácidos (< 2.8) prevalece la especie protonada en el N3, que tiene capacidad de aceptar protones, mientras que a pH superiores prevalece la especie deprotonada.

En general, el comportamiento observado en medio acuoso mixto se ajusta al comportamiento clásico para especies nitroaromáticas reivindicando el comportamiento de tipo aromático que tiene el anillo imidazólico. De acuerdo a este comportamiento, en el medio ácido, el pico obedece a la siguiente reacción:

$$RNO_2 + 4H^+ + 4e^- \rightarrow RNHOH + H_2O \quad (17)$$

Por otra parte, en el medio alcalino la onda aparentemente reversible que aparece a potenciales menos catódicos correspondería a la transferencia monoelectrónica del grupo nitro para generar el correspondiente anión radical nitro de acuerdo a la bien conocida ecuación:

$$RNO_2 + e^- \leftrightarrows RNO_2^{\bullet -} \quad (1)$$

y el pico irreversible que aparece a potenciales mayores correspondería a la posterior reducción del anión radical nitro para generar el derivado hidroxilamínico:

$$RNO_2^{\bullet -} + 3e^- + 4H^+ \rightarrow RNHOH + H_2O \quad (18)$$

De acuerdo a la anterior Ec. 17, el comportamiento del único pico observado en medio ácido es fuertemente dependiente del pH, como queda reflejado cuantitativamente en las representaciones del Potencial y Corriente de pico que se muestra en las figuras 14 y 15. En la Fig. 14 se muestra la dependencia del potencial del primer pico con el pH para lo

cual se ha considerado sólo el pico de la especie deprotonada. Se aprecia un comportamiento lineal con el pH con una pendiente de 30 mV.

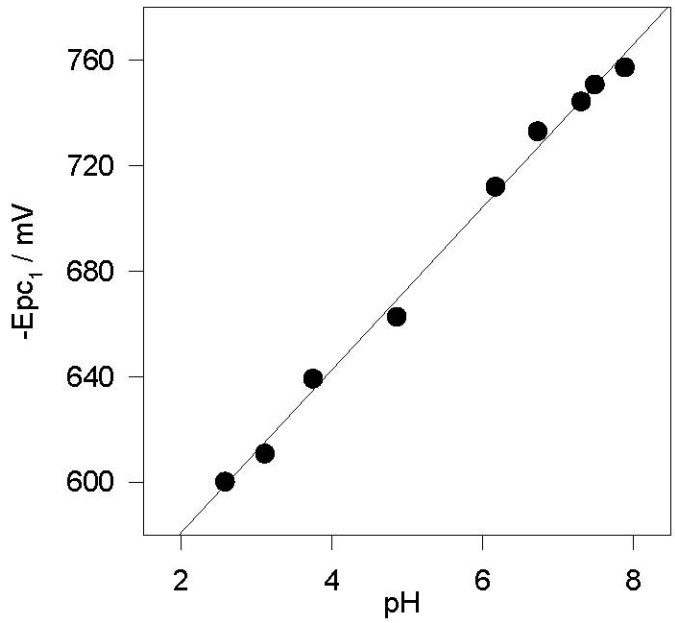

Fig. 14. Variación del Potencial de Pico (E_{PC1}) para el primer pico en medio ácido. O. Or = 519.1; Pend. = 30.830, r^2 = 0.9950. C°=1mM, v = 1V/s .

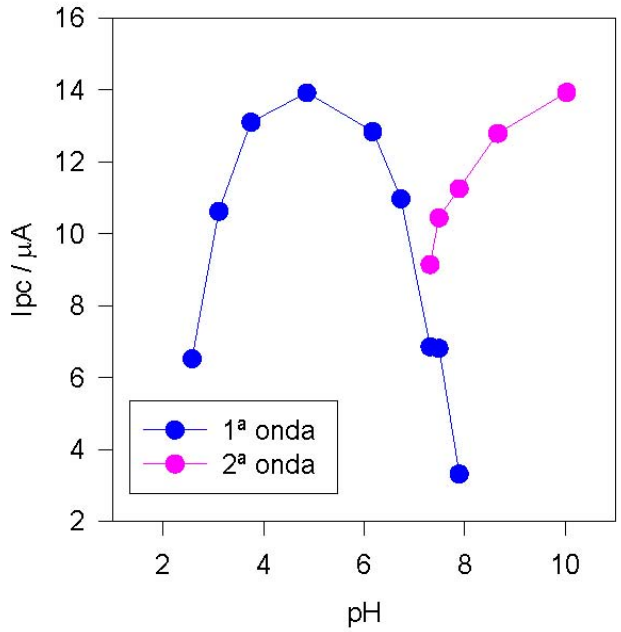

Fig. 15. Variación da la corriente de pico (i_{PC1}) para el primer pico en medio ácido. C°=1mM, v = 1V/s.

En la Fig. 15 se puede apreciar claramente el cambio de mecanismo que ocurre a pH cercanos a 7, en donde disminuye claramente la corriente del primer pico y aparece un segundo pico con corrientes crecientes. También se aprecia a pH ácidos, entre pH 2 y 4 un cambio en la corriente debido al equilibrio producto de la protonación del N3.

En los voltamperogramas sobre pH 7 se observa la aparición de un pico anódico asociado al primer pico catódico, generando una onda de aspecto aparentemente reversible. Esta onda, como se ha mencionado, corresponde a la generación de un radical nitro estable en la escala de tiempo de la Voltamperometría Cíclica lo que no fue posible de obtener en el medio no acuoso. Este hecho resuelta paradójico ya que es esperable que en un medio no acuoso sea más estable una especie radicalaria.

En consecuencia, a pH superiores a 7 y modificando adecuadamente las condiciones del barrido de potencial (Potencial de inicio y de cambio) es posible obtener un voltamperograma muy bien definido y que en definitiva corresponde a una visualización voltamperométrica del radical libre generado del 2NMZ.

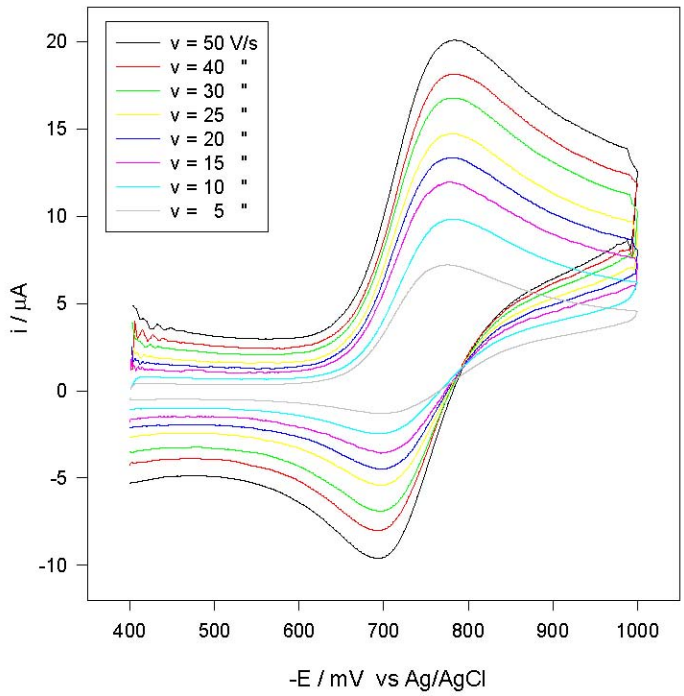

Fig. 16. Voltamperogramas cíclicos de la formación del radical libre de 2NMZ. C^{o}=1mM, Medio mixto, pH = 7.96.

Como se observa en la anterior Fig. 16, un efecto muy importante es la influencia que tiene sobre el voltamperograma la velocidad de barrido de potencial. Esta variación que se ilustra para algunas velocidades de barrido a un pH de 7.89 también se cumple para otros pH. A partir de estos voltamperogramas es posible calcular las razones de las corrientes de pico los cuales se han calculado de acuerdo a la expresión propuesta por Nicholson (49). En la siguiente Figura 17 se muestra la dependencia de la razón de corrientes, $i_{p,a}/i_{p,c}$, con la velocidad de barrido encontrando que ésta aumenta con el aumento de la velocidad de barrido hasta alcanzar un valor de 1 a velocidades suficientemente altas.

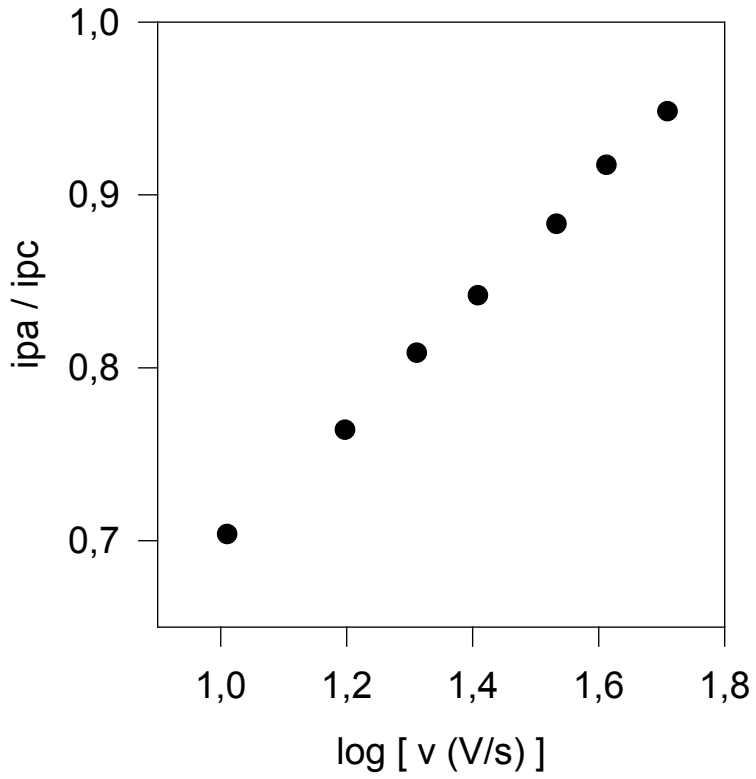

Fig. 17. Dependencia de las razones de corriente de los Voltamperogramas Cíclicos de la formación del radical libre de 2NMZ. Cº=1mM, Medio mixto, pH = 7.96.

El resultado encontrado implica que la reducción monoelectrónica del 2NMZ no corresponde a un proceso reversible ya que no se obtiene una razón de corriente igual a 1, a todas las velocidades analizadas. Por el contrario, en este caso, los resultados

encontrados implican que el anión radical nitro producido en el barrido catódico de ida no se oxida en un 100 % en el barrido anódico de vuelta, generando valores de razones de corriente diferentes de 1. La explicación se debe a que el anión radical nitro lleva a cabo una reacción química que consume al radical, impidiendo que éste se oxide en forma cuantitativa en el barrido de vuelta. En el caso de aniones radicales nitro en medios acuosos mixtos se ha descrito que esta reacción química es una disproporcionación (48). En consecuencia, el proceso que mejor representaría a la onda de aspecto reversible que aparece en los voltamperogramas obtenidos en medio acuoso mixto sería una primera etapa de transferencia de carga reversible seguida por una reacción de disproporcionación de acuerdo al siguiente esquema:

$$RNO_2 + e^- \leftrightarrows RNO_2^{\bullet -} \quad (1)$$

$$2\ RNO_2^{\bullet -} + 2\ H^+ \rightarrow RNO_2 + RNO + H_2O \quad (19)$$

Considerando que la reacción de disproporcionación es la vía de descomposición del radical en este medio es posible aplicar el procedimiento descrito por Olmstead y Nicholson (46), quien desarrolló una teoría la cual permite a partir de los voltamperogramas cíclicos obtener la constante cinética de segundo orden, $k_{2,disp}$, para la reacción química de disproporcionación.

A partir de los valores de razones de corrientes medidos experimentalmente desde los voltamperogramas cíclicos a distintas velocidades de barrido, es posible interpolar el valor del log ω desde las curvas teóricas descritas por Olmstead y Nicholson (46), ya que estas curvas relacionan las razones de corriente con el log ω. Este parámetro ω, se conoce como el parámetro cinético, se define para el caso de la disproporcionación como:

$$\omega = k_{2,disp}\, C^o\, \tau \quad (20)$$

donde $k_{2,disp}$ es la constante cinética para la reacción de disproporcionación, C^o es la concentración de 2NMZ en el seno de la disolución y τ es la constante de tiempo definida como :

$$\tau = | E_{ps} - E_{1/2} | / \upsilon \quad (21)$$

donde υ es la velocidad de barrido de potencial, E_{ps} representa el potencial de cambio (Potencial de Switching) y $E_{1/2}$ el potencial de media onda.

De acuerdo a la Ec. 20 existiría una relación lineal entre el parámetro cinético ω, obtenido interpolando en las curvas teóricas los valores experimentales de $i_{p,a}/i_{p,c}$, y la constante de tiempo τ, parámetro conocido de las condiciones experimentales aplicadas. En efecto, de acuerdo a lo que se aprecia en la siguiente Figura 18 la relación entre dichas variables es lineal.

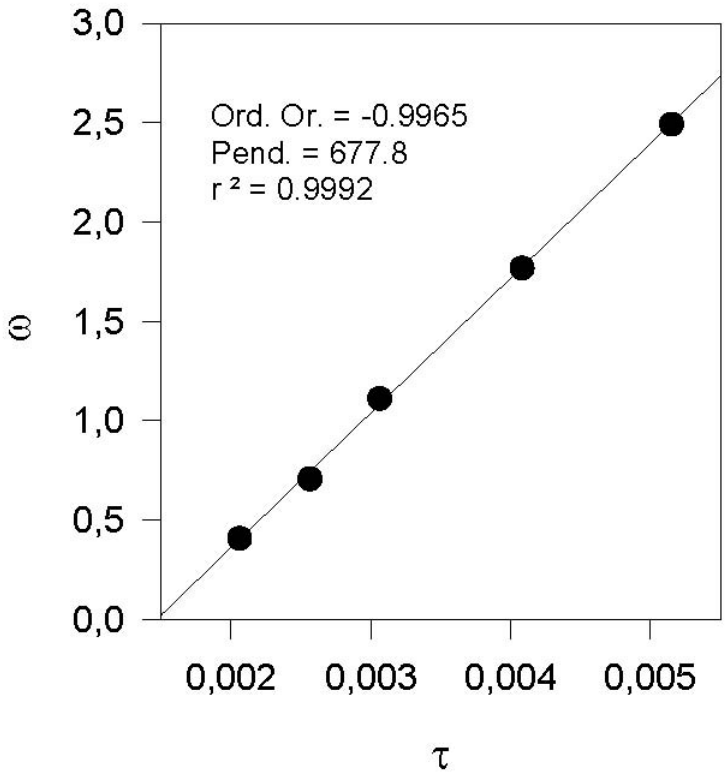

Fig. 18. Dependencia de ω versus τ para la disproporcionación de 2MNZ. C^o=1mM, Medio mixto, pH = 7.96.

Esta relación lineal entre ω y τ, es indicativa de que, efectivamente, la reacción química se ajusta bien al proceso propuesto inicialmente, quedando confirmada que dicha reacción corresponde a una disproporcionación del radical. Además, del valor de la pendiente de la recta se obtiene el valor de la constante $k_{2,disp}$. Para 2NMZ y considerando una concentración de 1 mM se obtiene una $k_{2,disp} = 677.8 \times 10^{3}\ M^{-1}\ s^{-1}$ para la disproporcionación del anión radical nitro del 2NMZ a un pH = 7.96 en el medio mixto acuoso estudiado. Considerando una reacción de segundo orden corresponde a un tiempo de vida media, $t_{1/2}$, para el anión radical nitro de 1.47 ms.

3.2.- 5-Nitroimidazoles

3.2.a Medio no acuoso

El estudio de los derivados 5-nitroimidazólicos se realizó sobre los compuestos 1-metil-5-nitroimidazol (M-NIm) y los derivados iodados: 1-metil-4-iodo-5-nitroimidazol (M-I-NIm) y 1-metil-2-iodo-4-iodo-5-nitroimidazol (M-I_2-NIm).

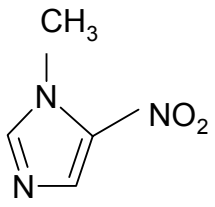

(M-NIm)

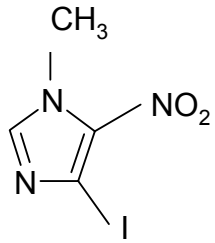

(M-I-NIm)

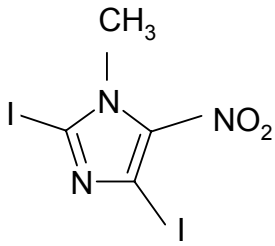

(M-I_2-NIm)

Se procede al estudio del comportamiento de los derivados 5-nitroimidazólicos en medio no acuoso, para ello se ha utilizado DMF (dimetilformamida) como disolvente y 0.1 M TBAP (Perclorato de tetrabutilamonio) como electrolito soporte.

En los voltamperogramas obtenidos, para las diferentes velocidades de barrido

de potencial, se registró la aparición de un pico catódico en el sentido del barrido catódico y su correspondiente pico anódico en el barrido anódico que corresponde a una onda aparentemente reversible que corresponde a la transferencia monoelectrónica del grupo nitro para generar el correspondiente anión radical nitro de acuerdo a la ecuación:

$$RNO_2 + e^- \leftrightarrows RNO_2^{\bullet -} \quad (1)$$

A objeto de ver el comportamiento de las respuestas voltamperométricas a diferentes escalas de tiempo del experimento, se realizaron medidas en las que se fue cambiando la velocidad de barrido del potencial. En todas las medidas, los Voltamperogramas para los derivados M-NIm y M-I-NIm resultaron ser equivalentes como se aprecia en la Figura 19.

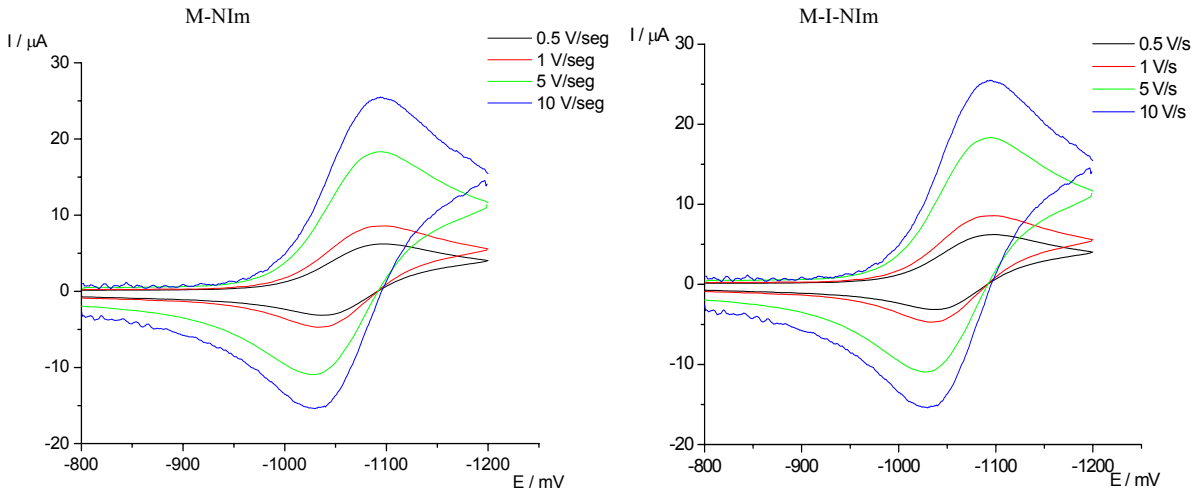

Fig. 19. Par redox RNO_2/ RNO_2^{-} a distintas velocidades de barrido para 1mM de M-NIm y M-I-MIm en DMF.

En el caso del compuesto di-iodado el comportamiento fue algo distinto ya que se apreció un pre-pico el que desapareció con el agregado de una base como NaOH

alcohólica (Figura 20). Este efecto fue interpretado en una primera etapa como

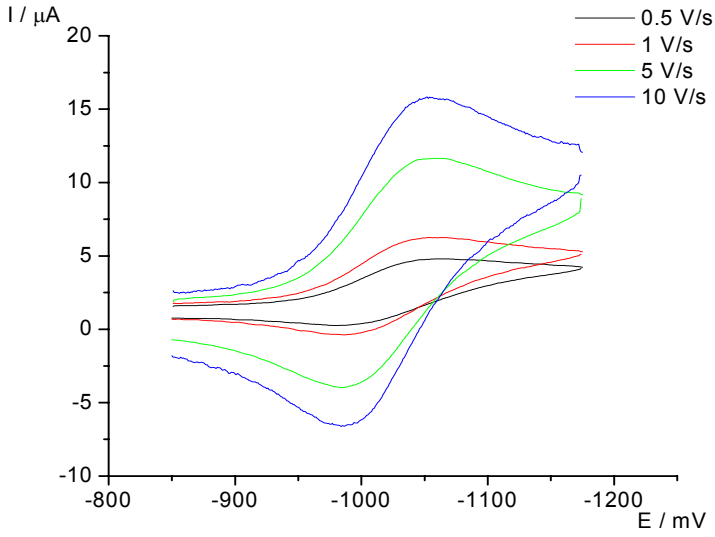

Fig. 20. Par redox RNO_2/ $RNO_2^{\cdot-}$ con y sin NaOH para 1mM de M-I_2-MIm en DMF.

debido a la existencia de un equilibrio ácido-base como el que se observó con el 2-nitroimidazol, sin embargo, esta conjetura fue descartada ya que no se observó la reversión del efecto cuando se agregó un ácido. En consecuencia, para el caso del compuesto di-iodado, se puede trabajar con la cupla completamente aislada sólo en presencia de la base. En la figura 21 se observa los voltamogramas cíclicos obtenidos usando NaOH para obtener una cupla sin pre-pico.

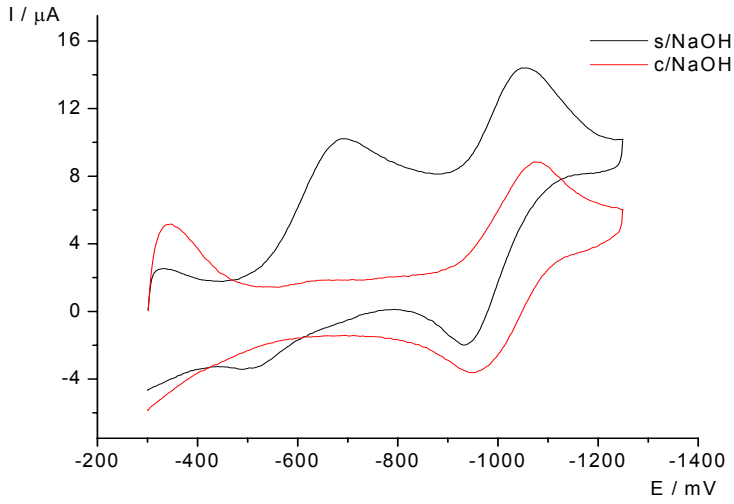

Fig. 21. Par redox RNO_2/ $RNO_2^{\cdot-}$ a distintas velocidades de barrido para 1mM de M-I_2-MIm en DMF con NaOH agregado.

A partir de las razones de corrientes calculadas para cada una de los cuplas y usando un procedimiento idéntico al especificado para el caso del derivado 2-nitroimidazol, tratado anteriormente, fue posible calcular la constante de estabilidad de segundo orden (dimerización) para el anión radical nitro del compuesto M-NIm y los correspondientes derivados iodados.

Compuesto	**E_{pc} (mV)**	**k_2 ($M^{-1}s^{-1}$)**	**$t_{1/2}$ (s)**
M-NIm	-1101	5.81×10^{2}	1.71
M-I-NIm	-1071	1.32×10^{4}	0.075
M-I_2-NIm	-1056	1.10×10^{5}	0.018

Tabla 1.- Valores de potenciales de pico catódico, (E_{pc}), para la reducción de los derivados 5-nitroimidazólicos y constantes de decaimiento y tiempos de vida media para el correspondiente anión radical nitro en medio aprótico .

En la tabla 1 se recoge los valores obtenidos tanto para la reducción de los derivados 5-nitroimidazólicos así como los parámetros que dan cuenta de la estabilidad del anión radical nitro generado. Si se compara los valores de E_{PC} se puede concluir que la presencia de los sustituyentes I en la molécula produce compuestos más fácilmente reducibles. Este efecto puede ser explicado por el carácter electro-atractor de electrones del sustituyente I, lo que provoca una disminución de la densidad electrónica en el anillo facilitando la reducción del grupo 5-nitro. Por otra parte la sustitución con I produce una considerable disminución en la estabilidad del anión radical nitro, lo que nos indica que el carácter electronegativo de los sustituyentes favorece la reactividad del radical libre. Probablemente los sustituyentes I ejercen su efecto electro-atractor sobre el anión radical disminuyendo su exceso de carga negativa facilitando la dimerización.

3.2.b Medio acuoso

El estudio en medio acuoso se realizó en buffer Britton-Robinson 0.1 M + 0.3 M KCl /EtOH : 70/30. Todos los compuestos 5-nitroimidazólicos fueron reducidos en el electrodo de goteo de mercurio (EGM) con señales que fueron dependientes del número de sustituyentes I en la molécula. En la figura 22 se puede observar los polarogramas de pulso diferencial (PPD) a 4 diferentes pH para cada uno de los 5-nitroimidazoles estudiados.

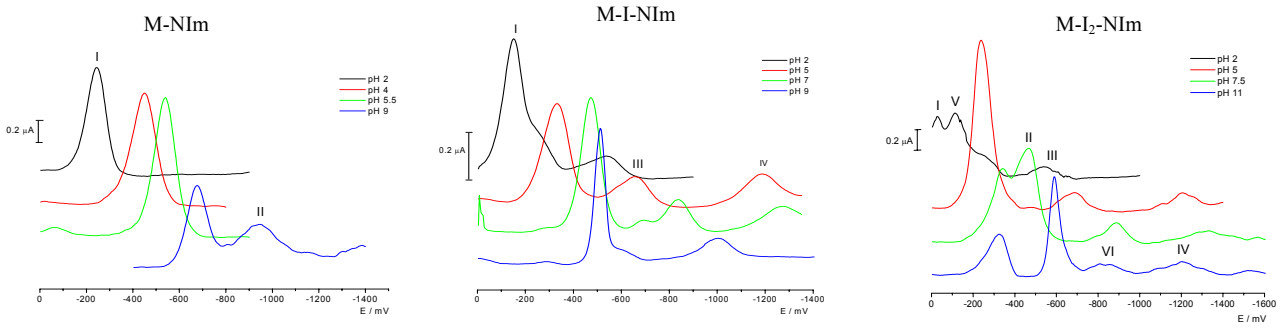

Fig. 22. Polarogramas de pulso diferencial para 0.1 mM de los derivados 5-nitroimidazólicos en buffer Britton-Robinson 0.1 M + 0.3 M KCl /EtOH : 70/30, a diferentes pH.

De acuerdo a estos polarogramas se aprecia una directa relación entre el número de los sustituyentes I y la complejidad de la respuesta observada. En el caso de los compuestos iodados los polarogramas están alterados por señales que corresponden a señales de adsorción como se comprobó en los polarogramas Tast (figuras no mostradas). En el caso del derivado M-NIm muestra una señal de reducción entre pHs 2 y 7.5 y dos señales sobre pH 8. Este mismo comportamiento fue previamente observado para el 4-nitroimidazol en medio acuoso [45], en donde la primera señal (I) corresponde a la reducción via 4-electrones y 4-protones como la anterior ecuación (17). El número de electrones transferidos fue corroborado por análisis culométrico donde se obtuvo un n = 4.02 ± 0.07. A pH superiores a 8 se produce la división de la onda (I) en las ondas (I) y

(II). Este comportamiento polarográfico para el M-NIm fue también corroborado y profundizado por voltamperometría cíclica. En la figura 23 se observa los voltamperogramas cíclicos para el derivado M-NIm a pH ácido y básico.

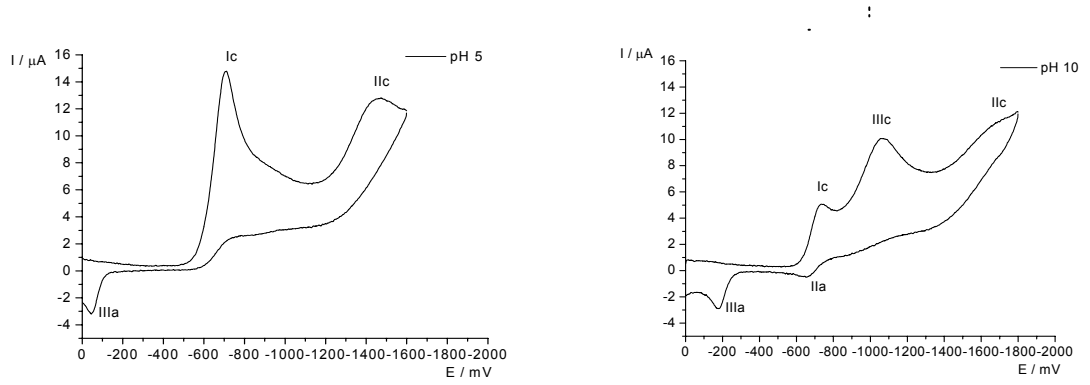

Fig. 23. Voltamperograma cíclica para 1 mM de M-NIm en buffer Britton-Robinson 0.1 M + 0.3 M KCl /EtOH : 70/30, a diferentes pH, 5 V/s.

A pH 5 se aprecian dos picos de reducción, el pico I_c que aparece con un E_p = – 0.71 V corresponde a la reducción via 4-electrones y 4-protones como la anterior ecuación (17) y el pico II_c que aparece con un E_p = - 1450 mV corresponde a la reducción del C=N del anillo imidazólico. En el barrido de vuelta no aparece ningún pico de oxidación indicando que ambos picos son irreversibles. En una zona de pH básico, pH = 10, el comportamiento es marcadamente diferente con la aparición de tres picos catódicos y dos picos anódicos. El pico catódico, I_c, que aparece a – 730 mV y el correspondiente pico anódico, II_a , que aparece a -670 mV, se debe a la cupla RNO_2/ RNO_2.-. El pico irreversible, IIIc, que aparece a – 1080 mV corresponde a la reducción a 3 e- y 4 H+ como se describe en la ecuación (18). El pico II_c que aparece con un E_p = -700 mV corresponde a la reducción del C=N del anillo imidazólico. El pico III_a anódico que aparece con un E_p = -190 mV corresponde a la oxidación del derivado hidroxilamínico generado en el barrido de ida de acuerdo a la ecuación:

$$RNHOH \rightarrow RNO + 2e^- + 2H^+ \quad (22)$$

En el caso de los derivados iodados se concluyó que en medio acuoso y en el electrodo de mercurio producían señales debidas a fenómenos de adsorción debido a alguna interacción del I de los derivados iodados con el Hg.

Como se puede apreciar del anterior resultado, la cupla que da cuenta del par redox RNO_2/ $RNO_2^{\cdot -}$ se manifiesta nítidamente a pH básico, lo que permite mediante una selección adecuada de los parámetros de potencial inicial y potencial de switching trabajar con dicha cupla en forma aislada. En el caso de los derivados iodados no se aprecia este comportamiento lo que implica que el radical de esos derivados no es estable en este medio. En la Figura 23 se puede apreciar el voltamperograma aislado para la cupla RNO_2/ $RNO_2^{\cdot -}$ la que se caracteriza de acuerdo a sus razones de corriente i_{pa}/i_{pc}.

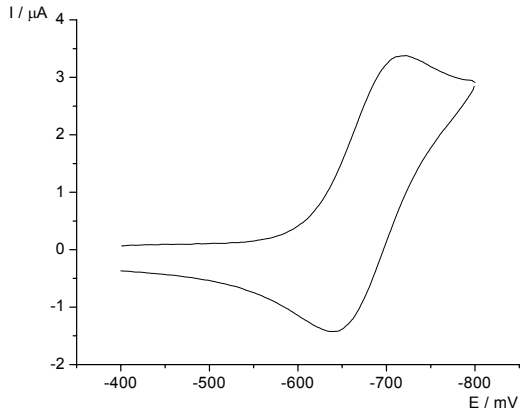

Fig. 23. Voltamperograma cíclico para 1 mM de M-NIm en buffer Britton-Robinson 0.1 M + 0.3 M KCl /EtOH : 70/30, pH = 10, 7 V/s.

A partir del aislamiento de la señal del par redox para el M-NIm, se realizaron estudios utilizando la aproximación de Nicholson para obtener los valores de Ipa/Ipc y evaluar su comportamiento con las velocidades de barrido. Se observó que a velocidades de barrido bajas la razón de corrientes presenta valores cercanos a 0.75 el cual aumenta a velocidades más altas, indicando que existe una reacción química acoplada a la etapa

electroquímica. También se analizó el comportamiento del potencial con la velocidad, observándose que el potencial de pico catódico es independiente de la velocidad de barrido, confirmándose que la reducción monoelectrónica del grupo nitro es reversible.

Usando el mismo procedimiento descrito en detalle para el caso del 2-nitroimidazol se obtuvo las constantes de estabilidad y tiempos de vida media para el derivado anión radical nitro del compuesto M-NIm a 3 pH distintos en medio básico. Estos resultados se recogen en la Tabla 2.

M-NIm	**k_2 ($M^{-1}s^{-1}$)**	**$t_{1/2}$ (s)***
pH 10	4.64×10^3	0.25
pH 11	2.18×10^3	0.45
pH 12	1.33×10^3	0.75

Tabla 2.- Valores de constantes de decaimiento y tiempos de vida media para el correspondiente anión radical nitro en medio acuoso básico, para la reducción del derivado M-NIm. * calculados a 1mM

La Figura 24 muestra la correlación que existe entre k_2 y el pH del medio de reacción, concluyendo que el anión radical es más inestable mientras bajo es el pH. Además, la dependencia de k_2 con el pH obedece a la siguiente ecuación de regresión:

$$\text{Log } k_2 = 6.36 - 0.27 \text{ pH } (r = 0.993)$$

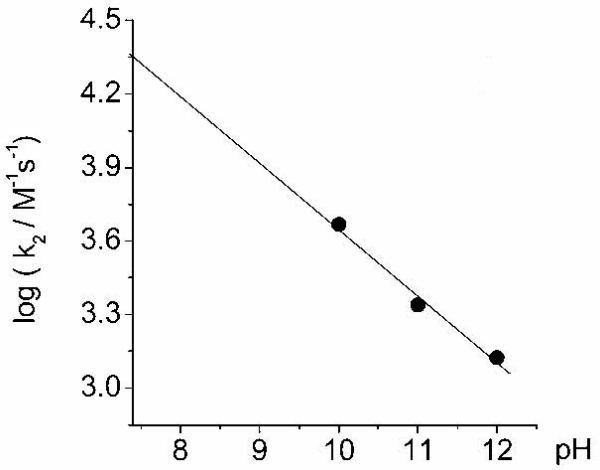

Fig. 24. Dependencia de la constante de decaimiento con el pH para el anión radical nitro de M-NIm.

Por extrapolación de la anterior relación con el pH es posible obtener el valor de k_2 a

diferentes pH. De acuerdo con esto el valor extrapolado para el pH fisiológico de 7.4 es $2.2 \times 10^{-4}\ M^{-1}s^{-1}$.

Como en el caso de los derivados iodados se concluyó que existían fenómenos de adsorción debido a interacciones químicas entre el I y el mercurio se estudió también el comportamiento en medio acuoso sobre electrodo de carbón.

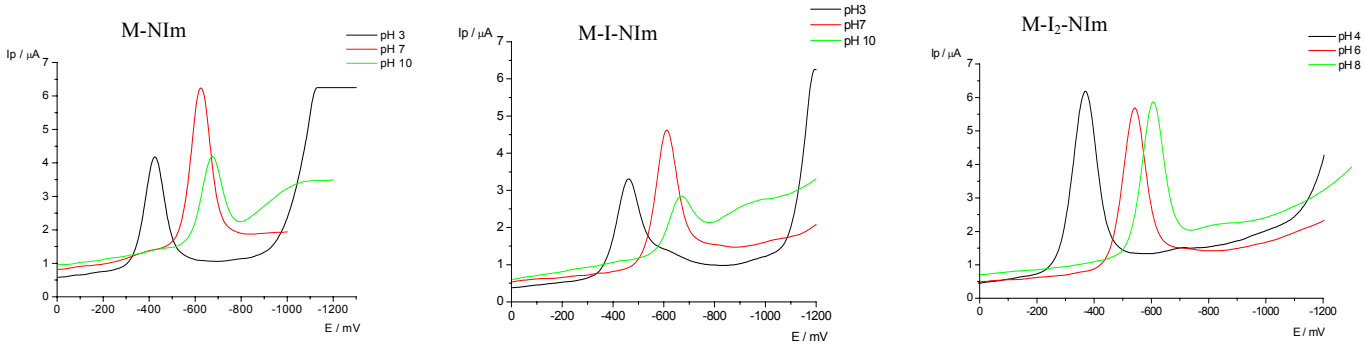

Fig. 25. Voltamperogramas de pulso diferencial sobre electrodo de carbono vítreo para los derivados 5-nitroimidazólicos a diferentes pH.

Como se aprecia en los voltamperogramas sobre electrodo de carbono, los tres compuestos presentaron una sola señal voltamétrica sin presentar fenómenos de adsorción lo que demuestra que estos se deberían a una interacción entre el I y el Hg.

Como se observa en la figura anterior, los potenciales de pico se desplazan a potenciales más negativos a medida que aumenta el pH del medio, es decir, la reducción involucrada necesita de mayor energía para llevarse a cabo en medio básico. Al comparar el potencial de pico de los compuestos a cualquier pH se observa que al igual que sobre mercurio, la substitución con yodo produce una marcada disminución del potencial de pico y por consiguiente una mayor facilidad de reducción, como se observa en la Tabla 3.

Compuesto	Ep (mV)
M-NIm	-752
M-I-NIm	-612
M-I_2-NIm	-572

Tabla 3.- Valores de potenciales de pico a pH 7, 0.1mM derivados 5-nitroimidazólicos, medio mixto.

3.3.- 4-Nitroimidazoles

El estudio de los derivados 4-nitroimidazólicos se realizó sobre los compuestos: 2-carboxialdehído- 4-nitroimidazol (NIm-CHO); 2-hidroximetil-4-nitroimidazol (NIm-OH); 1-metil-2-carboxialdehído- 4-nitroimidazol (M-NIm-CHO); 1-metil-2-hidroximetil- 4-nitroimidazol (M-NIm-OH) ; 1-metil-4-nitro-2-carboxiimidazole (M-NIm-COOH)

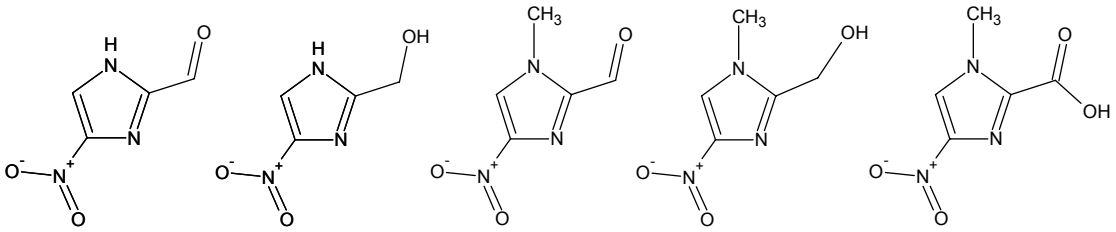

3.3.a. Medio no acuoso

El estudio mediante voltamperometría cíclica de los compuestos NIm-OH y M-NIm-OH en medio DMF con PTBA como soporte, arrojó los resultados que se detallan. Lo primero que se debe destacar es la gran diferencia que se aprecia en sus respuestas voltamperométricas, en donde para el caso del derivado M-NIm-OH muestra una señal correspondiente a un proceso reversible, la cual da cuenta de la reducción del grupo nitro a su anión radical nitro. Esto difiere con lo observado para el compuesto NIm-OH en este mismo medio, donde se ve una señal correspondiente a la reducción del grupo nitro a su anión radical nitro la cual no presenta reversibilidad.

Además, el compuesto NIm-OH presenta una señal cuasi-reversible a potenciales cercanos a -200 mV, lo cual se debería a la oxidación que experimenta el derivado hidroxilamínico formado.

La figura 26 nos muestra los voltamperogramas cíclicos para ambos compuestos a diferentes velocidades de barrido apreciándose que la sustitución en el N-1 afecta notoriamente dicho comportamiento, dónde para el caso del compuesto M-NIm-OH se observa un aumento en la intensidad de las corrientes de pico catódicas y anódicas a medida que se aumenta la velocidad de barrido. Por otra parte el anión radical nitro formado para el compuesto MNIm-OH experimenta un aumento en la intensidad de corriente de pico catódico a medida que aumentamos la velocidad de barrido, no observándose corrientes de pico anódicas, corroborando así la irreversibilidad del proceso de reducción del compuesto MNIm-OH en medio aprótico.

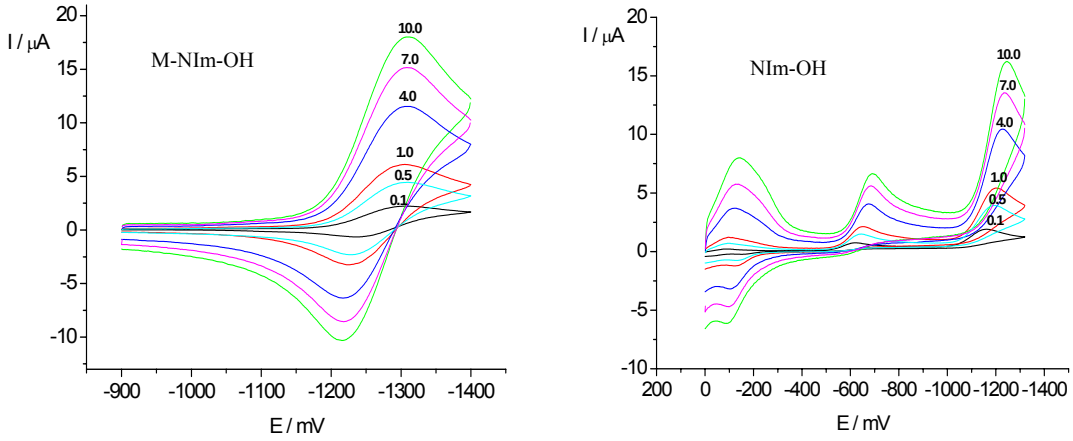

Figura 26.- Voltamperogramas cíclicos realizados a distintas velocidades de barrido (0.1; 0.5; 1.0; 4.0; 7.0; 10.0V/s) para los compuestos M-MNIm-OH y MNIm-OH en medio DMF.

Ahora bien, el comportamiento observado para el M-NIm-OH en medio aprótico es similar al observado por Vianello [44] para el 4-nitroimidazol en DMF. En

consecuencia los resultados muestran que no es posible aislar el par redox $RNO_2/RNO_2^{\cdot-}$ en DMF debido a una rápida reacción de autoprotonación que involucra la participación del NIm-OH inicial en lo que se denomina una reacción de tipo padre-hijo.

Para el caso del derivado M-NIm-OH se procedió a calcular la estabilidad del anión radical nitro de acuerdo al procedimiento mencionado anteriormente en esta tesis. Se procedió a utilizar el método propuesto por Olmstead para el cálculo de las razones de corriente, Ipa/Ipc, cuyo comportamiento a diferentes velocidades de barrido se aprecia en la Figura 27.

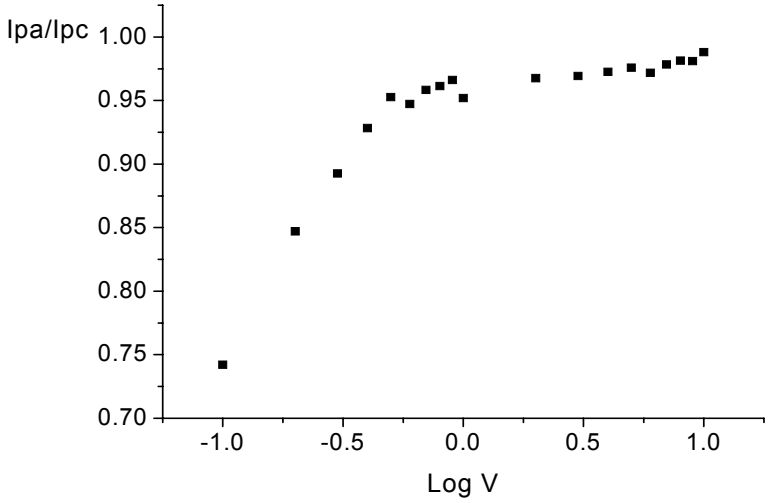

Figura 27.- Gráfico de la razón de corrientes (Ipa/Ipc) versus el logaritmo de la velocidad de barrido para M-MNIm-OH a una concentración 1mM. En medio aprotico.

Es importante señalar que a diferencia de los medios acuosos o mixtos donde el anión radical nitro formado sufre reacciones de decaimiento químico debido a la disponibilidad de protones en el medio, en este caso se plantea la dimerización como la reacción más probable, debido a la no disponibilidad de estos en el medio.

Considerando un procedimiento análogo al dado en la sección 3.1.b, podemos obtener para la reacción química de tipo dimerización [45], se puede calcular el valor de la constante $k_{2\ dim}$ desde la pendiente del gráfico Ω vs τ que se muestra a continuación.

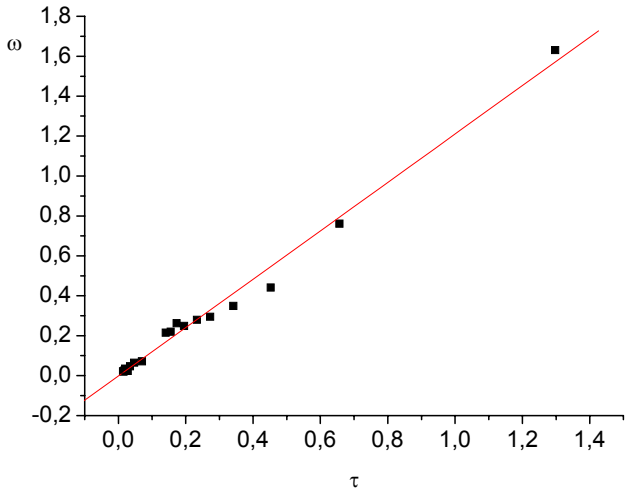

Figura 28.- Gráfico de ω versus τ para 1mM M-NIm-OH en medio no acuoso.

Se obtuvo un valor de k_{dim}= 1.1 × 10^3 $M^{-1}s^{-1}$ y un tiempo de vida medio, $t_{1/2}$ = 0.88 s para una concentración 1mM de M-NIm-OH.

De estos resultados se puede concluir que la sustitución con $–CH_3$ en la posición 1 del anillo nitroimidazólico produce la estabilización del anión radical nitro en medio no acuoso ya que bloquea la ocurrencia de la reacción de autoprotonación ya mencionada.

También se estudió el comportamiento ciclo voltámetrico de los derivados aldehído sustituido en posición 2, NIm-CHO y M-NIm-CHO, en medio DMF con PTBA como soporte.

En el caso del derivado NIm-CHO el comportamiento fue similar al del derivado NIm-OH ya que no fue posible obtener la estabilización de la señal para el anión radical nitro producto de la existencia de la reacción acoplada tipo padre-hijo gatillada por la

existencia del H en N-1. En el voltamperograma que se observa en la Figura 29 se aprecia los dos picos irreversibles originados por la reducción del grupo nitro, en forma análoga a lo observado en el derivado alcohólico. El pico de aparencia cuasi-reversible que aparece con un Epc de aproximadamente -2000 mV corresponde a una señal del blanco.

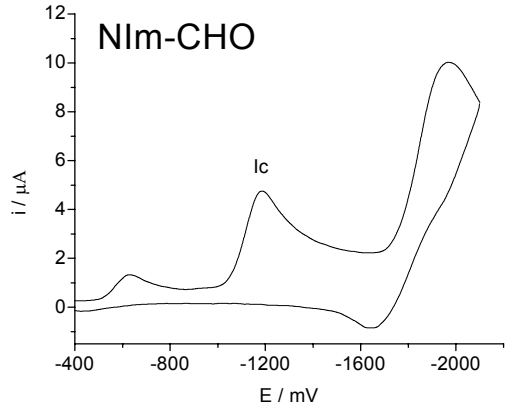

Figura 29.- Voltamperograma cíclico para el compuesto MNIm-CHO en medio DMF. V = 1V=s.

El compuesto M-MNIm-CHO presenta un comportamiento bastante diferente como se puede apreciar en la figura 30. En efecto al reemplazar el H del N imidazólico por el –CH_3 se evita el fenómeno de la reacción tipo padre-hijo y aparece una cupla cuasi-reversible debido a la reacción de reducción mono-electrónica del derivado nitro para producir el anión radical nitro el cual queda estabilizado en este medio.

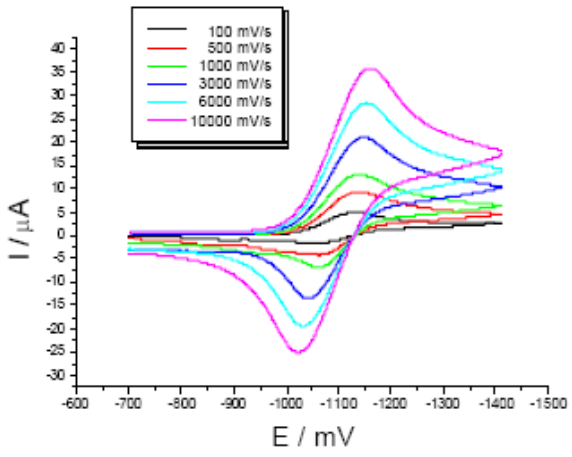

Figure 30.- Voltamperograma cíclico para 1mM de derivado M-NIm-CHO en medio 100 % DMF a distintas velocidades de barrido.

El derivado M-NIm-COOH presenta un comportamiento un tanto distinto a los anteriores compuestos producto del protón ácido que tiene en su estructura. En la figura 31 se muestra el voltamperograma cíclico de una solución que contiene 1 mM de M-NImCOOH en 100% DMSO con 0.1 M TBAP como soporte

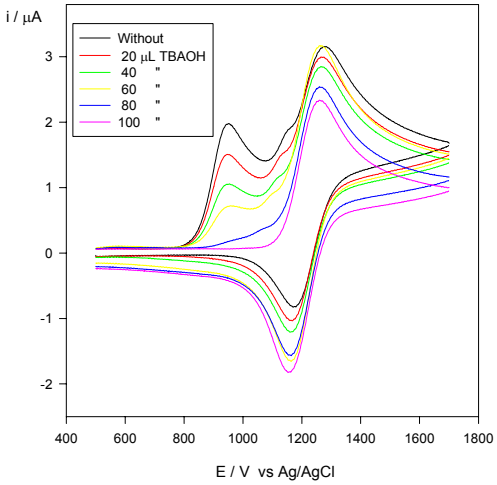

Figure 31.- Voltamperograma cíclico para 1mM de derivado M-NIm-COOH en medio 100 % DMSO sin y con diferentes cantidades agregadas de hidróxido de tetrabutil amonio. v = 1V/s.

En dicho voltamperograma se aprecian dos picos catódicos con potenciales de pico de -970 mV y -1270 mV, aproximadamente. El pico que aparece a potenciales más catódicos tiene un correspondiente pico anódico lo que origina una cupla aparentemente cuasi-reversible. Como se aprecia en la figura el pico que aparece a potenciales menos catódicos desaparece concomitante con el agregado de la base. Este fenómeno se revertió con el agregado de ácido (figura no mostrada). Estos experimentos apoyan la existencia de un equilibrio de disociación entre la especie neutra y la correspondiente base conjugada de acuerdo a:

$$\text{M-NIm-COOH} \quad = \quad \text{M-NIm-COO}^- \quad + \quad \text{H}^+ \quad (23)$$

Además, el mismo efecto se observó cuando se realizaron sucesivos barridos sobre el mismo electrodo (resultados no mostrados). Este hecho implica que el procedimiento de

electrólisis generó una especie (nitro radicales anión) que actúa como una base deprotonando el compuesto padre en una reacción de tipo padre-hijo según el siguiente esquema:

$$RNO_2COOH + e^- \rightarrow (RNO_2)^{\cdot-}COOH \qquad (24)$$

$$(RNO_2)^{\cdot-}COOH + RNO_2COOH \rightarrow RNO_2COO^- + (RNO_2)^{\cdot}COOH \qquad (25)$$

Además, mediante la apropiada selección del potencial de switching, el primer pico se estudió en forma aislada. En la figura 32 se aprecia el voltamperograma cíclico del primer pico de la reducción de N-MNIm-COOH a distintas velocidades de barrido. Se aprecia que el potencial de pico se desplaza hacia valores más catódicos con el aumento de la velocidad de barrido tal como se espera para un pico irreversible. Considerando los resultados anteriores y la información de trabajos previos [44] se puede concluir que el primer pico debido a la reducción del derivado M-NIm-COOH obedece a la siguiente reacción general:

$$5\ RNO_2COOH + 4e^- \rightarrow 4RNO_2COO^- + RNHOHCOOH + H_2O \qquad (26)$$

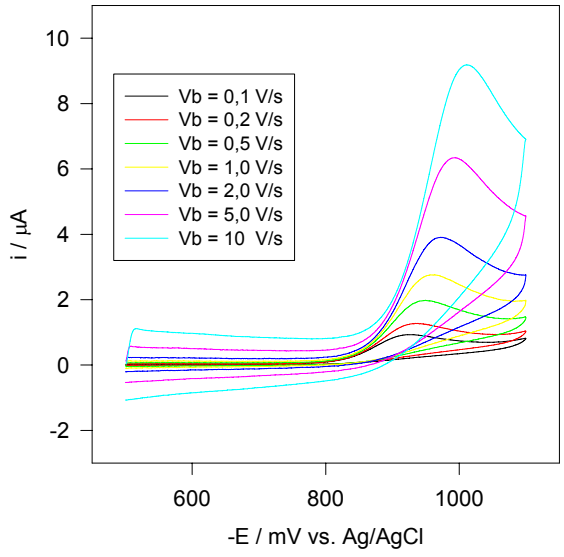

Figure 32.- Voltamperograma cíclico para el primer pico de 1mM de derivado M-NIm-COOH en medio 100 % DMSO a diferentes velocidades de barrido.

Por otra parte, el segundo pico sólo puede ser estudiado en forma aislada después de agregar base (TBAOH) y así eliminar la primera señal. En esta condición la respuesta voltamperométrica fue una cupla de apariencia reversible de acuerdo a la siguiente ecuación:

$$\mathbf{RNO_2COO^- + e^- \rightarrow (RNO_2)^{\cdot-}COO^-} \qquad (27)$$

En la figura 33 se aprecia la respuesta voltamperométrica que se obtiene a diferentes velocidades de barrido. De esta figura se puede apreciar que las separaciones de los picos anódicos y catódicos (ΔE_P) son más grandes que la esperada para un proceso reversible mono-electrónico (60 mV), ajustándose mejor a un proceso cuasi-reversible.

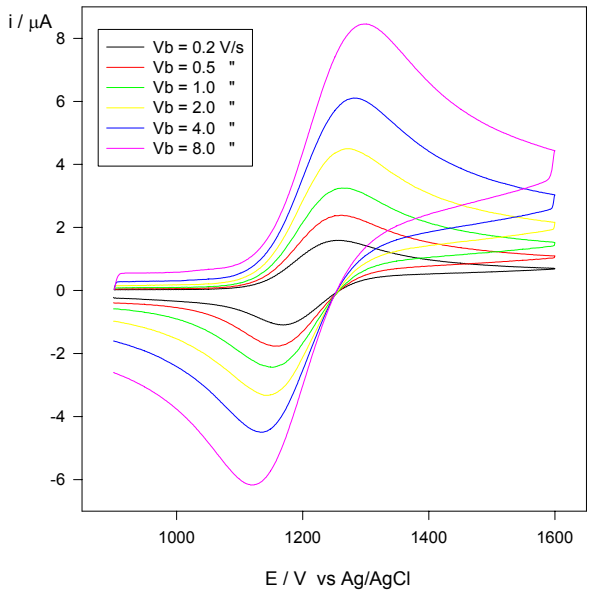

Figura 32.- Voltamperograma cíclico para la cupla cuasi-reversible de 1mM de derivado M-NIm-COOH en medio 100 % DMSO con TBOH agregado, a diferentes velocidades de barrido.

Desde estas condiciones de cuasi-reversibilidad, usando el método descrito por Nicholson [50] es posible estudiar la cinética de la reacción electródica y calcular la constante de velocidad heterogénea, k^0, para la reacción descrita en la ecuación 27. Los

valores de ΔE_p medidos desde los voltamperogramas son introducidos en la curva de trabajo descrita por Nicholson [50] para obtener el parámetro de transferencia ψ, desde el cual es posible obtener k^0 de acuerdo al procedimiento detallado en un trabajo previo [51]. Desde los valores obtenidos de los voltamperogramas de la figura 32 se obtuvo una $k^0 = 9.74\times10^{-3}$cm s^{-1}.

3.3.b Medio Acuoso

Los experimentos realizados por las técnicas de polarografía de pulso diferencial (PPD) y polarografía Tast arrojaron para ambos compuestos, NIm-OH y M-NIm-OH a pHs ácidos (Figura 33 se muestra sólo los resultados para M-NIm-OH) una señal inicial (I) bien definida. A medida que aumenta el pH de la solución, esta señal se desplaza a valores de potencial más negativos, junto con observarse a pHs básicos una segunda señal (II) la cual no se desplaza con el pH. Finalmente sobre pH 8.5 se advierte la formación de una tercera señal (III).

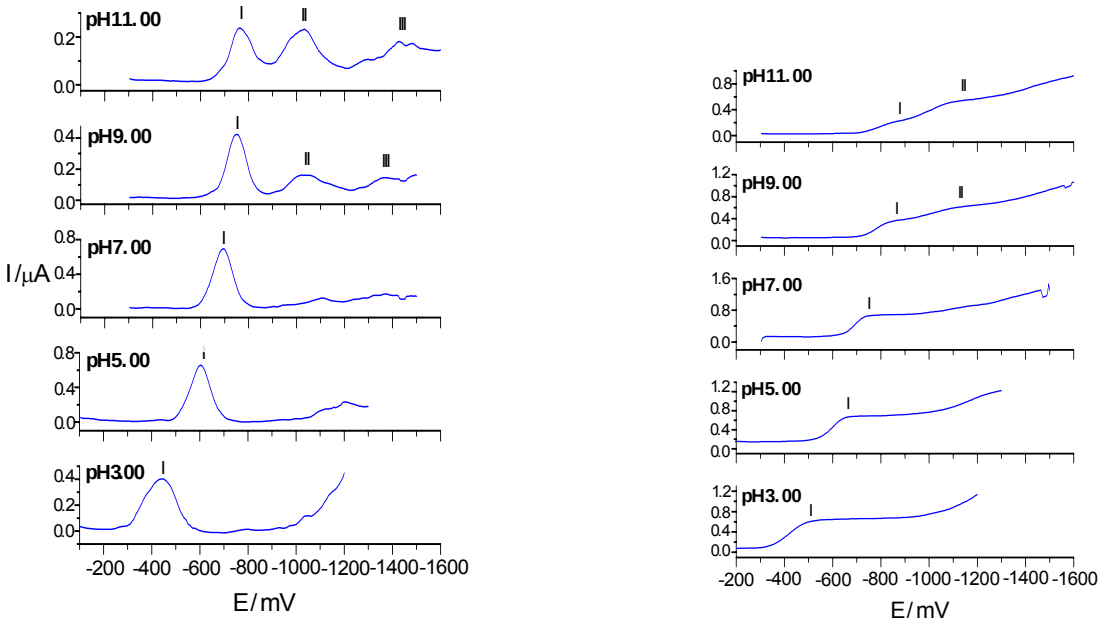

Figura 33.- Polarogramas de pulso diferencial (izquierda) y Tast (derecha) para la reducción de 0,1 mM de M-NIm-OH en 0,1 M EtOH/Britton Robinson (30/70).

En la Figura 34 se observa el comportamiento del potencial de pico de cada señal con respecto al pH para ambos compuestos, NIm-OH y M-NIm-OH. Para ambos casos la señal principal, la señal I, se observa en todo el rango de pH estudiado. Esta señal corresponde a la reducción del grupo nitro al correspondiente derivado hidroxilamínico de acuerdo a la siguiente ecuación:

$$RNO_2 + 4H^+ + 4e^- \rightarrow RNHOH + H_2O \qquad (28)$$

En la línea que marca el comportamiento del potencial de pico con el pH para la señal I se observan dos quiebres de tendencia, a pHs de aproximadamente 4 y 8,5, lo que podría indicar la existencia de dos pKa polarográficos a pHs cercanos a dichos valores, lo que se corroborará más adelante mediante espectrofotometría UV-Vis.

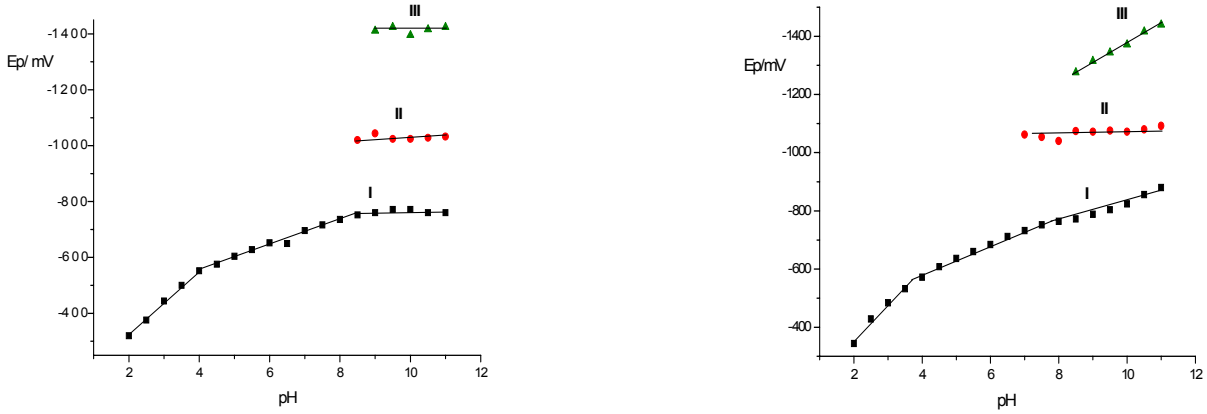

Figura 34.- Variación del potencial de pico (Ep) en función del pH a una concentración de 0,1mM para el M-NIn-OH (izquierda) y el NIm-OH (derecha). En medio EtOH/Britton Robinson (30/70) 0,1M.

En relación a los picos II y III que aparecen en los polarogramas se esperará el análisis por voltamperometría cíclica para realizar su asignación. Del anterior comportamiento con el pH podemos extraer los valores de potenciales de pico que reflejan el grado de dificultad de la reducción del grupo nitro en los dos compuestos y diferentes pHs. En la Tabla 4 se aprecia los valores de los potenciales de pico para

ambos compuestos en condiciones ácida, neutra y básica.

COMPUESTO	E_P / V (pH = 3)	E_P / V (pH = 7)	E_P / V (pH = 11)
M-NIm-OH	-0,45	-0,70	-0,76
NIm-OH	-0,48	-0,74	-0,88

Tabla 4.- Potenciales de pico catódicos para la reducción polarográfica de los derivados 4-nitroimidazólicos en distintas condiciones de acidez del medio EtOH/britton Robinson (30/70).

De acuerdo a los resultados mostrados en la Tabla 4 se puede concluir que para ambos compuestos la reducción del grupo nitro ocurre más fácil a pH ácidos, lo que estaría de acuerdo con el mecanismo de la ecuación 28. Por otra parte, al comparar los potenciales de pico (Ep) obtenidos para ambos nitrocompuestos a pHs 3, 7 y 11, se observa que el compuesto M-NIm-OH presenta menores potenciales de reducción que el compuesto NIm-OH, lo que explica por la presencia del substituyente metil en la posición 1 del anillo imidazólico, el cual produciría un bloqueo estérico parcial entre los electrones no enlazantes del N1 del anillo imidazólico, provocando que estos electrones no contribuyan al sistema π del anillo, disminuyendo así la densidad de electrones sobre el grupo nitro y por ende facilitando su reducción.

Con el objeto de explicar los quiebres que se aprecian en la línea que describe el comportamiento E_P-pH de la señal principal se procedió a estudiar el comportamiento espectroscópico a distintos grados de acidez del medio. El estudio espectrofotómetrico del compuesto M-NIm-OH mostró como resultado espectros de absorción dependientes del pH de la solución, observándose dos bandas de absorción a 245nm (I) y 304nm (II). La primera banda de absorción (I) muestra una absorbancia mínima a pH 6,0 donde posteriormente comienza a aumentar hasta llegar a un máximo a pH 12,0. Por otro parte el segundo máximo de absorción (II) presenta una absorbancia mínima a pH 2,5, punto en el cual comienza a aumentar hasta llegar a un máximo a pH 8,0, donde

posteriormente se mantiene en niveles de absorbancia constantes (Figura 35).

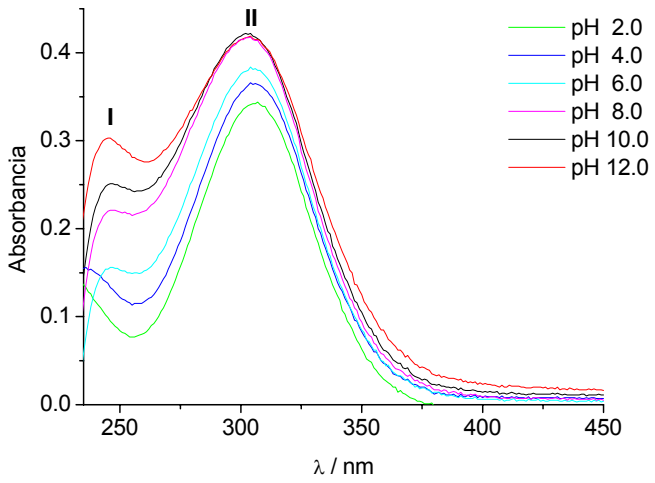

Figura 35.- Espectro UV-visible del compuesto M-NIm-OH a una concentración de $5x10^{-5}$M en medio Britton Robinson 0,1M , a diferentes pH.

En el caso del compuesto demetilado en la posición N-1, NIm-OH, el espectro de absorción arrojó 3 bandas de absorción a 224, 298 y 352 nm . Esta última es dependiente del pH y permitió determinar un valor de pKa aparente que fue igual a 9,2 ± 0.1 (Fig. 36). Este pKa se debería a la desprotonación del N en posición 1, que en el otro compuesto esta sustituido, por lo que no presenta este equilibrio. Por otra parte la banda a las longitudes de onda más bajas (220- 240 nm) se debería al protón del N en posición 3 del anillo imidazólico que origina un pKa de aproximadamente 5.

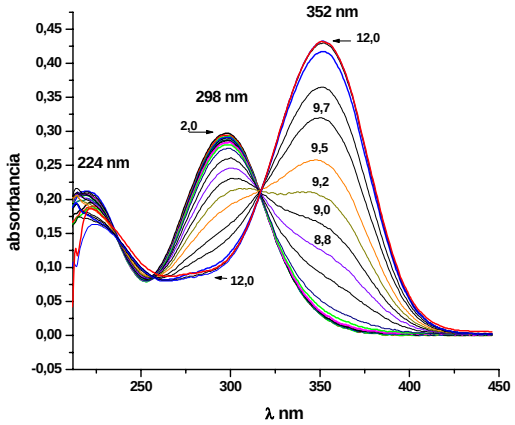

Figura 35.- Espectro UV-visible del compuesto NIm-OH a una concentración de $5x10^{-5}$M en medio Britton Robinson 0,1M , a diferentes pH.

Comparando estos valores de pK con los valores de pKa polarográficos se encuentra una adecuada correspondencia indicando que los quiebres en el gráfico Ep-pH se deben a cambios en el mecanismo electródico como consecuencia de la presencia de distintas especies. En los siguientes esquemas se muestran las distintas especies y los correspondientes equilibrios que originan los pKa:

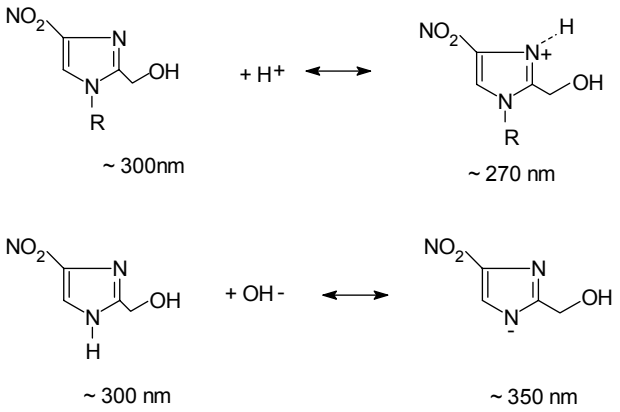

La Figura 36 resume el comportamiento ciclo voltamperométrico de los derivados M-NIm-OH y NIm-OH a diferentes pHs y a una velocidad de barrido de 1V/seg. Observándose que la señal correspondiente a la reducción del grupo nitro a su derivado hidroxilamínico tiende a desplazarse a valores de potencial más negativos a medida que se aumenta el pH y que existe un desdoblamiento de esta señal principal en la zona de pHs básicos.

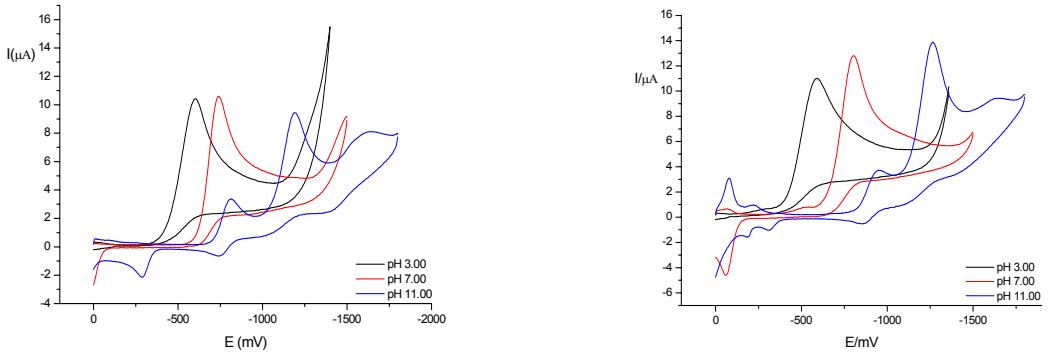

Figura 36.- Voltamperogramas cíclicos realizados a pH 3 , 7 y 11 , a una velocidad de barrido de 1 V/s para los compuestos M-NIm-OH (izquierda) y NIm-OH (derecha) a una concentración 1 mM, en medio EtOH/Britton Robinson (30/70) 0,1 M.

Como se puede apreciar, los picos catódicos que aparecen en los voltamperogramas coinciden con los picos (I, II, III) de los polarogramas de pulso diferencial vistos anteriormente. No obstante lo anterior desde los voltamperogramas se puede apreciar claramente como a pH básicos ocurre el desdoblamiento del pico principal generando una cupla reversible y un pico irreversible que estaría de acuerdo con un mecanismo descrito por las anteriores ecuaciones (1) y (18). Esto significa que en medio básico es posible estabilizar el anión radical observándose claramente la cupla redox $RNO_2/RNO_2^{\cdot -}$ la cual puede ser aislada y estudiada con mayor detalle.

Dado la reversibilidad observada a pHs básicos en los dos compuestos nitroimidazólicos en estudio, se procedió a analizar la formación y estabilidad de los correspondientes aniones radicales nitro a pHs 9, 10, 11.

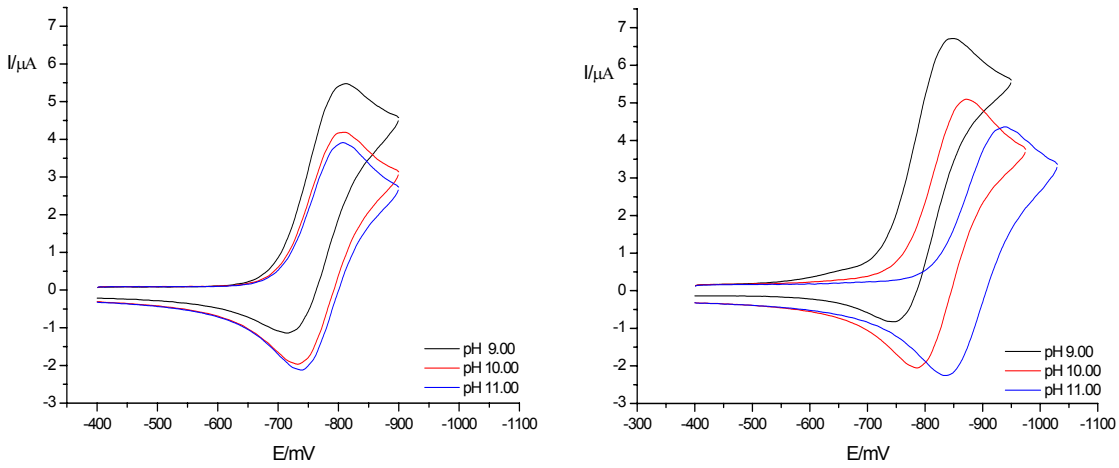

Figura 37.- Voltamperogramas cíclicos del par redox reversible realizados a pH 9 , 10 y 11 , a una velocidad de barrido de 1V/s para los compuestos M-NIm-OH (izquierda) y NIm-OH (derecha) a una concentración 1mM. En medio EtOH/Britton Robinson (30/70) 0,1M.

En la figura 37 se observa como el cambio de pH afecta notoriamente los voltamogramas cíclicos de la cupla $RNO_2/RNO_2^{\cdot -}$, especialmente en lo que se refiere,

primero, al corrimiento de las señales a valores más negativos de potencial (en el caso del NIm-OH**)** y segundo, al cambio de la intensidad de corriente observando un decrecimiento en la corriente de pico catódico (Ipc) y un incremento en la corriente de pico anódica (Ipa) a medida que aumenta el pH. Se observa claramente una diferencia entre el comportamiento de los compuestos metilado y no-metilado en la posición 1 en relación al pH. En el caso del derivado metilado el potencial de pico permanece constante con el pH lo que está de acuerdo con el mecanismo mono-electrónico descrito por la anterior Ec. 1. En el caso del derivado de-metilado se observa un leve desplazamiento del potencial de pico lo que se debe a que en este compuesto la reducción está afectada por el equilibrio que ocurre entre la especie protonada y la no-protonada en el N-1. De hecho el pKa para dicho equilibrio se midió como anteriormente como 9,1. Al cambiar la velocidad de barrido del experimento (Fig. 38) se observa que con el aumento de dicha velocidad se produce el aumento de la intensidad de las corrientes en ambos compuestos estudiados.

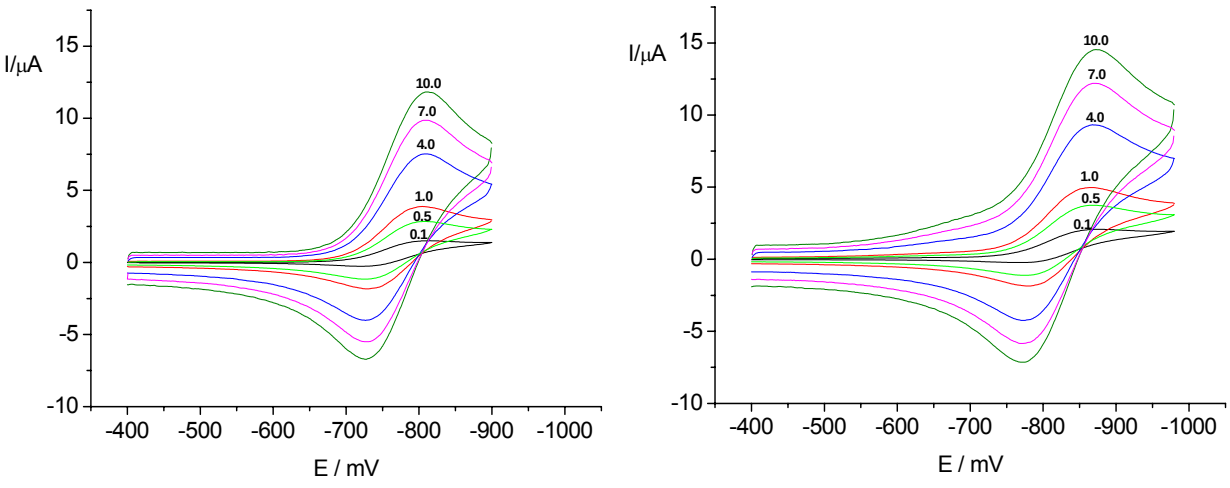

Figura 38.- Voltamperogramas cíclicos a pH 11, a distintas velocidades de barrido (0,1; 0,5; 1,0; 4,0; 7,0; 10,0V/s) para los compuestos M-NIm-OH (izquierda) y NIm-OH (derecha) a una concentración 1mM. En medio EtOH/Britton Robinson (30/70) 0,1M.

Si bien ambas corrientes aumentan sus valores, la razón entre ellas no se mantiene constante (Fig. 39)observándose que los valores de Ipa/Ipc tienden a 1.0 a medida que aumenta la velocidad de barrido.

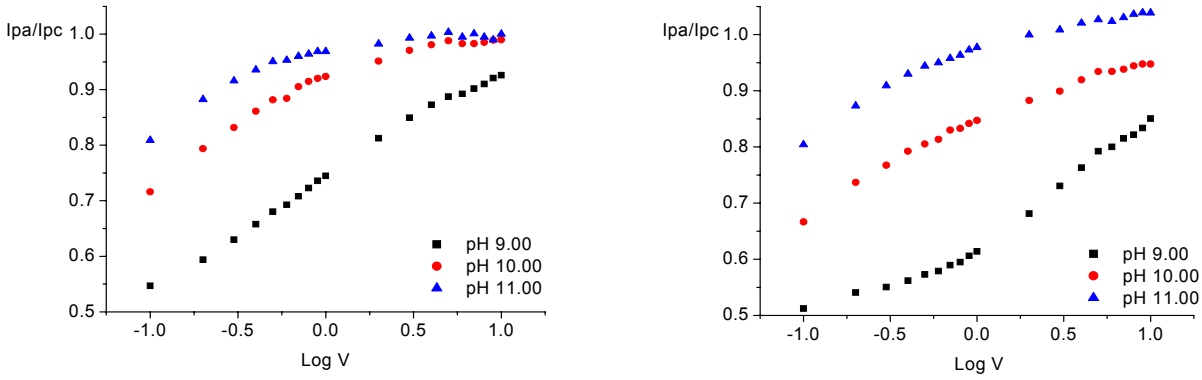

Figura 39.- Gráfico de la razón de corrientes (Ipa/Ipc) versus el logaritmo de la velocidad de barrido (Log V) a pH 9, 10 y 11 , para los compuestos M-NIm-OH (izquierda) y NIm-OH (derecha) a una concentración 1mM. En medio EtOH/Britton Robinson (30/70) 0.1M

De acuerdo a este comportamiento de las razones de corriente se puede afirmar que el proceso involucrado para ambos nitrocompuestos estudiados corresponde a un mecanismo de tipo Eci, es decir, que a la transferencia electrónica se encuentra acoplada a una reacción química la cual corresponde a una dismutación tal cual lo describe la ecuación (19). Posteriormente se procedió a aplicar el procedimiento de acuerdo a lo descrito por Olmstead y Nicholson [46] y que ya fue detallado en el caso de los 2-nitroimidazoles. La linealidad de los gráficos Ω versus τ (resultados no mostrados) confirma el carácter de segundo orden de la reacción química acoplada (dismutación).

En la Tabla 5 se muestran los resultados obtenidos para las constantes de degradación con sus correspondientes tiempos de vida media calculados para una concentración de anión radical nitro de 1 mM.

pH	Compuesto	$k_2 \cdot 10^{-3} / M^{-1}s^{-1}$	$t_{1/2}$ / s
pH 9.00	M-NIm-OH	50.6 ± 14.2	0.019
	NIm-OH	126.3 ± 5.6	0.008
pH 10.00	M-NIm-OH	4.21 ± 0.1	0.237
	NIm-OH	7.23 ± 1.2	0.138
pH 11.00	M-NIm-OH	1.70 ± 0.1	0.588
	NIm-OH	1.98 ± 0.2	0.505

Tabla 5.- Valores de las constantes de decaimiento (k_2) y tiempos de vida media ($t_{1/2}$), para los nitrocompuestos M-NIm-OH y NIm-OH a pH 9, 10 y 11 a una concentración de 1mM. En medio EtOH/Britton Robinson (30/70) 0.1M.

Al analizar los valores obtenidos para las constantes de decaimiento del anión radical nitro en medio acuoso, se observa que el nitrocompuesto M-NIm-OH presenta un menor valor de k_2 que el NIm-OH, indicándonos que el anión radical nitro formado a partir del derivado metilado es más estable. Esto significa que el grupo metilo en la posición 1 estabiliza al anión radical probablemente por la menor densidad electrónica de la nube π debido al efecto estérico del grupo metilo sobre los electrones desapareados del N-1.

El estudio del compuesto NIm-CHO arrojó un comportamiento diferente al de su compuesto análogo revisado arriba. En efecto este derivado nitroimidazólico sólo produce una señal irreversible en todo el rango de pH, sin aparición de un derivado anión radical nitro estabilizado (Figura 40), lo que implica que el cambio del sustituyente en la posición 2, desde $–CH_2OH$ a –CHO, produjo dicha desestabilización. Como se aprecia en la figura 40 la variación del potencial de pico con la velocidad de barrido obedece a una respuesta irreversible la cual se ajusta a una reducción del grupo

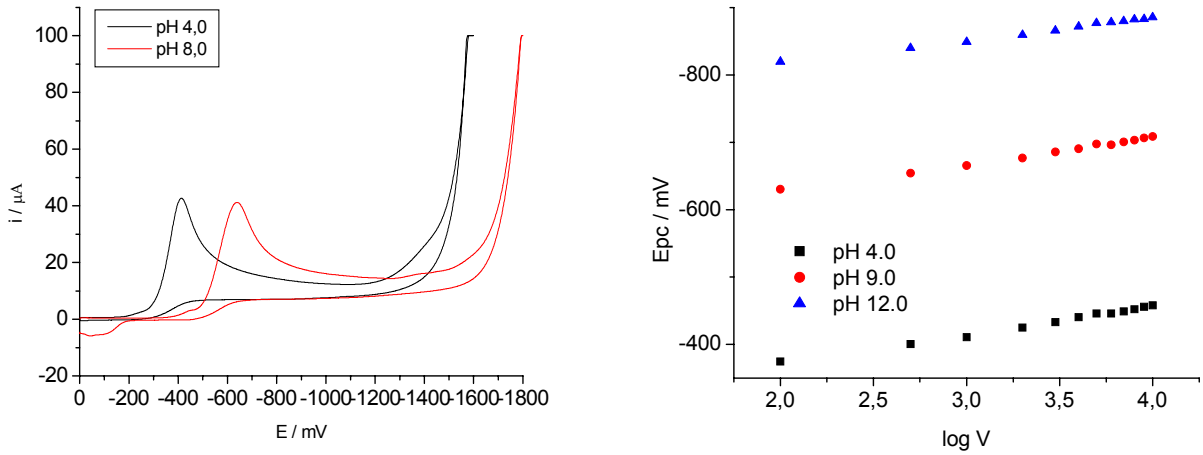

Figura 40.- Voltamperogramas cíclicos para el compuesto NIm-CHO en medio EtOH/Britton Robinson (30/70) 0,1M a dos distintos pHs y gráfico que muestra la variación del Potencial de Pico con la velocidad de barrido a pH 4, 9 y 12 (izquierda) y MNIm-OH (derecha) a una concentración 1mM.

nitro mediante 4-electrones y 4-protones para generar un derivado hidroxilamínico de acuerdo a la anterior ecuación (17).

Para el caso del compuesto metilado, M-NIm-CHO el comportamiento resultó un tanto diferente ya que en este caso aparecen dos picos irreversibles en todo el rango de pH estudiado. En la figura 41 se aprecia un pico catódico irreversible principal Ic que aparece a potenciales de aproximadamente – 0,63 V a pH 3 y que se desplaza a valores más catódicos a medida que el pH aumenta. Este pico corresponde a la reducción del grupo nitro mediante 4-electrones y 4-protones para generar un derivado hidroxilamínico de acuerdo a la anterior ecuación (17), tal como se observó para el derivado NIm-CHO. Además, se aprecia el pico IIc irreversible que aparece a potenciales de aproximadamente -0,80 V a pH 3 y que también se desplaza a potenciales más catódicos a medida que sube el pH. El pico IIc se asignó como debido a la reducción del C=O del sustituyente en posición 2, lo que fue corroborado por comparación con el voltamperograma cíclico correspondiente al 2-carboxialdehido-1-metilimidazol.

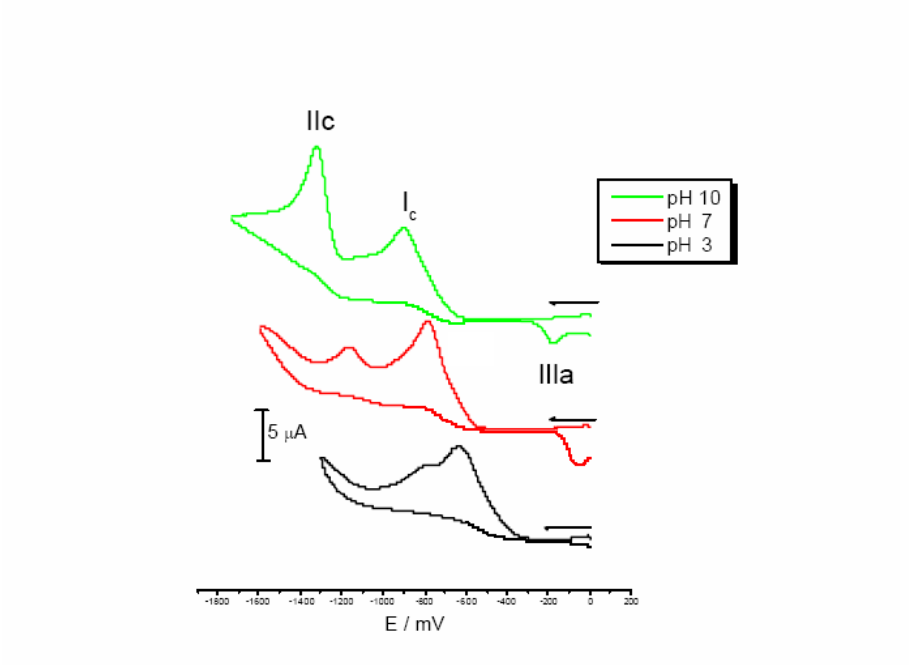

Figura 41.- Voltamperogramas cíclicos para el compuesto M-NIm-CHO en medio EtOH/Britton Robinson (30/70) 0,1M a tres distintos pHs. v = 1 V/s.

Para el caso del derivado M-NIm-COOH es posible trabajar en un medio 100 % Britton-Robinson para lo cual se realizaron polarogramas de pulso diferencial (PPD) y Tast a diferentes pH, desde pH 2 a 11. En los polarogramas se observa una única señal de reducción en todo el rango de pH, tanto en PPD como por Tast (Figura 42) . Las señales obtenidas se desplazan a potenciales más negativos a medida que aumenta el valor de pH. La onda o pico polarográfico obedece a la respuesta debida a la reducción vía 4-electrones, 4-protones del grupo nitro para generar el correspondiente derivado hidroxilamínico como se detalló en la anterior ecuación (17).

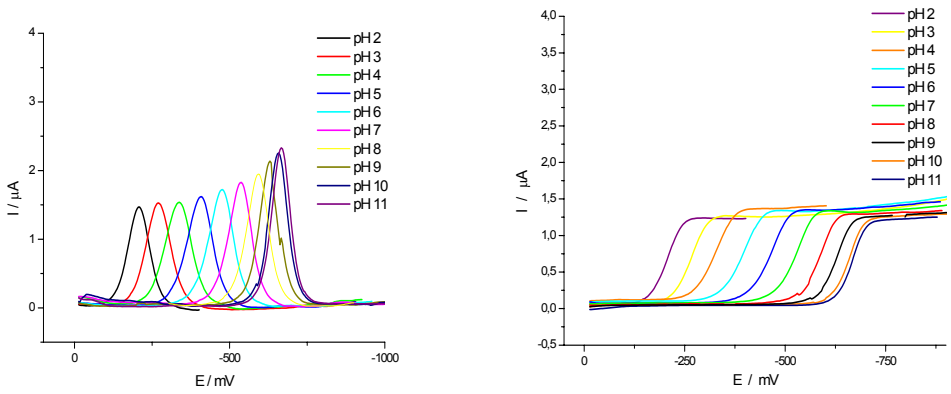

Figura 42.- Polarogramas de pulso diferencial (izquierda) y polarogramas tast (derecha) para 0,1 mM del compuesto M-NIm-COOH en medio 100 % Britton Robinson a diferentes pHs. v = 1 V/s.

La respuesta ciclovoltamperométrica resultó equivalente a lo encontrado por la técnica polarográfica encontrándose sólo un pico irreversible y dependiente del pH en todo el rango de pH entre 1 y 12. Sin embargo al agregar al medio 100 % Britton Robinson un co-solvente como Et-OH de tal manera que el nuevo medio de trabajo sea EtOH/Britton Robinson (30/70).

En la Figura 43 se despliegan los polarogramas PPD como TAST donde se observa una única señal de reducción hasta pH 7, la cual se desplaza a potenciales más negativos a medida que aumenta el pH de la solución. A partir de pH 8 se produce un desdoblamiento de la señal de reducción.

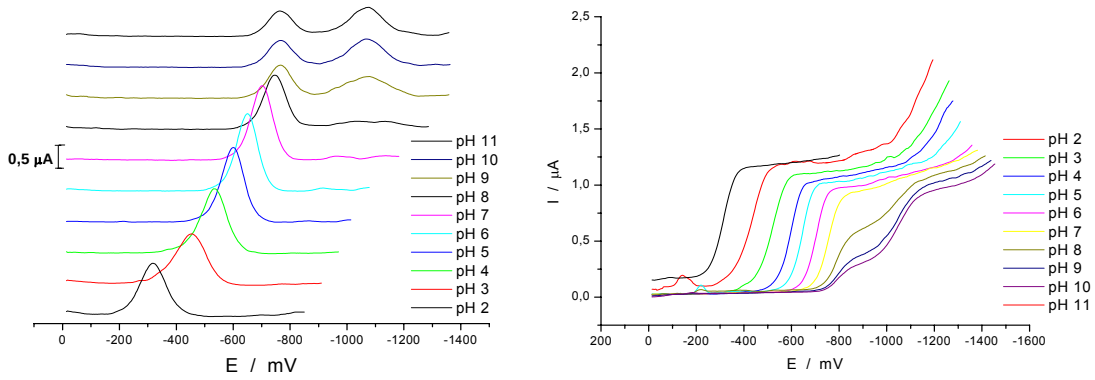

Fig 43.- Polarogramas de Pulso Diferencial (izquierda) y Polarogramas TAST (derecha) a distintos pH, para 0,1 mM de M-NIm-COOH en medio Britton Robinson – Etanol (70/30).

Mediante la técnica de polarografía tast se aprecia en forma muy clara el desdoblamiento que ocurre en la onda de reducción del grupo nitro a 4-electrones y 4-protones para generar dos nuevas ondas en medio básico. Este comportamiento revela el cambio de mecanismo que ocurre en la reducción del grupo nitro en un medio donde escasean los protones. La escasez de protones provoca que la protonación del anión radical ocurra con mayor dificultad, lo que genera una separación de la onda debido a la transferencia monoelectrónica del grupo nitro para formar el anión radical nitro y la posterior reducción del anión vía 3-electrones y 4-protones para generar el derivado

hidroxilamínico (Ecuación 18).

Además, lo anterior se corroboró por voltamperometría cíclica en la solución Britton Robinson – Etanol (70/30) a distintos pH como se observa en la figura 44. En ésta se observa que a pH ácido se obtiene una sola señal irreversible, la que corresponde a la reducción vía cuatro electrones cuatro protones para generar un derivado hidroxilamínico (Ecuación 17). A pH básico se observa la aparición de una cupla I/I'de aspecto reversible, debido a la formación del dianión radical nitro a partir de la forma aniónica del compuesto nitro derivado (Ej.- M-NIm-COO$^-$), (Ecuación 27), en una primera etapa, y la formación del derivado hidroxilamínico en la etapa posterior (II) (Ecuación 18). Además se observa una señal (III) correspondiente a la oxidación del derivado hidroxilamínico a derivado nitroso, (Ecuación 22).

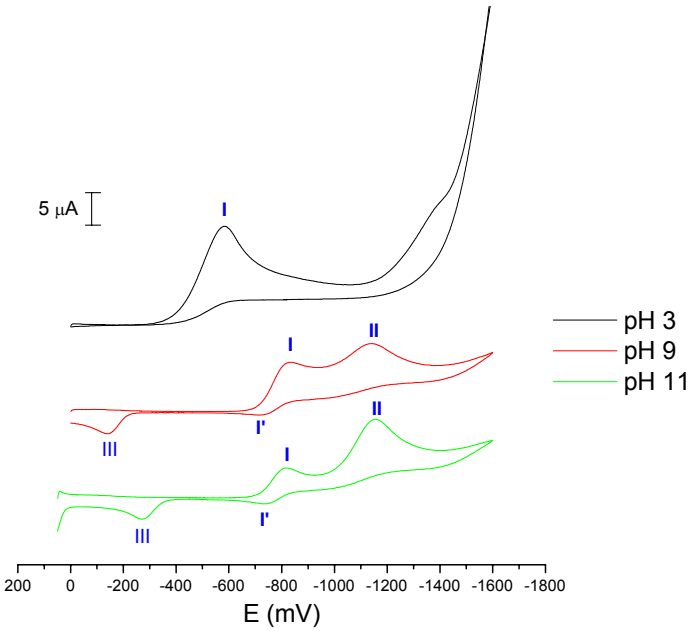

Fig 44.- Voltamperogramas de M-NIm-COOH 1 mM a pH 3, 9, 11. Velocidad de barrido 500 mV/s en medio Britton Robinson – Etanol (70/30).

Debido a que a pH 11 se obtiene una mejor estabilización del anión radical, se aisló la señal correspondiente al anión radical nitro desde -600 a -910 mV (Fig. 45), la cual se muestra a diferentes velocidades de barrido (desde 0,5 hasta 30 V/s). Se observa que al aumentar la velocidad de barrido, se obtiene un aumento en la intensidad de la

corriente y la señal tiende a ser más cuasi-reversible.

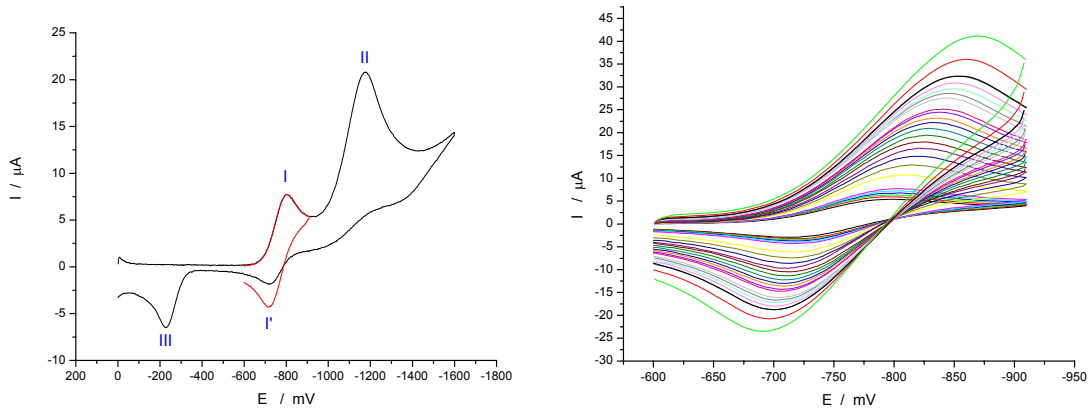

Fig 45.- Voltamperogramas de 1 mM de M-NIm-COOH a pH 11 y par redox (I/I') en rojo (izquierda). Par redox aislado a diferentes velocidades de barrido, pH 11, en medio Britton Robinson - Etanol (70/30).

Este comportamiento de cuasi-reversibilidad (ΔEp > 57 mV), es confirmado por los gráficos Epc vs Log v y ΔEp vs Log v (Resultados no mostrados), en los cuales se observa que al aumentar la velocidad de barrido, el potencial de pico catódico se desplaza a potenciales más negativos, y el ΔEp mínimo es de 80 mV el cual aumenta con la velocidad. Además, se encontró que la pendiente de la relación lineal log Ipc vs log v, es aproximadamente 0,5 lo que indica que el proceso está controlado por difusión. Se utilizó el método descrito por Nicholson [50] para la determinación de la constante de transferencia heterogénea en reacciones cuasi-reversibles, siendo el valor obtenido de la constante heterogénea en este medio de $k° = 2{,}98 \times 10^{-2}$ cm/s. De acuerdo al comportamiento obtenido anteriormente para este mismo compuesto en medio 100 % no acuoso se había obtenido una $k° = 9{,}74 \times 10^{-3}$ cm/s confirmando que el carácter prótico del medio favorece la reacción de transferencia.

3.3.c. Medio micelar

Con el objeto de encontrar condiciones que nos permitieran trabajar en condiciones similares a condiciones de pH *in-vivo*, soluciones acuosas de pH 7,4, se estudió el comportamiento del anión radical nitro generado en estos derivados 4-nitroimidazólicos en medios micelares. Para este estudio se tomó como modelo el compuesto M-NIm-OH. Se utilizó diferentes compuestos surfactantes, entre ellos, surfactantes aniónicos como SDS (Sulfato de dodecil sodio), no iónicos como Triton X y catiónicos como Hyamina y CTAB (Bromuro de cetil trimetil amonio). Se estudió que las micelas catiónicas son las que mejor estabilizan el anión radical.

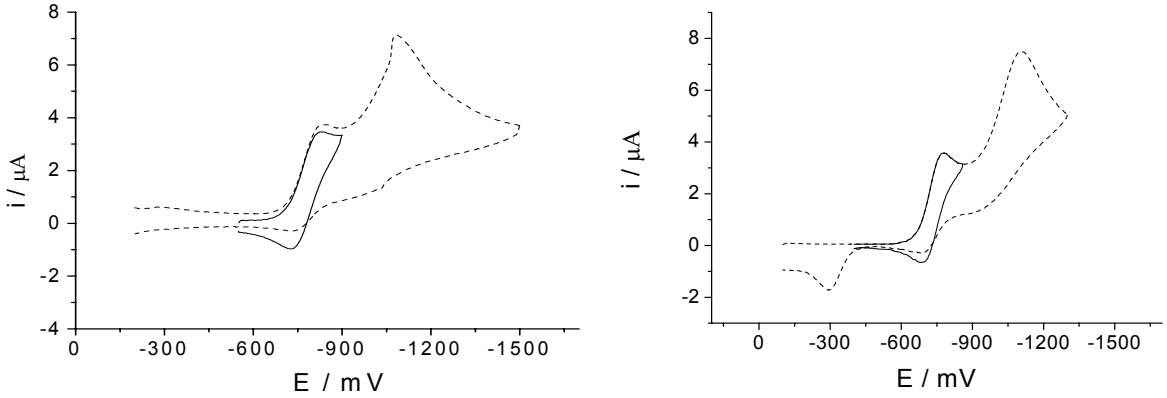

Fig 46.- Voltamperogramas de 1 mM de M-NIm-OH en 0,1 M Britton Robinson a pH 8,4 con 15 mM de CTAB (izquierda) y Hyamina (derecha). La línea completa indica el par redox $RNO_2/RNO_2^{\cdot-}$.

En la Figura 46 se aprecia que es posible obtener la generación de la cupla correspondiente al anión radical nitro en buffer Britton Robinson en presencia de surfactantes catiónicos. En esta condición es posible estudiar la respuesta del anión radical en forma aislada a diferentes velocidades de barrido.

En la figura 47 se muestran los voltamperogramas cíclicos obtenidos para soluciones de M-NIm-OH en buffer Britton Robinson a pH 8,4 donde se ha agregado 15 mM de Hyamina como surfactante.

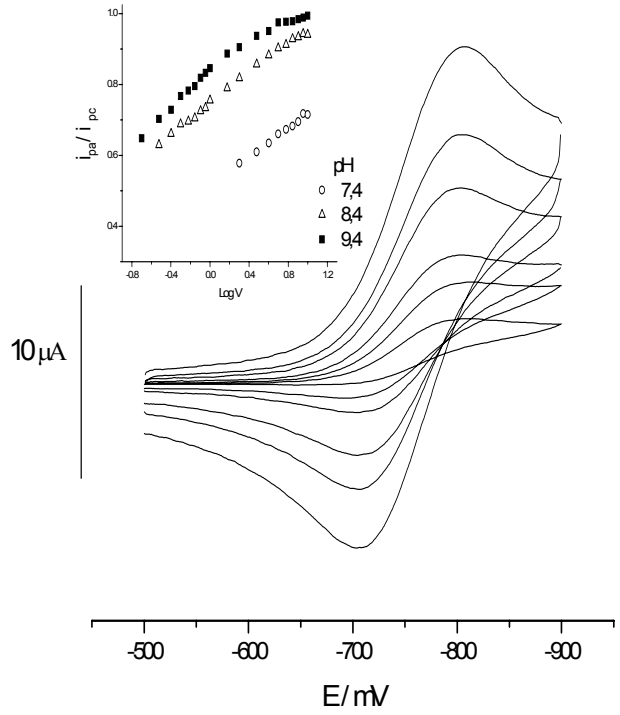

Fig 47.- Voltamperogramas de 1 mM de M-NIm-OH en 0,1 M Britton Robinson a pH 8,4 con 15 mM de Hyamina. En el inserto se muestra los gráficos de la dependencia entre la razón de corriente y la velocidad de barrido.

Aplicando el mismo procedimiento ya descrito anteriormente en esta tesis se calcularon los valores de la constante de estabilidad del anión radical nitro y los correspondientes tiempos de vida media para una concentración de 1 mM de M-NIm-OH en diferentes medios y pH. Estos resultados se muestran en la Tabla 6 en donde los datos a pH 9.4[a] son para una solución acuosa en 100 % buffer Britton Robinson con 5mM de micelas de Hyamina. Los resultados del pH 10[b] corresponde a soluciones en un medio mixto 30/70: Etanol/ Buffer Britton-Robinson sin micelas y la solución de pH 10[c] corresponde a soluciones en un medio mixto 60/40 : DMF/ buffer citrato, KCl sin micelas. De los resultados obtenidos con la misma concentración de micelas pero a distintos pH se observa que el pH afecta fuertemente la estabilidad del anión radical

(valores de k_2) sin embargo no afectan la energética de la reducción del grupo nitro (valores de $E_{p,c}$). Estos resultados confirman la pH-dependencia de la reacción de disproporcionación y la pH-independencia de la reducción mono electrónica para generar el anión radical nitro.

pH	**$k_2 \times 10^{-4}$ / l $mol^{-1}s^{-1}$**	**$t_{1/2}$ / ms**	**- $E_{P,C}$ / mV**
7.4	104 ± 2.11	0.96	804
8.4	4.30 ± 0.43	23.25	802
9.4	1.37 ± 0.21	72.99	796
9.4[a]	8.77 ± 0.62	11.40	774
10[b]	0.59 ± 0.03	169.49	760
10[c]	1.36 ± 0.21	73.52	727

Tabla 6.- Constantes de estabilidad y tiempos de vida media para el anión radical nitro, y potenciales de pico catódico para el par RNO_2/ $RNO_2^{\cdot}$ formado desde soluciones acuosas con 15 mM de micelas Hyamina a diferentes pH.

4. CONCLUSIONES

- Todos los compuestos nitroimidazólicos estudiados fueron suceptibles de ser reducidos tanto en medios próticos como apróticos no obstante que el mecanismo de la reducción es fuertemente influenciada por el grado de proticidad del medio.

- Al comparar compuestos equivalentes de 2-nitroimidazol, 4-nitroimidazol y 5-nitroimidazol en el mismo medio (Buffer acuoso, pH 8: etanol, 70:30) se encontró que el orden de facilidad de reducción sigue la siguiente secuencia para los derivados 2-Nitroimidazol (E_P = -660 mV) > 5-Nitroimidazol (-750 mV) > 4-Nitroimidazol (- 830 mV). Probablemente la mayor facilidad de reducción de los derivados de 2-nitroimidazol se debe a que en estos compuestos el grupo nitro se encuentra en medio de dos átomos de N electronegativos que provocan una disminución de la densidad electrónica sobre el grupo nitro facilitando así su reducción.

- A pesar que los derivados 2-nitroimidazol y 4-nitroimidazol presentan una notoria diferencia en su facilidad de reducción siguen mecanismos similares. En medio no acuoso el mecanismo está fuertemente influenciado por la ionización del N imino en la posición 1 del anillo nitroimidazólico generando un equilibrio entre la especie neutra y la base conjugada. La especie neutra produce una respuesta irreversible debido a la siguiente ecuación:

$$5\ \ HNRNO_2 + 4\,e^- \ \rightarrow\ \ 4\ ^-NRNO_2 + HNRNHOH + H_2O$$

Por otra parte la base conjugada o nitranión produce una onda cuasi reversible debido a la reducción monoelectrónica del nitranión generando un dianión.

-El anión radical nitro producido del 2-nitroimidazol resulta ser bastante más reactivo que el del 4-nitroimidazol, lo que podría explicar, en parte, la mayor inactividad biológica que se ha encontrado para los derivados 4-Nitroimidazólicos

De acuerdo al estudio con distintos sustituyentes realizados con el derivado 4-nitroimidazol se puede concluir que la sustitución en posición 2 del anillo nitroimidazólico no produce diferencias significativas en la capacidad de reducción del grupo nitro. Sin embargo el reemplazo del H en la posición 1 del N imidazólico por un grupo CH_3 produjo diferencias notables en la energética de la reducción del nitro, en la estabilidad del anión radical generado y en el mecanismo de la reducción.

-El efecto que genera el grupo metilo en la posición N-1 del anillo imidazólico se debe al efecto estérico que ejerce sobre los electrones no enlazantes del N que hace que estos electrones no contribuyan al sistema π del anillo, disminuyendo así la densidad de electrones sobre el grupo nitro y por ende facilitando su reducción. Por otra parte el cambio del H en la posición N-1 por el grupo metilo genera cambios en el mecanismo ya que evita la generación de reacciones acopladas del tipo padre-hijo que impiden la estabilización del anión radical.

5. REFERENCIAS

1. D.Thall, G. Rosner, C. Azuma, M. Mc Entee, J. Raleigh. Radiotherapy & Oncology 44, 171-176 (1997)

2. F. Riché, A. du Molinet, S. Sèpe, L. Riou, D. Fagret and M. Vidal. Biorg. Med. Chem. Lett. 11, 71-74 (2001)

3. S.A. Everett, M.A. Naylor, K.B. Patel, M.R. Stratfordand, P. Wardman. Biorg. Med. Chem. Lett. 9, 1267-1272 (1999)

4. G.E. Adams, I.J. Stratford, R.G. Wallace, P. Wardman, M.E. Watts. J.Natl.Cancer.Inst. 64, 555-560 (1980)

5. D.I. Edwards. Progress Med. Chem., 18, 87 (1981)

6. D.I. Edwards. J.Antimicrobiol. Chemo ther., 31, 9-20 (1993)

7. D.I. Edwards. Biochem. Pharmacol., 35, 53-58 (1986)

8. P.Wardman, Environ Health. Perfect., 64, 309-320 (1985)

9. M.Muller, Scand. J.Infect. Dis. (Suppl.) 26, 31 (1981)

10. H.Van den Bassche, Nature 273, 626 (1978)

11. D.I. Edwards. J.Antimicrobiol. Chemother., 31, 9-20 (1993)

12. W. Bone, N. Jones, G. Kamp, C. Yeung, T Cooper. J. Reprod. Fertility 118, 127-135 (2000)

13. D. Menéndez, E. Rojas, L. Herrera, M. Lopez, M. Sordo, G. Elizondo, P. Ostrosky-Wegman. Mut. Res. 478, 153-158 (2001)

14. P. Hrelia, C. Fimognari, F. Maffei, B. Brighenti, L. Garuti, S. Burnelli, G. Cantelli. Mut. Res. 397, 293-301 (1998)

15. S. Trinh, G. Reisset. Mut. Res. 398, 55-65 (1998)

16. M. Lopez-Nigro, A. Gadano, M. Carballo. Toxicology in Vitro 15, 209-213

(2001)

17. C. Viodé, N. Battache, N. Cenas, L. Krauth-Siegel, G. Chauviere, N. Bakalara, J. Perie; Biochem. Pharmacol. 57, 549 (1999)

18. R.P. Mason , J.L. Holtzman, Biochem. 14,1626-32 (1975)

19. R.P. Mason , J.L. Holtzman, Biochem. Biophys.Res.Commun 67, 1267-74 (1975)

20. P. Wardman, Repts. Prog. Phys. 41, 259 (1978)

21. R.P. Mason, Free radical intermediates in the metabolism of toxic chemicals, en: W.A. Prior (Ed.), Free radicals in Biology, Vol.V, Academic Press, New York, 1982, p.161.

22. J.A. Squella, J. Mosre, M. Blázquez, L.J. Núñez-Vergara, J. Electroanal. Chem. 319, 177(1991).

23. L.J. Núñez -Vergara, S. Bollo, A. Alvarez, M. Blázquez, J.A. Squella, J. Electroanal. Chem. 345, 121 (1993).

24. Carbajo, S. Bollo, L.J. Núñez -Vergara, P. Navarrete, J.A. Squella, J. Electroanal. Chem. 494, 69 (2000).

25. J.H. Tocher, D.I. Edwards, Int. J. Radiat. Biol. 57. 45 (1990)

26. J.A. Squella, C. Solabarrieta, L.J. Núñez -Vergara, Chem-Biol.Interact. 89, 197(1993).

27. J.H. Tocher, D.I. Edwards, Biochem. Pharmacol. 50, 1367(1995).

28. L.J. Núñez -Vergara, M.E. Ortiz, S. Bollo, J.A. Squella, Chem-Biol. Interact. 106, 1(1997).

29. S.Bollo, L.J.Núñez-Vergara, M.Bonta, G. Chauviere, J.Périé and J.A.Squella. J. Electroanal. Chem. 511, 46-54 (2001)

30. L.J.Núñez-Vergara, M.Bontá, P.A.Navarrete-Encina and J.A.Squella.

Electrochim. Acta. 46, 4289-300 (2001)

31. M.Bontá, G.Chauviere, J. Périé, L.J.Núñez-Vergara and J.A.Squella. Electrochim. Acta 47, 4045-4053 (2002).

32. S.Bollo, L.J.Núñez-Vergara, C.Martinez, G.Chauviere, J. Périé and J.A.Squella. Electroanalysis 15 (1) 19-25 (2003)

33. D. Church, H. Rabin, E. Laishley. Journal of Antimicrobial Chemotherapy 25, 15-23 (1990)

34. D. Dumanovic, J. Volke, V. Vajgand, J. Pharm. Pharmacol. 18, 507(1966).

35. S.A. Ozcan, Z. Senturk, I. Biryol, Int. J. Pharm. 157, 137 (1997).

36. A. Radi, S. El-Laban, Abdel-Ghany El-Kourashy, Electroanalysis 9, 625 (1997).

37. S.A. Okzan, Analusis 25, 130 (1997).

38. S. Bollo, L.J. Núñez-Vergara, M. Bontá, G. Chauviere, J. Perie. J.A. Squella, Electroanalysis 13, 936 (2001)

39. J.H. Tocher, D.I. Edwards, Free. Radical Res. Commun. 16, 19 (1992).

40. J.H. Tocher, D.I. Edwards, Free. Radical Res. Commun. 9, 49 (1990).

41. D. Barety, B. Resibois, G. Vegoten, Y. Moschetto. J. Electroanal. Chem. 162, 335-341 (1984).

42. S. Bollo, L.J. Núñez-Vergara, M. Bontá, G. Chauviere, J. Perie, J.A. Squella, J. Electroanal. Chem. 511, 46 (2001).

43. M.L. Arguelho, G. Silva, N. Stradiotto. J. Electrochem. Soc. 148 (2) D1-D3 (2001)

44. S. Roffia, C. Gottardi, E. Vianello. J. Electroanal. Chem. 142, 263-275 (1982)

45. J. Carbajo, S. Bollo, L.J. Núñez-Vergara, A. Campero, J.A.Squella. J.

Electroanal. Chem. 531, 187-194 (2002)

46. M.L. Olmstead, R.S. Nicholson, Anal. Chem. 41, 862 (1969)

47. J. Arguello, L.J. Núñez-Vergara, J.A.Squella. Electrochemical Communications 7, 53-57 (2005)

48. J.A.Squella, S. Bollo, L.J. Núñez-Vergara. Current Organic Chemistry 9 (6), 565-581 (2005)

49. R. S. Nicholson. Analytical Chemistry 36, 1406 (1964)

50. R. S. Nicholson. Analytical Chemistry 37, 1351 (1965)

51. M.E. Ortiz, L.J. Núñez.Vergara y J.A.Squella 549, 157-160 (2003)

ELSEVIER

Journal of Electroanalytical Chemistry 531 (2002) 187–194

Journal of Electroanalytical Chemistry

www.elsevier.com/locate/jelechem

Cyclic voltammetric study of the disproportionation reaction of the nitro radical anion from 4-nitroimidazole in protic media

J. Carbajo [b], S. Bollo [a], L.J. Núñez-Vergara [a], A. Campero [b], J.A. Squella [a,*]

[a] Bioelectrochemistry Laboratory, Chemical and Pharmaceutical Sciences Faculty, University of Chile, P.O. Box 233, 1007 Olivos, Santiago 1, Chile
[b] Departamento de Química Física y Química Orgánica, Escuela Politécnica Superior, Universidad de Huelva, Huelva, Spain

Received 9 April 2002; received in revised form 25 June 2002; accepted 20 July 2002

Abstract

We have chosen 4-nitroimidazole (4-NIm) as a prototype of nitroimidazolic compounds in order to carry out an exhaustive cyclic voltammetric study in protic media, 0.1 M Britton–Robinson buffer+0.3 M KCl with ethanol as a co-solvent. The one electron reduction of 4-NIm in protic media at alkaline pH produces a stable nitro radical anion on the time scale of the cyclic voltammetric technique. The nitro radical anion decays according to a coupled chemical reaction and we have focused the study to follow this reaction using cyclic voltammetric methodology. The one electron reduction of the 4-NIm to form the nitro radical anion and the subsequent reaction of the radical obey an EC_2 mechanism that follows very well the cyclic voltammetry theory for the disproportionation reactions previously described by Olmstead and Nicholson (Anal. Chem. 41 (1969) 862). We have obtained the disproportionation rate constant k_2 which is strongly dependent on both pH and ethanol content according to the following regression equations: $\log k_2 = -0.932\mathrm{pH} + 12.771$ and $\log(10^{-3}\ k_2) = -1.998\log[\%\ \mathrm{EtOH}] + 3.873$. The results obtained from this study in protic media differ substantially from previous studies in aprotic media wherein the nitro radical anion was not stabilized.

Keywords: 4-Nitroimidazole; Nitro radical anion; Cyclic voltammetry

1. Introduction

Nitroimidazoles are used extensively in the treatment of infectious illnesses in both human and non-human therapeutics [1,2]. The antimicrobial action of nitroimidazoles is produced inside pathogenic microorganisms wherein some reduced form of the nitro group interacts with the microbial DNA, thus causing damage in the microbial structure hindering its reproduction. Consequently, it is vital for the mechanism of action that the microorganisms have an enzymatic system capable of reducing the nitro group. The reduction of nitroimidazoles can be produced via two different routes according to the media conditions i.e. aerobic or anaerobic [3,4], but under both conditions the requirement of the first step of the reduction is the one-electron reduction to form the nitro radical anion:

$$RNO_2 + e^- \rightarrow RNO_2^{\bullet -} \quad (1)$$

Under anaerobic conditions, the nitro radical anion formed can undergo further reductions producing nitroso, hydroxylamine and amine derivatives:

$$RNO_2^{\bullet -} + e^- + 2H^+ \rightarrow RNO + H_2O \quad (2)$$

$$RNO + 2e^- + 2H^+ \rightarrow RNHOH \quad (3)$$

$$RNHOH + 2e^- + 2H^+ \rightarrow RNH_2 + H_2O \quad (4)$$

On the other hand, under aerobic conditions, the nitro radical anion formed would be re-oxidized to regenerate the initial nitro compound and to produce superoxide ($O_2^{\bullet -}$) provoking a so called 'futile cycle':

$$RNO_2^{\bullet -} + O_2 \rightarrow RNO_2 + O_2^{\bullet -} \quad (5)$$

As can be seen the nitro radical anion plays a crucial and important role in the mechanism of the action of nitroimidazole compounds and consequently a knowledge of its behaviour is a permanent challenge because its radical chemistry is central to the use of nitroimidazoles in medicine.

* Corresponding author. Tel.: +56-2-678-2928/2927; fax: +56-2-737-1241
E-mail address: asquella@ll.ciq.uchile.cl (J.A. Squella).

0022-0728/02/$ - see front matter
PII: S0022-0728(02)01071-9

The prototropic properties and natural lifetimes of nitro radical anions have been studied mainly by using electron spin resonance (ESR) and pulse radiolysis techniques [5–7] but lately electrochemical techniques i.e. cyclic voltammetry, have also been shown to play an advantageous role in the study of nitro radical anions [8–14]. Under suitable conditions of the medium, the one electron reduction of nitroaromatic and nitroheterocyclic compounds produces very well resolved cyclic voltammograms due to the nitro/nitro radical anion couple ($RNO_2/RNO_2^{\bullet -}$). By using appropriately the wide versatility of the cyclic voltammetric technique, it is possible to study the feasibility of formation of nitro radical anions [8,9], their prototropic behavior [10], their natural lifetimes [11,12] and their reactivity with other molecules [13,14].

There are numerous studies related to electrochemical aspects of nitroimidazoles. Generally these are focused on the electroanalytical determination of some nitroimidazoles of importance in medicine such as metronidazole [15], ornidazole [16], secnidazole [17], tinidazole [18], and megazol [19]. Furthermore, the use of cyclic voltammetry in order to obtain the lifetimes of nitro radical anions from some nitroimidazoles such as misonidazole, metronidazole and megazol [20–22] has been also reported.

In this work we have centered our study on the nitro radical anion produced from a molecule such as 4-nitroimidazole (4-NIm) wherein the only substituent on the nitroimidazole moiety is the nitro group thus avoiding any possible distortion effect from other substituents. There has been only one previous report devoted to the electrochemical behaviour of 4-NIm in aprotic media wherein the autoprotonation of the nitro radical anion was shown but, consequently, that work did not involve a study of the nitro radical anion [23]. In the present study we report an exhaustive cyclic voltammetric study of the prototropic properties and the natural lifetime of the nitro radical anion obtained from 4-NIm. Specifically we have focused our study on the disproportionation reaction of the nitro radical anion from 4-NIm in a protic medium containing ethanol as a co-solvent. The influences of pH, ethanol content and 4-NIm concentrations on the disproportionation rate constant were investigated in depth.

2. Experimental

2.1. Reagents and solutions

4-NIm 97% pure was obtained from Aldrich Chem. Co. and was used without prior purification. All the other reagents employed were of analytical grade. Nitrogen gas was from Alphagas-Air liquide with maximum impurities of $H_2O < 3$ ppm; $O_2 < 2$ ppm; $C_nH_m < 0.05$ ppm.

All the voltammetric experiments were obtained after bubbling with N_2 for 10 min in the cell before each run. The temperature was kept constant at 25 ± 0.1 °C in all experiments.

Solutions for cyclic voltammetry were prepared starting from a 0.2 M stock solution of 4-NIm in DMF prepared daily. Final solutions (20 ml) in the voltammetric cell were prepared by diluting an appropriate quantity of the stock solution in order to obtain a final concentration of 1 mM (Except in the 4-NIm concentration study).

Experiments for the pH study were made in Britton–Robinson buffer 0.1 M + 0.3 M KCl + EtOH (70//30). The pH was adjusted by addition of concentrated solutions of NaOH or HCl depending on the desired final pH. For the study of the dependence on the EtOH content, the EtOH% was varied appropriately in the above solution.

2.2. Apparatus

Voltammetric curves were recorded on an Autolab (Eco Chemie model PGSTAT 20) instrument attached to a PC computer with appropriate software (GPES 4.8 for Windows) for total control of the experiments and data acquisition and treatment. A static mercury drop electrode (SMDE) (Metrohm VA 663) with a drop area of 0.42 mm^2 was used as the working electrode and a glassy carbon rod as the counter electrode. All potentials were measured against Ag/AgCl/3 M KCl.

All pH measurements were carried out with a Crison model Basic 20 pH meter equipped with a glass electrode Crison 52-01 (resolution 0.01, precision ±0.01). The standard solutions used for calibration were Crison 4.00 and 7.02 and Probus 10.00.

2.3. Methods

The return-to-forward peak current ratio I_{pa}/I_{pc}, for the reversible first electron transfer (the $R–NO_2/R–NO_2^{\bullet -}$ couple) was measured for each cyclic voltammogram, varying the scan rate from 0.05 up to 150 V s^{-1} according to the procedure described by Nicholson [24]. A reproducibility study involving ten independent runs at different sweep rates (0.5, 1 and 10 V s^{-1}) produced variation coefficients of 0.1 and 0.7% for potential peak and current ratio measurements, respectively.

Using the theoretical approach of Olmstead and Nicholson [25], the I_{pa}/I_{pc} values measured experimentally at each scan rate were inserted into a working curve to determine the parameter ω, which incorporates the effects of the rate constant, 4-NIm concentration and scan rate. A plot of ω versus τ resulted in a linear

relationship described by the equation

$$\omega = k_2 c_o \tau$$

where k_2 is the second-order rate constant for the decomposition of $RNO_2^{\bullet -}$, c_o is the nitrocompound concentration and $\tau = (E_\lambda - E_{1/2})/v$. Consequently we can obtain the second order rate constant for the decomposition of the nitro radical anion from the slope of the straight line ω versus τ.

3. Results and discussion

4-NIm can be electrochemically reduced over the whole pH range at the mercury electrode in protic media (0.1 M Britton–Robinson buffer+0.3 M KCl with ethanol as a co-solvent), but its reduction is strongly affected by pH changes. Consequently, the cyclic voltammetric response of the 4-NIm reduction is also pH-dependent. In fact, at pH values < 7 the cyclic voltammetric response corresponds to only one irreversible reduction peak without any oxidation peak appearing in the corresponding positive sweep. Obviously this reduction peak is due to the well-known [26] four-electron four-proton reduction of the nitro group to produce the corresponding hydroxylamine derivative:

$$RNO_2 + 4H^+ + 4e \rightarrow RNHOH + H_2O \quad (6)$$

In Fig. 1 we can observe the behaviour of this voltammetric reduction peak in acidic media. At pH values > 7 the cyclic voltammetric response is rather different but follows the well-known [27] general pattern due to nitrocompound in aprotic media or in the presence of inhibitors. In fact the single signal observed in acidic media was divided into two different new signals according to the pH increase (Fig. 1). Consequently, at alkaline pH, the equations describing the new two signals correspond to:

$$RNO_2 + e^- \rightleftarrows RNO_2^{\bullet -} \quad (7)$$

$$RNO_2^{\bullet -} + 3e^- + 4H^+ \rightarrow RNHOH \quad (8)$$

In Fig. 2 we have summarized the pH effect on both cathodic peak current and negative peak potentials of both signals. As the aim of this paper is the cyclic voltammetric study of the nitro radical anion ($RNO_2^{\bullet -}$) produced by the one electron reduction of 4-NIm we have centered our study on the corresponding first reversible couple obtained at pH values > 7.

By working at sufficiently alkaline pH and adjusting the switching potential appropriately we can study the nitro/nitro radical anion couple ($RNO_2/RNO_2^{\bullet -}$) in isolation. In Fig. 3, a very good resolved cyclic voltammograms obtained after two consecutives sweeps is shown. Furthermore, we have obtained a ΔE_p value of approximately 60 mV (Table 1) confirming the one electron character of the couple.

With the aim of obtaining the pH-dependence of the $RNO_2/RNO_2^{\bullet -}$ couple we have carried out a very

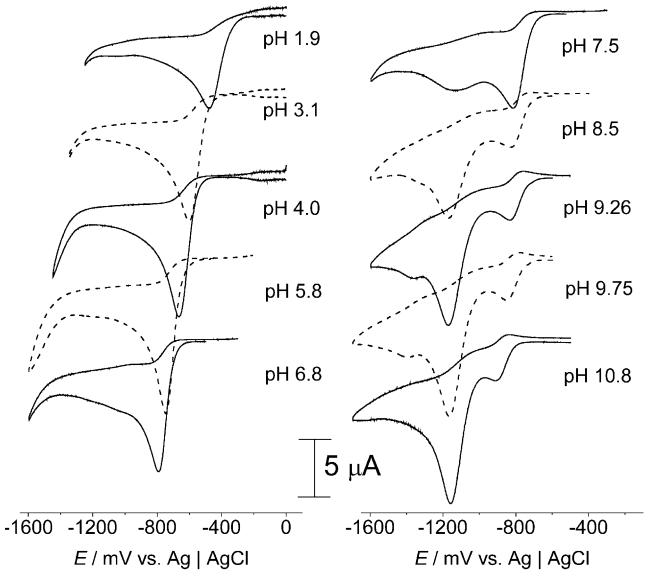

Fig. 1. Cyclic voltammograms of 1 mM 4-NIm in protic media (0.1 M Britton–Robinson buffer+0.3 M KCl+EtOH (70//30)) at different pH values. Sweep rate 1 V s^{-1}.

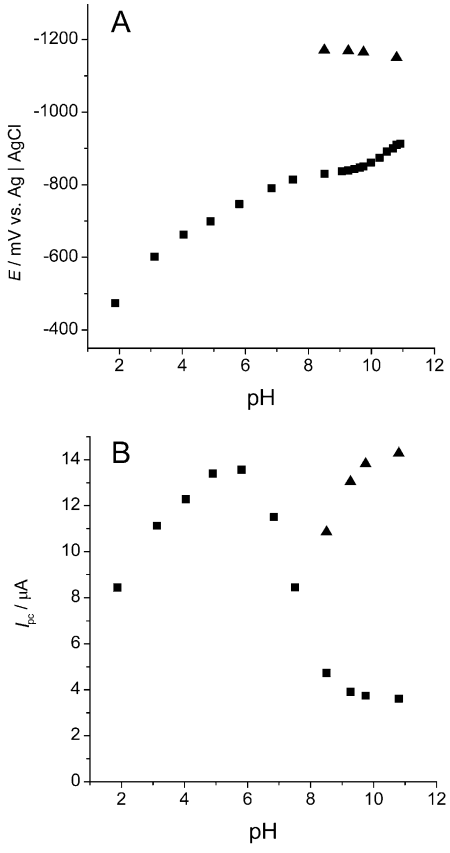

Fig. 2. Peak potential (A) and peak current (B) dependence with pH for 1 mM 4-NIm in protic media. ■, first peak; ▲, second peak. Other conditions as in Fig. 1.

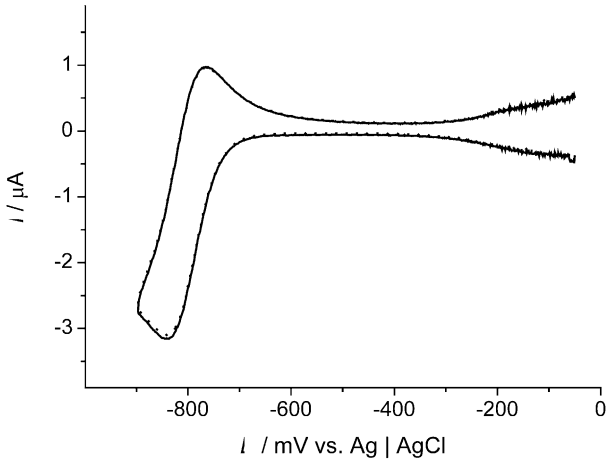

Fig. 3. Two consecutives cyclic voltammograms due to the $RNO_2/RNO_2^{\bullet -}$ couple from 1 mM 4-NIm in protic media. pH 9.10, $v = 1.0$ V s^{-1}. Other conditions as in Fig. 1.

Table 1
ΔE_p values of the $RNO_2/RNO_2^{\bullet -}$ couple obtained from 1 mM 4-NIm cyclic voltammograms in protic media, 30% EtOH, pH 9.15 at different sweep rates

v/V s^{-1}	ΔE_p/V
1.0	0.070
2.0	0.067
3.0	0.062
5.0	0.061
7.0	0.059

exhaustive study in a rather narrow zone ($8 < pH < 10$). The change of pH clearly affects the cyclic voltammograms of the $RNO_2/RNO_2^{\bullet -}$ couple. Specifically, we observe two main changes when the pH increases; first, a shift of the wave to more negative values and second, a change in the peak current intensities, i.e. a decrease in the cathodic peak current and an increase in the anodic peak current. These changes are summarized in Fig. 4. Obviously, this observed pH-influence indicates that the one electron reduction of 4-NIm is not explained well by only one equation such as the above Eq. (7). Probably a chemical reaction involving protons should be coupled with the one-electron electrochemical reaction. This assumption is also supported by the observed behaviour of the couple when the sweep rate is varied. According to the Nicholson and Shain criteria [28] we can affirm that the process corresponds to an electron transfer with a coupled chemical reaction i.e. an EC mechanism. Consequently an increase of the current ratio (I_{pa}/I_{pc}) with an increase of the sweep rate (v) was observed at all the pH values studied, as is shown in Fig. 5. In order to investigate the order of the coupled chemical reaction we have tested cyclic voltammograms at different 4-NIm concentrations. According to the dependence obtained between I_{pa}/I_{pc} and the 4-NIm concentration (Fig. 6a)

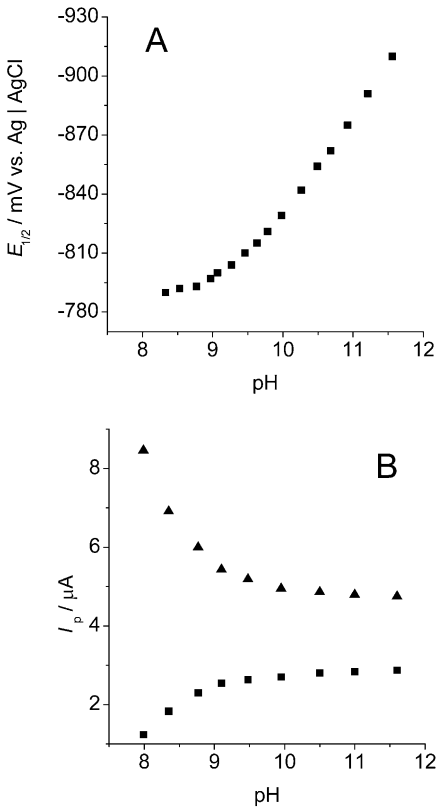

Fig. 4. Half-wave potential (A) and peak current (B) dependence on pH of the $RNO_2/RNO_2^{\bullet -}$ couple from cyclic voltammograms of 1 mM 4-NIm in protic media at different pH values. ▲, I_{pc}; ■, I_{pa}. Sweep rate 1 V s^{-1}. Other conditions as in Fig. 1.

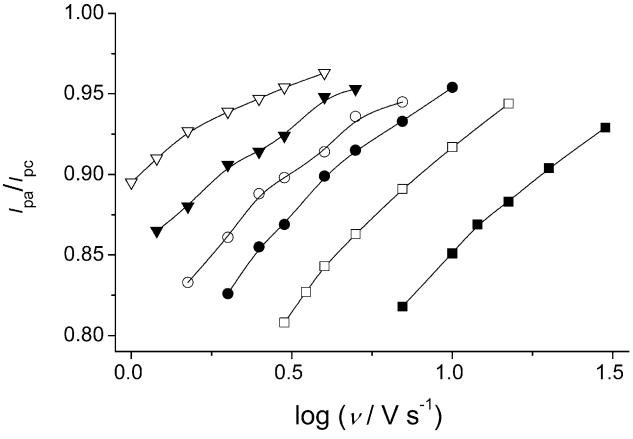

Fig. 5. Current ratio dependence on sweep rates of the $RNO_2/RNO_2^{\bullet -}$ couple from cyclic voltammograms of 1 mM 4-NIm in protic media at different pH values. ▽, 9.45; ▼, 9.19; ○, 8.95; ●, 8.70, □, 8.44; ■, 8.19. Other conditions as in Fig. 1.

we can affirm that the order of the coupled reaction was different from order 1 and from the slope of the plot of the half-wave potential ($E_{1/2}$) versus the natural logarithm of 4NIm concentration (Fig. 6b) [29] we obtained an order of 2 for the coupled chemical reaction. Consequently from this conclusive experimental evi-

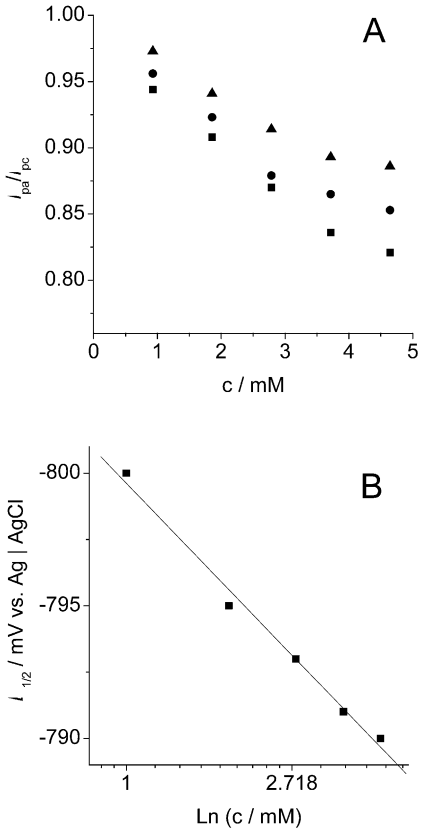

Fig. 6. (A) Current ratio dependence on the 4-NIm concentration at different sweep rates: ▲, 7.0; ●, 5.0; ■, 4.0 V s^{-1} and (B) half-wave potential dependence with the natural logarithm of 4-NIm concentration in protic media. pH 9.10. Other conditions as in Fig. 1.

dence and the well-known fact (7) that nitro radical anions can suffer a disproportionation reaction we can affirm that the second order coupled chemical reaction corresponds to a disproportionation reaction, producing the following EC_2 mechanism:

$$RNO_2 + e^- \rightleftarrows RNO_2^{\bullet -} \quad (7a)$$

$$2RNO_2^{\bullet -} + 2H^+ \rightarrow RNO_2 + RNO + H_2O \quad (9)$$

In order to confirm the proposed mechanism we applied the cyclic voltammetry theory for the disproportionation reaction described by Olmstead and Nicholson [25]. In fact we obtained straight lines in the plots of the kinetic parameters ω versus τ in perfect accordance with that anticipated by the theory (Fig. 7A). Furthermore, according to the theory, for values $a\tau = 4$, it should be noted that $\omega = k_2 c^{o} \tau$; consequently, we can obtain the disproportionation rate constant (k_2) from the slope of the straight lines between ω and τ. We have calculated the k_2 values and the corresponding half-life times ($t_{1/2}$) for the nitro radical anion from 4-NIm at different pH values (Table 2). As can be seen from these results the stability of the nitro radical anion is related directly to the proton concentration of the medium i.e. a lower proton concentration implies higher stability. Moreover, the logarithm of the disproportionation rate constant follows a linear dependence with pH (Fig. 7B). From this behaviour it is possible to obtain the following regression curve: $\log k_2 = -0.932\text{pH} + 12.771$ ($r^2 = 0.9949$); which permits the k_2 value at different pH values to be calculated by extrapolation. By using the above equation we have obtained a k_2 value of 7.48×10^5 M^{-1} s^{-1} and a $t_{1/2}$ of 1.33×10^{-3} s at pH 7.4. Obviously these values are in accord with the experimental fact that the nitro radical anion cannot be observed on the time scale of the cyclic voltammetric experiment at pH 7.4 in protic media.

In order to study the dependence of 4-NIm concentration on the stability of the nitro radical anion we have selected pH 9.10. As was shown above (Fig. 6) both the I_{pa}/I_{pc} and the $E_{1/2}$ fulfilled the requirements for a second order chemical reaction. In order to examine the character of the limiting current we have studied the behaviour of the cathodic peak current, I_{pc}, with the sweep rate at different 4-NIm concentrations. The logarithmic plot of these parameters is shown in Fig. 8. As can be observed we have obtained a linear dependence with a slope of 0.5 showing that the one-electron reduction of 4-NIm corresponds to a diffusion controlled process without adsorption interference.

Furthermore, in a similar way as shown above, we have used the theory described by Olmstead and Nicholson [25] to calculate the disproportionation rate constant, k_2, at different 4-NIm concentrations. In Fig. 9 we can observe the experimentally obtained linear behaviour of the kinetic parameters ω versus τ at different 4-NIm concentrations. From the slopes of these lines we have obtained both k_2 and $t_{1/2}$ at different 4-NIm concentrations (Table 3). From these results we can observe that k_2 remains practically constant at different 4-NIm concentrations as is expected for a rate constant. However, as is expected for a second order chemical reaction, the $t_{1/2}$ of the nitro radical anion is dependent of the 4-NIm concentration. At lower concentrations of 4-NIm the nitro radical anion is more stable. As in-vivo concentrations would be relatively low, probably the in-vivo nitro radical anion stability would be high which could have dangerous consequences.

In order to study the influence of the media in the stability of the nitro radical anion we have varied the ethanol content in the solutions studied. The appearance of the cyclic voltammogram of the one-electron redox couple was affected by the quantity of ethanol in the medium. This change can be shown clearly from some cyclic voltammetric parameters such as $E_{1/2}$ and I_{pa}/I_{pc} as is shown in Fig. 10. From these results it is clear that an increase in the ethanol content produces both a shift in $E_{1/2}$ and an increase in I_{pa}/I_{pc}; however, different quantities of ethanol did not affect the mechanism of the disproportionation reaction as is deduced from the

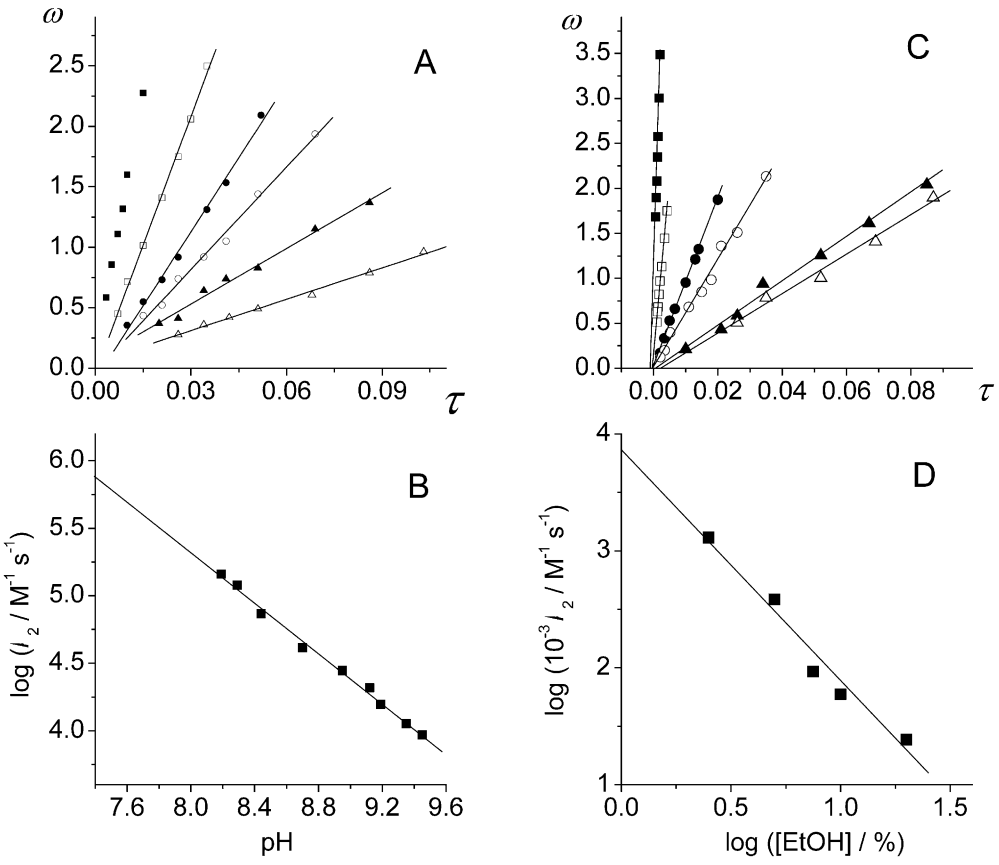

Fig. 7. (A–C) Plots of the kinetic parameter, ω, with the time constant, τ, for 1 mM 4-NIm and 30% EtOH at different pHs: ■, 8.19; □, 8.44; ●, 8.70; ○, 8.95; ▲, 9.19; △, 9.45 (plot A) and at different ethanol percentages, pH 9.10: ■, 2.5; □, 5.0; ●, 7.5; ○, 10.0; ▲, 20.0, △, 30.0% (plot C). (B–D) Disproportionation rate constant dependence on pH for 30% EtOH (plot B) and for an ethanol content at pH 9.10 (plot D) for 1 mM 4-NIm in protic media. Other conditions as in Fig. 1.

Table 2
Disproportionation rate constant and half life times values for $RNO_2/RNO_2^{\bullet -}$ couple obtained from 1 mM 4-NIm in protic media, 30% EtOH at different pHs

pH	10^{-3} k_2/l mol^{-1} s^{-1}	10^2 $t_{1/2}$/s
8.19	145	0.68
8.29	120	0.83
8.44	73.7	1.5
8.70	41.2	2.6
8.95	27.9	3.6
9.12	20.7	5.2
9.19	15.8	6.3
9.35	11.3	8.8
9.45	9.31	12

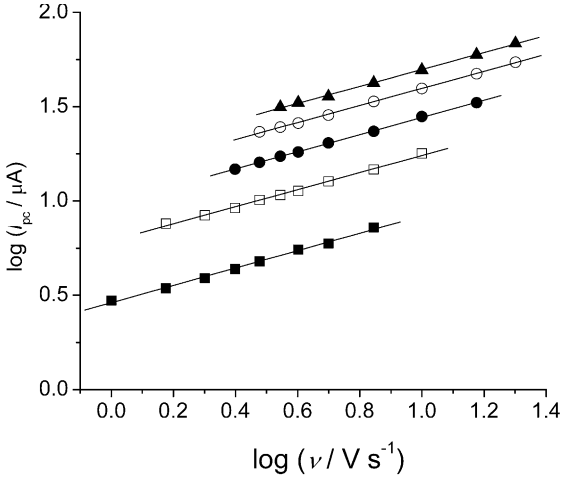

Fig. 8. Log–log dependence of the cathodic peak current of the $RNO_2/RNO_2^{\bullet -}$ couple on sweep rate at different 4-NIm concentrations in protic media, pH 9.10. ▲, 4.65; ○, 3.72; ●, 2.79; □, 1.86; ■, 0.93 M. Other conditions as in Fig. 1.

linear behaviour obtained for ω versus τ shown in Fig. 7C. From the slopes of these lines we have obtained both k_2 and $t_{1/2}$ at different ethanol contents. As can be seen from the results in Table 4, both the disproportionation rate constant, k_2, and the half-life time, $t_{1/2}$, have a strong dependence on the ethanol content in the medium. At lower ethanol concentrations ($< 10\%$) the variation of k_2 and $t_{1/2}$ are very pronounced but at ethanol concentrations $> 20\%$, the k_2 and $t_{1/2}$ values remain practically constant. Moreover, the logarithm of the disproportionation rate constant follows a linear dependence with the ethanol content in the medium

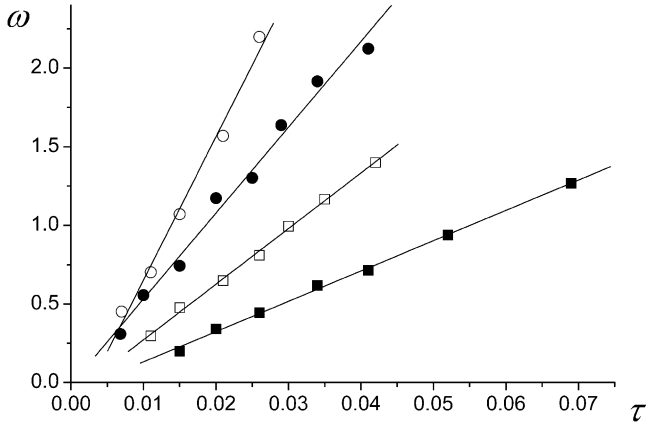

Fig. 9. Plot of the kinetic parameter, ω, vs. the time constant, τ, for different concentrations of 4-NIm in protic media, pH 9.10. ■, 0.93; □, 1.86; ●, 2.79; ○, 4.65 M. Other conditions as in Fig. 1.

Table 3
Disproportionation rate constant and half life times values for $RNO_2/RNO_2^{\bullet -}$ couple obtained from different concentrations of 4-NIm in protic media, 30% EtOH, pH 9.15

[4-NIm]/mM	10^{-3} k_2/l mol^{-1} s^{-1}	10^2 $t_{1/2}$/s
0.93	20.7	5.2
1.86	18.9	2.9
2.79	19.7	1.8
3.72	21.0	1.3
4.65	20.0	1.1

(Fig. 7D). From this behaviour, it is possible to obtain the following regression equation: $\log 10^{-3}k_2 = -1.998 \log[\%\ \mathrm{EtOH}] + 3.873$ ($r = 0.998$), for [% EtOH] ≤ 20%. Then, by using this linear relationship we obtained an extrapolated k_2 value of 7.46×10^6 M^{-1} s^{-1} and a $t_{1/2}$ value of 1.33×10^{-4} s at 1% EtOH concentration. Obviously from these results we can conclude that ethanol in the medium stabilizes the nitro radical anion strongly.

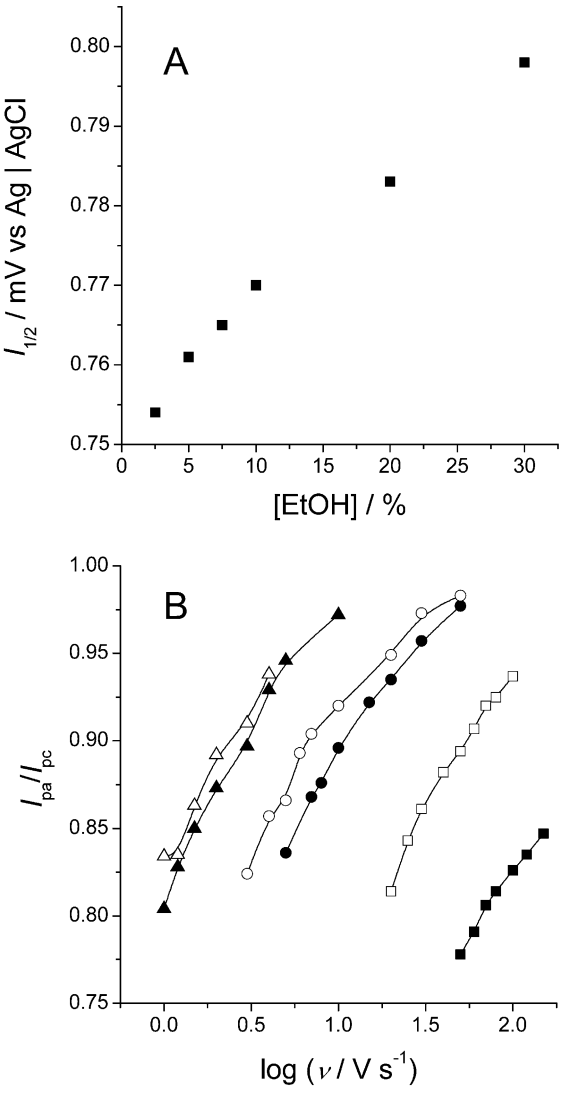

Fig. 10. (A) Half-wave potential dependence on the ethanol concentration and (B) peak current ratio dependence with the sweep rate at different ethanol concentrations: ■, 2.5; □, 5; ●, 7.5; ○, 10; ▲, 20; and △, 30%, for the $RNO_2/RNO_2^{\bullet -}$ couple from 1 mM 4NIm in protic medium at pH 9.10. Other conditions as in Fig. 1.

4. Conclusion

The results of experimental work presented above as well as those of previous workers can be summarized in the following points.

4-NIm was easily reduced in a protic media but by a totally different mechanism to that previously reported for this compound in aprotic (DMF, AN) media by Roffia et al. [23]. The cyclic voltammogram in aprotic media displayed two reduction peaks. The first peak was irreversible up to a sweep rate of 250 V s^{-1} while the second one appeared to be reversible even at low sweep rates. The first irreversible peak was attributed to the following overall electron reaction:

Table 4
Disproportionation rate constant and half life times values for $RNO_2/RNO_2^{\bullet -}$ couple obtained from 1 mM 4-NIm in protic media, pH 9.15, at different EtOH percentages

EtOH/%	10^{-3} k_2/l mol^{-1} s^{-1}	10^2 $t_{1/2}$/s
2.5	1300	0.08
5.0	385	0.26
7.5	93.2	1.1
10.0	59.4	1.7
20.0	24.5	4.1
30.0	21.9	4.6

$$5HRNO_2 + 4e^- \rightarrow HRNHOH + 4RNO_2^- + H_2O \quad (10)$$

and the second reversible peak was attributed to the following reduction reaction which generates a radical nitro dianion:

$$RNO_2^- + e^- \rightleftarrows RNO_2^{2-\bullet} \quad (11)$$

On the other hand our results in protic media reveal cyclic voltammograms displaying: (a) at $pH < 7$; one irreversible reduction peak described by Eq. (6); and (b) at $pH > 7$; one reversible and one irreversible peak described by Eqs. (7) and (8).

According to Vianello's paper in aprotic media the $RNO_2/RNO_2^{\bullet -}$ couple cannot be recorded due to a rapid decay of the $RNO_2^{\bullet -}$ because of a fast protonation reaction by the starting nitroimidazole (a father–son type of reaction) with the formation of the conjugate base $RNO_2^{\bullet -}$ and of the neutral radical $RNO_2H^{\bullet}$. Paradoxically our results demonstrate that the $RNO_2/RNO_2^{\bullet -}$ couple can be very well stabilized in protic media but at alkaline pH, due to the autoprotonation, the couple is not favoured in this medium.

On the other hand, 4-NIm is a rare case wherein its nitro radical anion is sufficiently stabilized in protic media to be detected on the time scale of the cyclic voltammetric technique. Usually the detection of this radical requires the presence of inhibitors or aprotic solvent, besides alkaline pH. Furthermore, this nitro radical anion, generated from 4-NIm, is a very good example of the accomplishment of the theory for the disproportionation reactions previously described [29]. In spite of cyclic voltammetry results proving to be a very good tool in the study of nitro radical anions, care should be taken in the use of a co-solvent because it affects the stability of the radicals strongly.

Acknowledgements

This research was supported by grant 8000016 from FONDECYT. The support of DID Universidad de Chile is also recognized.

References

[1] D.I. Edwards, Progress Med. Chem. 18 (1981) 87.
[2] D.I. Edwards, J. Antimicrob. Chemother. 31 (1993) 9.
[3] D.I. Edwards, Biochem. Pharmacol. 35 (1986) 53.
[4] C. Viodé, N. Bettache, N. Cenas, L. Krauth-Siegel, G. Chauviere, N. Bakalara, J. Périé, Biochem. Pharmacol. 57 (1999) 549.
[5] P. Wardman, Repts. Prog. Phys. 41 (1978) 259.
[6] R.P. Mason, Free-radical intermediates in the metabolism of toxic chemicals, in: W.A. Pryor (Ed.), Free Radicals in Biology, vol. V, Academic Press, New York, 1982, p. 161.
[7] P. Wardman, Environ. Health Persp. 64 (1985) 309.
[8] J.A. Squella, J. Mosre, M. Blázquez, L.J. Núñez-Vergara, J. Electroanal. Chem. 319 (1991) 177.
[9] L.J. Núñez-Vergara, S. Bollo, A. Alvarez, M. Blázquez, J.A. Squella, J. Electroanal. Chem. 345 (1993) 121.
[10] J. Carbajo, S. Bollo, L.J. Núñez-Vergara, P. Navarrete, J.A. Squella, J. Electroanal. Chem. 494 (2000) 69.
[11] J.H. Tocher, D.I. Edwards, Int. J. Radiat. Biol. 57 (1990) 45.
[12] J.A. Squella, C. Solabarrieta, L.J. Núñez-Vergara, Chem-Biol. Interact. 89 (1993) 197.
[13] J.H. Tocher, D.I. Edwards, Biochem. Pharmacol. 50 (1995) 1367.
[14] L.J. Núñez-Vergara, M.E. Ortiz, S. Bollo, J.A. Squella, Chem-Biol. Interact. 106 (1997) 1.
[15] D. Dumanovic, J. Volke, V. Vajgand, J. Pharm. Pharmacol. 18 (1966) 507.
[16] S.A. Ozcan, Z. Senturk, I. Biryol, Int. J. Pharm. 157 (1997) 137.
[17] A. Radi, S. El-Laban, Abdel-Ghany El-Kourashy, Electroanalysis 9 (1997) 625.
[18] S.A. Okzan, Analusis 25 (1997) 130.
[19] S. Bollo, L.J. Núñez-Vergara, M. Bonta, G. Chauviere, J. Perie, J.A. Squella, Electroanalysis 13 (2001) 936.
[20] J.H. Tocher, D.I. Edwards, Free. Radical Res. Commun. 16 (1992) 19.
[21] J.H. Tocher, D.I. Edwards, Free. Radical Res. Commun. 9 (1990) 49.
[22] S. Bollo, L.J. Núñez-Vergara, M. Bonta, G. Chauviere, J. Perie, J.A. Squella, J. Electroanal. Chem. 511 (2001) 46.
[23] S. Roffia, C. Gottardi, E. Vianello, J. Electroanal. Chem. 142 (1982) 263.
[24] R.S. Nicholson, Anal. Chem. 36 (1964) 1406.
[25] M.L. Olmstead, R.S. Nicholson, Anal. Chem. 41 (1969) 862.
[26] H. Lund, Cathodic reduction of nitro and related compounds, in: H. Lund, O. Hammerich (Eds.), Organic Electrochemistry, 4th ed., Marcel Dekker, New York, 2001, p. 379.
[27] B. Kastening, Free radicals in organic electrochemistry. L. Nitro and nitroso compounds, in: P. Zuman, L. Meites (Eds.), Progress in Polarography, vol. III, Wiley-Interscience, New York, 1972, p. 259.
[28] R.S. Nicholson, I. Shain, Anal. Chem. 36 (1964) 706.
[29] G. Bontempelli, F. Magno, G.A. Mazzochin, R. Seeber, Ann. Chim. 3–4 (1989) 146.

Journal of The Electrochemical Society, **152** (6) J46-J51 (2005)
0013-4651/2005/152(6)/J46/6/$7.00 © The Electrochemical Society, Inc.

Voltammetric Behavior of a 4-Nitroimidazole Derivative

Nitro Radical Anion Formation and Stability

C. Yañez, J. Pezoa, M. Rodríguez, L. J. Núñez-Vergara, and J. A. Squella[z]

Bioelectrochemistry Laboratory, University of Chile, Santiago, Chile

A new synthesized compound, 1-methyl-4-nitro-2-hydroxymethylimidazole (4-MNImOH), was electrochemically reduced at the mercury electrode in aqueous, mixed, and aprotic media. In an aqueous medium, only one voltammetric peak was observed because of the four-electron, four-proton reduction of the nitro group to the hydroxylamine derivative in the 2-12 pH range. For the mixed and nonaqueous media, it was possible to observe a reversible couple due to the first one-electron reduction step of the nitro group to the nitro radical anion.The nitro radical anion decays by a disproportionation reaction in mixed media and by dimerization in a nonaqueous medium. Both disproportionation and dimerization rate constants, k_2, were determined according to Olmstead's approach, obtaining a value of 1460 ± 110 M^{-1} s^{-1} in aprotic medium. In mixed media, the values were dependent both on pH and on the nature of the cosolvent.After comparison of 4-MNImOH with the parent compound, 4-nitroimidazole, we concluded that the substitution with 1-methyl and 2-hydroxymethyl produces a more easily reducible nitro compound and a less stable nitro radical anion than the unsubstituted 4-nitroimidazole. According to the electrochemical results, the 4-MNImOH derivative would be more suitable for enzymatic reduction and less toxic to the host than 4-nitroimidazole.
 [DOI: 10.1149/1.1904983]

Manuscript submitted October 21, 2004; revised manuscript received December 29, 2004. Available electronically April 26, 2005.

In the last decades, nitroimidazoles have been the source of many investigations because of their properties as antibiotics, radiosensitizers, and antiprotozoans.[1-3] The biological activity of nitroimidazoles is dependent on the nitro group reduction process due to the formation of active intermediate species that interact with DNA and cause biochemical damage. The reduction of these compounds can follow two different routes depending on whether the medium is aerobic or anaerobic,[4,5] however, both routes share a common first step, *i.e.*, the one-electron reduction of the nitro group to form the nitro radical anion ($RNO_2^{\bullet -}$). Consequently, $RNO_2^{\bullet -}$ is a key intermediate in the biological activity, and the understanding of its behavior is a permanent challenge for these type of compounds.

Three types of nitroimidazole derivatives have been currently used, namely, 2-, 4-, and 5-nitrosubstituted derivatives; however, there are still no conclusive results about the incidence of the nitro substitution in their biological activity. A study on the reduction of 2-, 4- and 5-nitroimidazole drugs by hydrogenase 1 in *Clostridium pasteurianum*[6] revealed that the rate of reduction of the nitroimidazole compounds correlated with their one-electron reduction potential. However, the reduction rates for the drugs did not correlate with the antibacterial activity against *Clostridium pasteurianum*, suggesting that other factors are also important for determining the antimicrobial potencies of these compounds. Another study on the activity of nitroimidazoles against *Trichomonas vaginalis*[7] revealed that the potency of this activity follows the order 5-nitroimidazole $>$ 2-nitroimidazole $>$ 4-nitroimidazole. However, the description of the mutagenic and carcinogenic properties of some 2- and 5-nitroimidazoles have increased interest in the minor mutagenic 4-nitroimidazoles.[8-14]

The electrochemical studies of nitroimidazoles are mainly focused on the analytical determination of some pharmacologically important 5-nitroimidazoles, such as metronidazole, ornidazole, secnidazole, tinidazole, and megazol.[15-19] In addition, cyclic voltammetric studies of nitro radical anions produced from 5-nitroimidazole derivatives have been reported, demonstrating the usefulness of this technique to the study of nitro free radicals.[20-24] However, electrochemical studies of 4-nitroimidazole derivatives are scarce and restricted to a polarographic study of several 1,2-dialkyl-4-nitroimidazoles[25] and some electrochemical studies on the cyclic voltammetric behavior of 4-nitroimidazole in aportic[26] and protic media.[27] The results obtained from these studies differ widely, depending on the protic or aprotic medium. The one-electron reduction of 4-nitroimidazole in protic medium at alkaline pH produces a stable nitro radical anion on the time scale of the cyclic voltammetry. But, in aprotic medium, the nitro radical anion cannot be stabilized because of a rapid decay of the nitro radical produced by a fast protonation reaction by the starting 4-nitroimidazole (father-son type reaction).

In the scope of our current investigations to find new pharmacological important compounds that use the nitro radical anion as the active specie, we have synthesized 1-methyl-4-nitro-2-hydroxymethylimidazole (4-MNImOH) (Fig. 1), a new 4-nitroimidazole derivative substituted in positions 1 and 2. Our first aim is studying its electrochemical behavior with the focus on the formation and stability of the nitro radical anion in aqueous, mixed, and nonaqueous media. This is our first attempt to reveal the incidence of different substitutions in the 4-nitroimidazole ring to find nitro radical anions with improved pharmacological potency.

Experimental

Reagents and solutions.— 4-MNImOH was synthesized and characterized in our laboratory. All the other reagents employed were of analytical grade. Ultrapure water (18.2 MΩ cm) obtained from interchanged columns (Millipore Milli-Q system) was used.

Stock solutions of 4-MNImOH were prepared at a constant concentration of 10^{-2} M in ethanol. The polarographic and cyclic voltammetric working solutions were prepared by diluting the stock solution until final concentrations of 0.1 or 1 mM were obtained. The dilution solutions were Britton-Robinson buffer (0.1 M) for aqueous media, a mixture of 30/70: ethanol/Britton-Robinson buffer (0.1 M) or 60/40: dimethylformamide (DMF)/citrate buffer (0.015 M) KCl (0.3 M) for mixed media, and 100% DMF containing 0.1 M tetrabutylammonium perchlorate (TBAP), as supporting electrolyte, for nonaqueous solvent. The pH was adjusted with small aliquots of concentrated NaOH or HCl, respectively, in the aqueous and mixed solvents. All the polarographic experiments were obtained after a purge with N_2 for ten min in the cell before each run. All the experiments were carried out at room temperature.

Synthesis of 4-MNImOH.— 4-MNImOH (10 g, 0.09 mol) and potassium nitrate (20.5 g, 0.20 mol) were mixed and added slowly to sulfuric acid (5.4 mL, 0.10 mol) taking care not to exceed 50°C. The mixture was then maintained in a hot water bath for 3 h and stirred for 15 h at room temperature. The solution was carefully neutralized with sodium hydrogen carbonate. The product was extracted with ethyl acetate. The white solid was desiccated in vacuum. The yield of the recrystallized product in ethanol was 40%. ^{1}H NMR (300 MHz, D_2O): δ 3.2 (s, 1H, — OH) 3.8 (s, 3H, —N — CH_3) 4.5 (s, 2H, —CH_2—) 8.0 (s, 1H, —C ═ CH — N — CH_3) ^{13}C NMR (75 MHz, D_2O): 30.0 (—CH_3). 55.0 (—CH_2 — OH). 120.0 (O_2N — C ═ CH — N — CH_3). (2 × 149.8) (O_2N

[z] E-mail: asquella@ciq.uchile.cl

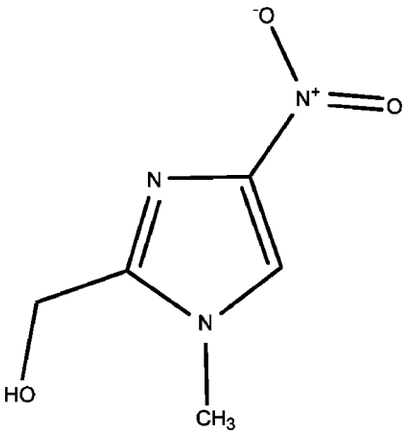

Figure 1. Chemical structure of 1-methyl-4-nitro-2-hydroxymethylimidazole (4-MNImOH).

— C(═CH) — N ═ C — CH_2OH). Elemental analysis for $C_5H_7O_3N_3$. Calculated: C: 38.22; H: 4.49; N: 26.74. Found: C: 37.90; H: 4.58; N: 26.52. melting point: 180-181°C Rf(benzene:methanol:acetic acid/45:8:1; Silica Gel 60 F, Merck) = 0.38

Apparatus.— Electrochemical experiments, differential pulse polarography (DPP), tast polarography, coulometry, and cyclic voltammetry were performed with a totally automated BAS-100 voltammetric analyzer attached to a PC with proper BAS 100W version 2.3 software for total control of the experiments and data acquisition and treatment. A controlling growth mercury electrode (CGME) polarographic stand was used with a dropping mercury electrode (DME) as the working electrode, a platinum wire as the counter electrode, and an Ag/AgCl electrode as the reference electrode. For differential pulse (DP) and tast polarography, the CGME stand was used in a CGME mode and for cyclic voltammetric experiments a static mercury drop electrode mode was used.

Spectrophotometric measurements were carried out with an ATI Unicam Model UV3, UV-vis spectrophotometer using a 1 cm quartz cell and equipped with a PC with the Vision acquisition and treatment program.

All pH measurements were carried out with a WTW microprocessor-controlled standard pH ion meter pMX 3000/pH equipped with a glass pH-electrode Sen Tix 81. The standard solutions used for calibration were WTW 4.006, 6.865, and 9.180. Measurements of pH were corrected according to the following equation:[28] $pH^* - B = \log U^o_H$, where pH^* equals $-\log a_H$ in the mixed solvent, B is the pH meter reading, and the term $\log U^o_H$ is the correction factor for the glass electrode, which was calculated from the different mixtures of DMF and aqueous solvent, according to a procedure reported previously.[29]

Methods.—*Polarography*.—Differential pulse polarograms were carried out with a DME under the following operating conditions: scan rate 4 mV/s, pulse amplitude 50 mV, pulse width 50 mV, sample width 17 ms, and drop time 1000 ms. TAST polarograms (TPs) were carried out using a DME with the following operating conditions: scan rate 4 mV/s, sample width 17 ms, and drop time 1000 ms.

Cyclic voltammetry.—For the kinetic analysis carried out in alkaline pH, the return-to-forward peak current ratio I_{pa}/I_{pc} for the reversible one-electron couple ($ArNO_2/ArNO_2^{\bullet -}$) was measured for each cyclic voltammogram (CV) according to the procedure described by Nicholson.[30] The scan rate (υ) ranged from 0.1 to 10 V s^{-1}. Using the theoretical approaches of Olmstead *et al.*,[31,32] the I_{pa}/I_{pc} values measured experimentally at each scan rate were inserted into a working curve to determine the parameter ω, which incorporates the effects of the rate constant, nitro compound concentration, and scan rate. A plot of ω *vs.* τ resulted in a linear relationship described by the equation $\omega = k_2 C^o \tau$, where k_2 is the second-order rate constant for the chemical reaction of $ArNO_2^{\bullet -}$, C^o is the nitro compound concentration, $\tau = (E_\lambda - E_{1/2})/\upsilon$, E_λ is the switching potential, and $E_{1/2}$ is the cyclic voltammetric half-wave potential; and υ is the sweep rate. Consequently, we can obtain the second-order rate constant for the decomposition of the nitro radical anion from the slope of the straight line ω *vs.* τ. The assumption that the decomposition of $ArNO_2^{\bullet -}$ follows second-order kinetics is supported by the linear relation between the kinetic parameter ω and the time constant τ.

Considering that the decay of $ArNO_2^{\bullet -}$ follows second-order kinetics, it is possible to calculate the half-lifetime, $t_{1/2}$, from the well-known equation, $t_{1/2} = (k_2 C^o)^{-1}$.

Coulometry.—Coulometry was carried out on a mercury pool electrode in 0.1 M Britton-Robinson buffer/ethanol 70/30 at pH 4 and 7. The potential applied was −530 and −676 mV for pH 4 and 7, respectively. Oxygen was removed with pure and dry presaturated nitrogen. A three-electrode circuit with an Ag/AgCl electrode was used as reference and a platinum mesh as a counter electrode. A BAS-CV 50 assembly was used to electrolyze the compound.

Solutions containing an accurately weighed amount of 4-MNIm-OH were subjected to successive short electrolysis for 6 min to ensure that all the original compound had been consumed. This procedure was followed until the charge obtained was equal to the background charge. The net charge was calculated by correcting the estimated background current. The total net charge corresponds to the sum of all the individual processes. The number of electrons is obtained by application of the well-known Coulomb law

$$Q = nFe \qquad [1]$$

where, Q = total net charge, n = mole number of electroactive specie in solution, F = Faraday's constant, and e = the number of electrons. The number of electrons was obtained after five runs at each pH.

Spectrophotometry: determination of pK'_a.—The sensitivity of the band at 304 nm with pH was used to determine the spectrophotometric apparent pK'_a. The pH solution was changed each 0.5 unit. The temperature was kept constant at 25°C. The concentration was 1×10^{-4} M for the entire pH scale. The value of pK_a' obtained was calculated by the linear regression method.[33]

Simulations.—Simulated CV curves were obtained by using the DIGISIM 2.1 CV simulator for Windows software (BAS, USA). The software was run using a Gateway 2000 PC.

Electrolysis: Electron spin resonance (ESR) measurements.—The ESR spectra from the nitroimidazole derivative were recorded *in situ* in the cavity of a Bruker ECS 106 spectrometer with 100 kHz field modulation at microwave band X (9.68 GHz) and at room temperature. The hyperfine splitting constants were considered to be accurate within 0.05 G. The electrolysis was performed by reduction at −900 mV in the ESR cell using a platinum wire electrode and an $Ag/AgCl/KCl_{sat}$ reference electrode. The concentration of the 4-MNImOH was 5 mM in DMF with 0.1 M of TBAP as supporting electrolyte.

Results and Discussion

The new synthesized compound, 4-MNImOH, was electrochemically reduced at the mercury electrode in different media, but its reduction was strongly affected by solvent and pH changes. In a totally aqueous medium containing 100% Britton-Robinson 0.1 M, only one signal in all the pH scale was detected (Fig. 2a). In the polarograms (mainly at acid pH) one can observe a polarographic maximum, probably because of the adsorption of the 4-MNImOH or some reaction product on the mercury surface. This assumption was

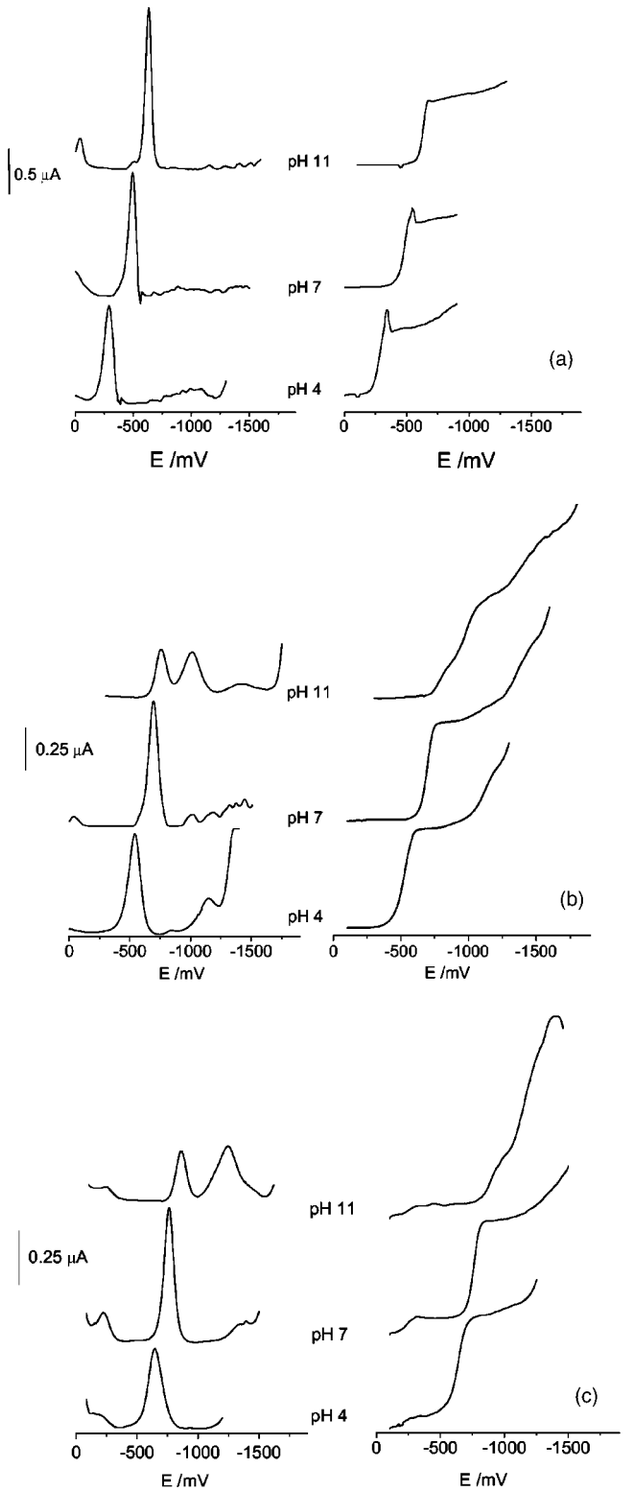

Figure 2. Differential pulse and tast polarograms of 4-MNImOH in (a) aqueous (0.1 M, Britton-Robinson buffer) and mixed: (b) DMF/citrate and (c) ethanol/Britton-Robinson buffer media at different pH.

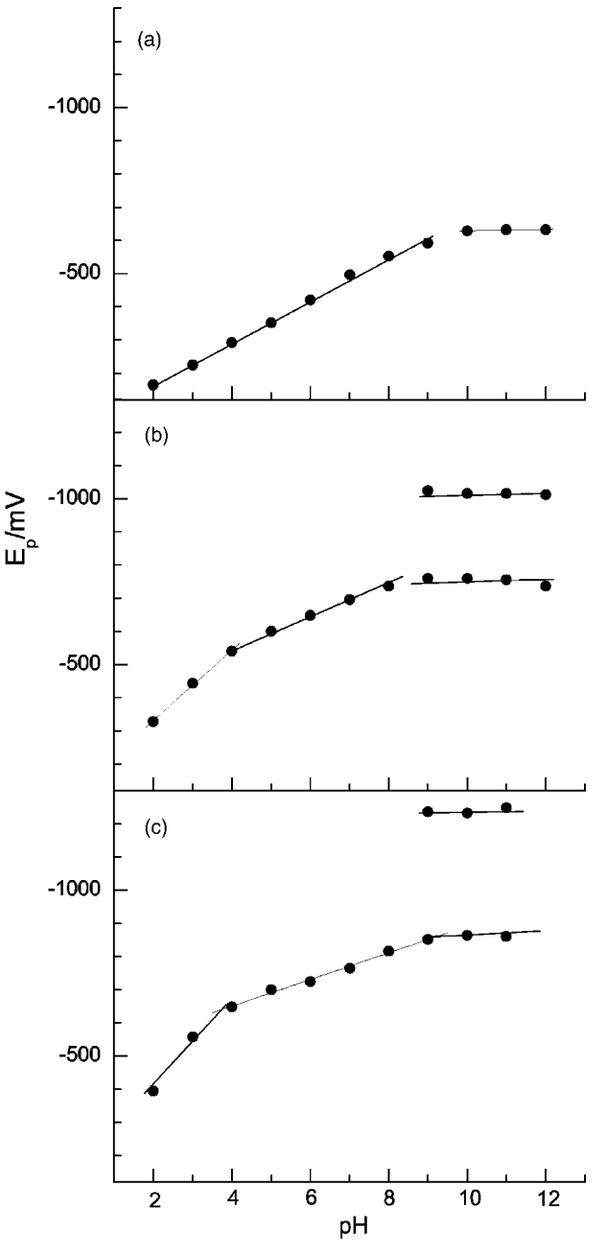

Figure 3. Peak potential dependence with pH in (a) aqueous medium (0.1 M, Britton-Robinson buffer) and mixed media: (b) DMF/citrate and (c) ethanol/Britton-Robinson buffers.

corroborated by electrocapillary curves (data not shown). Consequently, to avoid adsorption problems, we changed the electrolyte from aqueous to mixed media, adding a cosolvent to the buffer, *i.e.*, ethanol or DMF. As observed in Fig. 2b, the addition of a cosolvent permitted us to eliminate the polarographic maxima by avoiding adsorption problems in the electrodic process.

For mixed media, using either ethanol or DMF as cosolvent, the behavior was different, showing two peaks (or waves) at alkaline pH (Fig. 2b and c). In this medium, the peak appearing at acid pH splits into two peaks at pH $>$ 8. Under all conditions, the signal was pH dependent only up to pH 8, as observed in the potential peak *vs.* pH plot displayed in Fig. 3. At pH values beyond 8, the signals were pH independent, showing a change in the mechanism, meaning that there are no protons involved before the rate-determining step. Furthermore, the limiting currents obtained by tast polarography were pH independent, claiming a diffusion-controlled process.

From the E_P *vs.* pH plot, we can observe two different breaks: First, the previously mentioned break at pH 8 as a consequence of the change of mechanism and second the break at pH 3.5 due to the

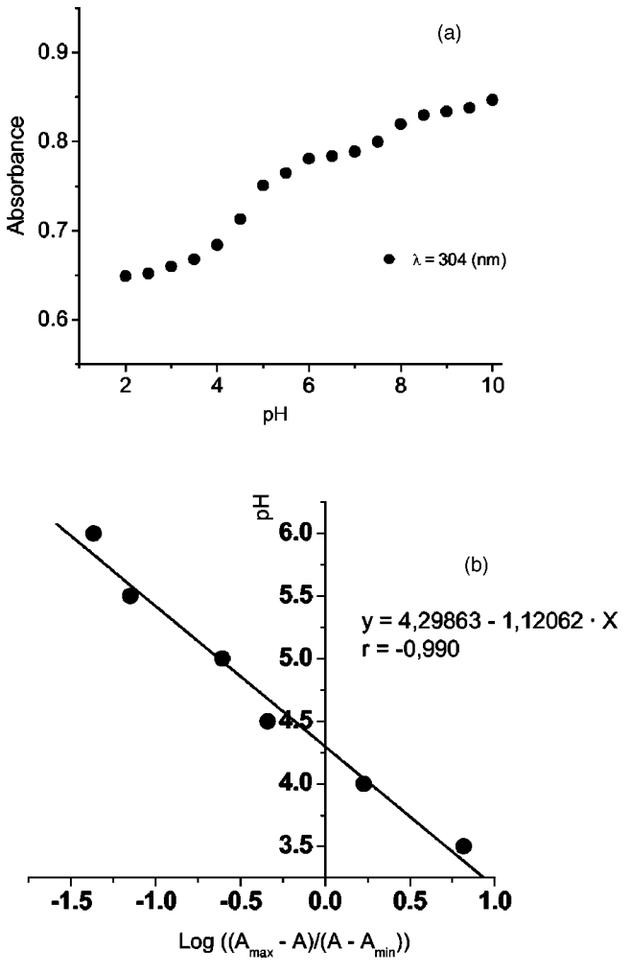

Figure 4. (a) Absorbance dependence of wave at λ = 304 nm of 4-MNImOH at different pH. (b) pK_a calculation according to linear regression method.

pK_a of the nitro-nitro protonated acid base equilibrium. To validate this point, we have calculated an equivalent pK_a value by using UV-spectrophotometry. UV spectra at different pH values reveal one pH-dependent absorption signal at 304 nm. The sensitivity of this signal to pH was used to determine the spectroscopic apparent pK_a (Fig. 4). The value of pK_a obtained for 4-MNImOH was 4.3, and it was calculated by the linear regression method. This value agrees with the break at 3.5 in the E_p *vs.* pH plot obtained with the DPP technique.

To elucidate the number of electrons transferred in the reduction process, we compared the limiting current of 4-MNImOH with the limiting current of equimolar solutions of the previously studied 4-nitroimidazole[27] under the same experimental conditions (pH < 7). 4-MNImOH showed the same value of the limiting current measured by tast polarography, which indicates that the same four electrons are transferred (data not shown). We also carried out coulometric experiments at pH 7, finding that the number of electrons transferred was slightly lower than four, as shown in Table I (3.7 ± 0.1). However, coulometric experiments at pH < 4 provided lower values, indicating that probably a part of the starting material is disappearing in a nonfaradaic process, as reported by Vianello *et al.*[26]

According to the well-known mechanism of 4-nitroimidazole,[27] we can assume that the observed irreversible peak at acid and neutral pH is due to the four-electron, four-proton reduction of the nitroimidazole group to yield the hydroxylamine derivative according to the following overall reaction

$$\text{R-NO}_2 + 4\bar{e} + 4\text{H}^+ \rightarrow \text{R-NHOH} + \text{H}_2\text{O} \quad [2]$$

In the same way, the equations describing the two new signals at alkaline pH correspond to

$$\text{R-NO}_2 + \bar{e} \leftrightarrows \text{RNO}_2^{\bullet -} \quad [3]$$

$$\text{RNO}_2^{\bullet -} + 3\bar{e} + 4\text{H}^+ \rightarrow \text{R-NHOH} + \text{H}_2\text{O} \quad [4]$$

The observed splitting at alkaline pH by using DPP was also confirmed by cyclic voltammetry. Figure 5 displays CVs at three different pH conditions. In acid and neutral media, it is possible to observe only one irreversible signal due to the four-electron, four-proton reduction of the nitro compound to generate the hydroxylamine derivative according to Reaction 2. In alkaline conditions, we can observe the reversible couple, I_a/I_c, corresponding to the one-electron reduction of the 4-MNImOH according to Reaction 3 and the irreversible peak II_c corresponding to the further reduction of the nitro radical anion to the hydroxylamine derivative, according to Reaction 4. Furthermore, in the reverse sweep, an anodic peak,

Table I. DPP cathodic peak potentials ($E_{p,c}$) obtained from 4-MNImOH solutions in ethanol/Britton-Robinson buffer.

pH	$-E_{p,c}$ (mV)	n[a]
4	530	3.3 ± 0.1
7	676	3.7 ± 0.1

[a] The number of electrons transferred (n) was coulometrically obtained as the mean of five runs.

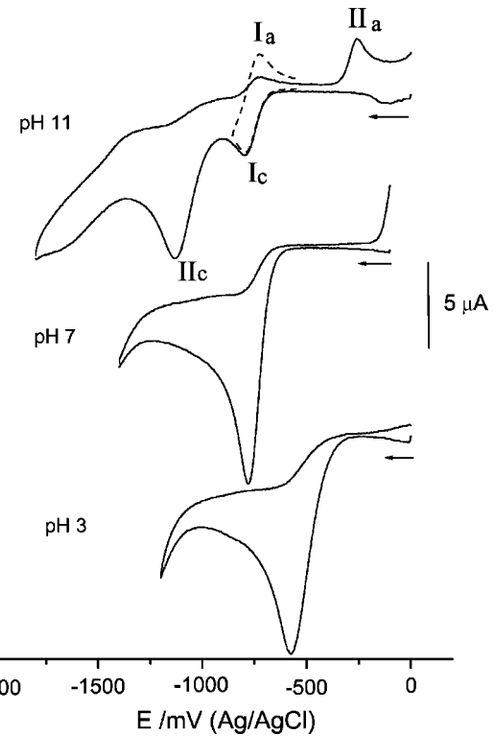

Figure 5. CVs of 1 mM 4-MNImOH in ethanol/Britton-Robinson buffer 0.1 M at different pH values. Sweep rate 1 V s^{-1}. Dashed line shows a short sweep with $RNO_2/RNO_2^{\bullet -}$ isolated couple. Arrow indicates the scan direction.

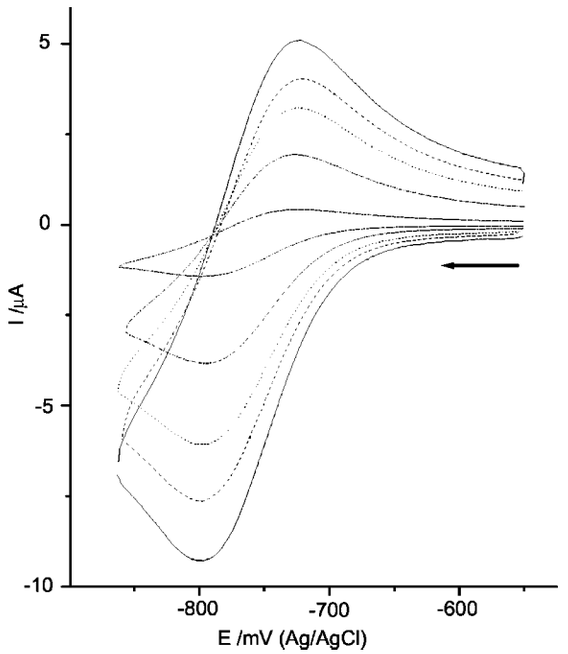

Figure 6. CVs showing the reversible couple due to the one-electron reduction of 4-MNImOH in nonaqueous medium at different sweep rates. Arrow indicates the scan direction.

II_a, at −256 mV was observed. This corresponds to the two-electron oxidation of the hydroxylamine derivative, which forms during the first negative-going sweep, to form the nitroso derivative

$$\text{R-NHOH} \rightarrow \text{R-NO} + 2\overline{e} + 4H^+ \qquad [5]$$

Adjusting the switching potential appropriately, we can study the nitro/nitro radical anion couple ($RNO_2/RNO_2^{\bullet -}$) in isolation (dashed line in Fig. 5). To complete the electrochemical characterization to study the properties of the nitro radical anion in the absence of protonation reactions, we also studied an aprotic medium. In a totally nonaqueous medium containing 100% DMF with 0.1 M TBAP, we obtained a perfectly isolated couple (Fig. 6) corresponding to the one-electron reduction of the nitroimidazole parent compound to produce the nitroimidazole radical anion derivative. The generation of the nitro radical anion derivative was also characterized by ESR. The radical was prepared *in situ* by controlled potential electrolysis at −900 mV *vs.* Ag/AgCl in DMF. The nitroimidazole free radical displays a well-resolved ESR spectrum (Fig. 7). The interpretation of the ESR spectra led us to determine the coupling constants for all

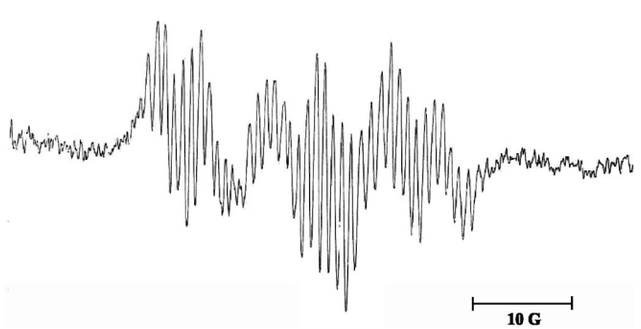

Figure 7. ESR experimental spectrum of radical anion of 4-MNImOH in DMF. Spectrometer conditions: microwave frequency 9.68 GHz, microwave power 20 mW, modulation amplitude 0.2 G, scan rate 1.25 G/s, time constant 0.5 s, number of scans: 15.

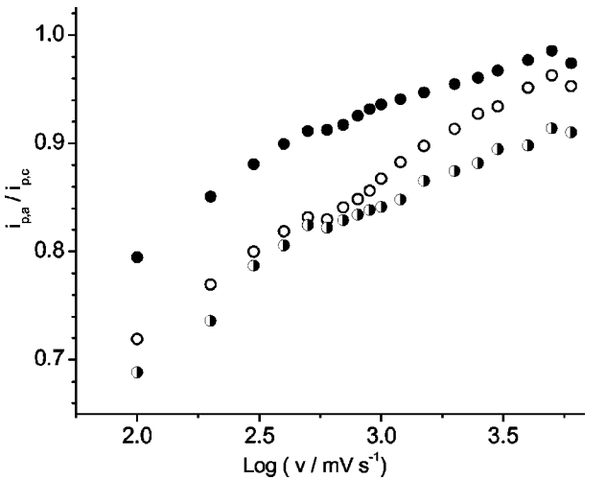

Figure 8. Current ratio dependence on sweep rates of $RNO_2/RNO_2^{\bullet -}$ couple from CVs of 1 mM 4-MNImOH in ethanol/Britton-Robinson buffer at different pH values.

magnetic nuclei. Thus, the obtained hyperfine constants were $a_N(NO_2)$ = 14.0 G, a_H = 4.5 G, a_N (ring) = 2.0 G, a_N (ring) = 1.2 G, and a_H (CH_3) = 0.4 G.

Using the preceding cyclic voltammetric response, we can study the kinetic stability of the nitro radical anion species in all the media conditions. In Fig. 8, we can observe the effect of different sweep rates on the current ratio, showing a similar general trend in all media, *i.e.*, the $i_{p,a}/i_{p,c}$ current ratio increases as the scan rate is increased. These results fulfill the requirements for an irreversible chemical reaction following a reversible charge-transfer step according to the classical Nicholson criteria,[30] but we also found that the current ratio was dependent on the 4-MNImOH concentration (data not shown), implying a second-order chemical step. To check what kind of second-order chemical reaction is involved, we tried both disproportionation and dimerization approaches. Using the theoretical approach of Olmstead *et al.* for disproportionation[31] and dimerization,[32] we calculated the second-order rate constant, k_2, obtaining different values depending on whether disproportionation or dimerization was assumed. To decide what type of mechanism adjusts better with the real mechanism, we used the simulation procedure described in a previous paper.[34] That procedure is based on the comparison between experimental and simulated curves, wherein the latter is simulated by both disproportionation and dimerization. In Fig. 9, we can observe a comparison of experimental and simulated CVs for 4-MNImOH considering either disproportionation or

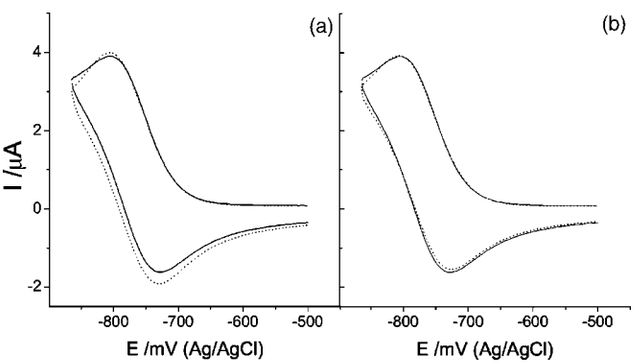

Figure 9. Comparison of experimental (solid line) and simulated (dashed line) CVs for 4-MNImOH in mixed medium considering (a) dimerization or (b) disproportionation as the chemical coupled reaction.

Table II. Disproportionation and dimerization rate constant and half-lifetime values for $RNO_2/RNO_2^{\bullet-}$ couple obtained for 4-MNlmOH in different media.

Medium	$10^{-3}k_2$ (M^{-1} s^{-1})	$t_{1/2}$ (s)
B/EtOH pH 10 [a]	5.97 ± 0.25 (disp)	0.17
B/EtOH pH 11	1.93 ± 0.24 (disp)	0.5
B/EtOH pH 12	2.23 ± 0.23 (disp)	0.45
DMF/citrate[b] pH 10	13.64 ± 2.13 (disp)	0.08
DMF	1.46 ± 0.11 (dim)	0.69

[a] 30/70: Ethanol/Britton-Robinson buffer (0.1 M).
[b] 60/40: DMF/citrate buffer (0.015 M), KCl (0.1 M).

dimerization in a mixed medium. From these results, one can see that in the case where disproportionation was considered, the fit between the simulation and experimental curves was clearly better. Moreover, we have obtained optimum correlation between experimental and simulated curves for disproportionation in mixed media (using ethanol or DMF as cosolvents) and dimerization in nonaqueous medium (100% DMF). Consequently, the change from mixed to nonaqueous medium produces a change in the decay mechanism of the radical anion passing from disproportionation in mixed medium to dimerization in a nonaqueous medium. This finding is in accord with previous results obtained for nitro radical anion produced from some nitrofuran derivatives.[34]

The obtained kinetic second-order rate constant, k_2, and the corresponding half-lifetime values for the nitro radical anion from 4-MNImOH in different media are shown in Table II. From these values, we can state that, as expected, the nitro radical anion was more stabilized in a totally nonaqueous medium, confirming that its optimal environment is the lipophilic one. However, when we compared different buffers at the same pH, we found different stabilities for the radical, showing that the proton activity is not the only factor promoting its decay. For the same buffer at strong alkaline conditions (pH 11-12), the results were statistically similar, showing the same stability. Furthermore, in Table III we compared the results obtained for 4-MNImOH with those obtained with 4-nitroimidazole. From these results, we can conclude that the new compound 4-MNImOH is more easily reducible than the 4-nitroimidazole, thus requiring less energy to produce the nitro radical anion. However, from the kinetic constants, we can conclude that the nitro radical anion from 4-MNImOH is less stable than the corresponding free radical from 4-nitroimidazole. Both of these results point to a product with enhanced capabilities to become a more useful bioactive compound than the parent molecule, 4-nitroimidazole. The new compound would be more suitable for enzymatic reduction and less toxic to the host than 4-nitroimidazole, meaning it would be a potential new bioactive 4-nitroimidazole compound.

Conclusions

The new synthesized compound, 4-MNImOH, was easily reducible in aqueous, mixed, and nonaqueous media, but only in mixed and nonaqueous media was it able to generate nitro radical anions capable of being detected in the time scale of the cyclic voltammetric technique. The nitro radical decayed according to a second-order chemical reaction, disproportionation in mixed media, and dimerization in a totally nonaqueous medium.

Table III. Comparison between cathodic potential peak values and nitro radical anion decay constants for one-electron reduction of 4-nitroimidazole and 4-MNImOH obtained in 30/70: ethanol/Britton-Robinson buffer (0.1 M), pH 10.

Compound	$-E_{p,c}$ (mV)	10^{-3} k_2 (M^{-1} s^{-1})
4-Nitroimidazole	850	2.82 ± 0.1
4-MNImOH	760	5.97 ± 0.2

According to the results, the new substituted 4-nitroimidazole derivative was more easily reducible than the nonsubstituted parent compound, and the corresponding nitro radical anion decays more rapidly than the nonsubstituted nitro radical. Both of these aspects are promising for finding more efficient bioactive compounds with sufficiently low reduction potentials in order to be enzymatically reduced and at the same time to have radicals not stable enough to produce damage in the host.

In addition, we believe that for compounds that act via free radicals, *e.g.*, nitroimidazole derivatives, the voltammetric determination of simple parameters, such as the reduction potential and stability constants, may be a very good option to carry out an *in vitro* first step screening to select a bioactive compound, avoiding more expensive and tedious procedures.

Acknowledgments

This research was supported by FONDECYT (grants 8000016 and 1050767). We are also grateful to Professor Claudio Olea (CEPEDEQ) for ESR measurements and Professor C. Telha for the English revision.

The University of Chile assisted in meeting the publication costs of this article.

References

1. D. I. Edwards, *J. Antimicrob. Chemother.*, **31**, 9 (1993).
2. P. Wardman, *Environ. Health Perspect.*, **64**, 309 (1985).
3. F. Riché, A. du Molinet, S. Sèpe, L. Riou, D. Fagret, and M. Vidal, *Bioorg. Med. Chem. Lett.*, **11**, 71 (2001).
4. D. I. Edwards, *Biochem. Pharmacol.*, **35**, 53 (1986).
5. W. Bone, N. Jones, G. Kamp, C. Yeung, and T. Cooper, *J. Reprod. Fertil.*, **118**, 127 (2000).
6. D. Church, H. Rabin, and E. Laishley, *J. Antimicrob. Chemother.*, **25**, 15 (1990).
7. C. Cosar, C. Crisan, R. Horclois, R. M. Jacob, J. Robert, S. Tchelitcheff, and R. Vaupre, *Arzneim.-Forsch.*, **16**, 23 (1966).
8. M. D'Auria, F. D'Onofrio, J. Suwinski, and K. Swierczek, *Tetrahedron*, **49**, 3899 (1993).
9. J. Suwinski, W. Szczepankiewicz, and M. Widel, *Arch. Pharm. (Weinheim)*, **325**, 317 (1992).
10. G. Elizondo, M. Gonsebatt, A. M. Salazar, I. Lares, P. Santiago, J. Herrera, E. Hong, and P. Ostrosky-Wegman, *Mutat Res.*, **370**, 75 (1996).
11. S. Gomez-Arroyo, S. Melchor-Castro, R. Villalobos-Pietrini, E. Melendez-Camargo, H. Salgado-Zamora, and M. Campos-Aldrete, *Toxicol. in Vitro*, **18**, 319 (2004).
12. S. Khabnadideh, Z. Rezaei, A. Khalafi, R. Bahrinajafi, R. Mohamadi, and A. Farrokhroz, *Bioorg. Med. Chem. Lett.*, **13**, 2863 (2003).
13. N. Boechat, A. Carvalho, E. Fernandez-Ferreira, R. Soares, A. Souza, D. Gibaldi, M. Bozza, and A. Pinto, *Cytobios*, **105**, 83 (2001).
14. T. Chu, S. Hu, B. Wei, Y. Wang, X. Liu, and X. Wang, *Bioorg. Med. Chem. Lett.*, **14**, 747 (2004).
15. D. Dumanovic, J. Volke, and V. Vajgand, *J. Pharm. Pharmacol.*, **18**, 507 (1966).
16. S. A. Ozcan, Z. Senturk, and I. Biryol, *Int. J. Pharm.*, **157**, 137 (1997).
17. A. Radi, S. El-Laban, and A.-G. El-Kourashy, *Electroanalysis*, **9**, 625 (1997).
18. S. A. Okzan, *Analusis*, **25**, 130 (1997).
19. S. Bollo, L. J. Núñez-Vergara, M. Bontá, G. Chauviere, J. Perie, and J. A. Squella, *Electroanalysis*, **13**, 936 (2001).
20. J. H. Tocher and D. I. Edwards, *Free Radical Res. Commun.*, **16**, 19 (1992).
21. D. Barety, B. Resibois, G. Vegoten, and Y. Moschetto, *J. Electroanal. Chem. Interfacial Electrochem.*, **162**, 335 (1984).
22. S. Bollo, L. J. Núñez-Vergara, M. Bontá, G. Chauviere, J. Perie, and J. A. Squella, *J. Electroanal. Chem.*, **511**, 46 (2001).
23. M. L. Arguelho, G. Silva, and N. Stradiotto, *J. Electrochem. Soc.*, **148**, D1 (2001).
24. P. C. Mandal, *J. Electroanal. Chem.*, **570**, 55 (2004).
25. D. Dumanovic, J. Jovanovic, D. Suznjevic, M. Erceg, and P. Zuman, *Electroanalysis*, **4**, 889 (1992).
26. S. Roffia, C. Gottardi, and E. Vianello, *J. Electroanal. Chem. Interfacial Electrochem.*, **142**, 263 (1982).
27. J. Carbajo, S. Bollo, L. J. Núñez-Vergara, A. Campero, and J. A. Squella, *J. Electroanal. Chem.*, **531**, 187 (2002).
28. A. G. Gonzalez, F. Pablos, and A. Asuero, *Talanta*, **39**, 91 (1992).
29. A. Asuero, M. A. Herrador, and A. G. Gonzalez, *Talanta*, **40**, 479 (1993).
30. R. S. Nicholson, *Anal. Chem.*, **36**, 1406 (1964).
31. M. L. Olmstead and R. S. Nicholson, *Anal. Chem.*, **41**, 862 (1969).
32. M. L. Olmstead, R. G. Hamilton, and R. S. Nicholson, *Anal. Chem.*, **41**, 260 (1969).
33. K. A. Connors, *Curso de análisis farmacéutico (Ensayo del medicamento)*, Editorial reverté, SA Barcelona, Spain, p. 145 (1980).
34. M. Bontá, G. Chauviere, J. Perie, L. J. Núñez-Vergara, and J. A. Squella, *Electrochim. Acta*, **47**, 4045 (2002).

Full Paper

Nitroradical Anion Formation from some Iodo-Substituted Nitroimidazoles

S. Bollo,[a] *L. J. Núñez-Vergara*,[a] *C. Barrientos*,[a] *J. A. Squella**[a]

[a] Bioelectrochemistry Laboratory, Chemical and Pharmaceutical Sciences Faculty, University of Chile, P. O.Box 233 Santiago 1, Chile
*e-mail: asquella@ciq.uchile.cl

Received: January 31, 2005
Final version: April 6, 2005

Abstract

The electrochemical behavior of iodo nitroimidazole derivatives such as 1-methyl-4-iodo-5-nitroimidazole (M-I-NIm) and 1-methyl-2,4-diiodo-5-nitroimidazole (M-I_2-NIm) and the parent compound 1-methyl-5-nitroimidazole (M-NIm), was studied in protic, mixed and non-aqueous media. The electrochemical study was carried out using Differential Pulse Polarography (DPP), Cyclic Voltammetry (CV), Differential Pulse Voltammetry (DPV) and coulometry and as working electrodes mercury and glassy carbon were used. As can be expected, in all media, the effect of introduce iodo as substituent in the nitroimidazole ring produced a decrease of the energy requirements of the nitro group reduction. Certainly, this fact can be explained by the electron withdrawing character of the iodo substituent that acts diminishing the electronic density on the nitro group thus facilitating their reduction. In all the studied media the reduction of M-NIm produced a detectable signal for a nitro radical anion derivative. In the case of M-I-NIm the nitro radical anion was only detectable in both mixed and non-aqueous media. On the other hand the nitro radical anion for the M-I_2-NIm was detected only in non-aqueous medium. When glassy carbon electrode was used as the working electrode in a mixed medium a detectable nitro radical anion derivative appeared for all compounds, thus permitting an adequate comparison between them. The obtained values of k_2 for M-NIm, M-I-NIm and M-I_2-NIm in non-aqueous medium were 5.81×10^2, 132×10^2 and 1100×10^2 M^{-1} s^{-1}, respectively. From the obtained k_2 and $t_{1/2}$ values in this medium, it is concluded that there is a direct dependence between the presence of iodo substitution in the nitroimidazole ring with the stability of the nitro radical anion.

Keywords: Nitro radical anion, Nitroimidazoles, Reduction, Decay constants

1. Introduction

The investigation of different types of nitrocompounds has been a very active research topic during several years probably due to its many applications. There are a lot of nitrocompounds which possess interesting biological properties such as antimicrobial [1, 2], antituberculosis [3], anti-protozoa and anticancer [4, 5] activities. Increasingly, the treatment of protozoa infections, such as Chagas disease, has become an important problem due to the emergence of drug resistance. Consequently, a series of nitro derivatives has been synthesized with the aim of finding new drugs. In previous studies, a 5-nitroimidazole derivative, megazol, showed a good activity against *Trypanosoma cruzi*, the causative agent of Chagas disease, better than the classic antichagasic drugs nifurtimox and benznidazole [6]. In that work the results indicated that nifurtimox and related compounds act as redox cycles, whereas, the 5-nitroimidazole megazol essentially acts as thiol scavenger particularly for trypanothione, the cofactor for trypanothione reductase, an essential enzyme in the detoxification process. The mechanism of megazol would imply the nitro radical anion formation which is converted to the nitroso derivative as a consequence of a disproportionation reaction.

In view of the good results obtained with megazol, a renewal interest in to obtain new synthesized nitroimidazole compounds required for pharmacological and toxicological investigations have been generated. In this way, a series of iodo nitroimidazole derivatives (Figure 1) were generated in the new synthetic route for obtaining megazol and are being studied for possible pharmacological applications.

In our laboratory we have conducted several electrochemical studies of nitro compounds in order to characterize the redox activation that implies the one electron transfer of the nitro group to produce the nitro radical anion [7, 8 – 11] In such studies we characterized the reduction potential of the $RNO_2/RNO_2^{\bullet -}$ couple, a well recognized parameter as a very appropriate index to define the type of biological

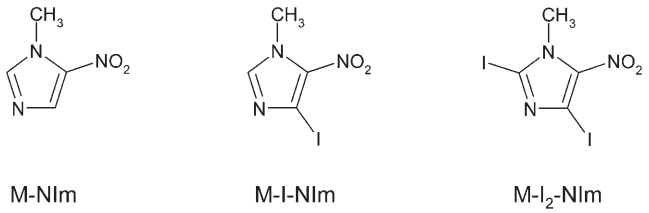

Fig. 1. Chemical structure of iodo nitroimidazole derivatives 1-methyl-4-iodo-5-nitroimidazole (M-I-NIm), 1-metil-2,4-diiode-5-nitroimidazole (M-I_2-NIm) and the parent compound 1-methyl-5-nitroimidazole (M-NIm).

  DOI: 10.1002/elan.200503271

properties of the different nitrocompounds as was demonstrate by Olive [12] on a series of nitroheterocyclic compounds. Furthermore, in those previous studies was revealed the voltammetric feasibility of quantitatively characterize the formation and stabilization of the nitro radical anion.

In the present work we are interested in to study the electrochemical significance of adding one or two iodo atoms in the 1-methyl-5-nitroimidazole moiety. The study will be mainly focused to reveal the effect of these iodo substituents in the formation and stability of the nitro radical anion derivatives in different media.

2. Experimental

2.1. Reagents and Solutions

All the compounds were synthesized and characterized by one of us. All the other reagents employed were of analytical grade.

Stock solutions of each compound were prepared at a constant concentration of 0.025 M in DMF. The polarographic and cyclic voltammetric working solutions were prepared by diluting the stock solution until to obtain final concentrations of 0.1 and 1 mM respectively. A mixture of 30/70: ethanol/Britton-Robinson buffer (KCl 0.3 M) for a protic medium and 60/40:DMF/citrate buffer (0.015 M) + KCl (0.3 M) for mixed media were used. The pH was adjusted with little aliquots of concentrated NaOH or HCl, respectively. Dimethylformamide (DMF) and tetrabutyl ammonium perchlorate (TBAP) as solvent and supporting electrolyte were used in non-aqueous media.

2.2. Apparatus

Electrochemical experiments were performed with a totally automated BAS CV-50W voltammetric analyzer. All experiments were carried out at a constant temperature of 25.0 $\pm$ 0.1 °C using a 10 mL thermostated cell. A mercury drop electrode (Controlling Growth Mercury Electrode, CGME stand of BAS) with a drop area of 0.42 mm^2 and a glassy carbon as working electrodes and a platinum wire as a counter electrode were used. All potentials were measured against Ag/AgCl 3 M.

For Differential Pulse Polarography (DPP) the CGME stand was used in a CGME mode, for cyclic voltammetric experiments the CGME stand was used as SMDE mode (static mercury drop electrode) and for DPV the GCME stand was used as C2 mode, i.e., for solid electrode operation, under the following conditions: scan rate 20 mV/s, pulse amplitude 50 mV, pulse width 50 mV, sample width 20 ms and pulse period 200 ms.

For the kinetic analysis, the return-to-forward peak current ratio I_{pa}/I_{pc} for the reversible one electron couple ($RNO_2/RNO_2^{\bullet -}$) was measured for each individual cyclic voltammogram according to the procedure described by Nicholson [13]. The scan rate was varied between 0.1 to 10 V/s.

Using the theoretical approach of Olmstead et al. for dimerization or disproportionation [14, 15], the I_{pa}/I_{pc} values measured experimentally at each scan rate were inserted into a working curve to determine the parameter ω, which incorporates the effects of rate constant, drug concentration and scan rate. A plot of ω versus τ resulted in a linear relationship described by the equation

$$\omega = k_2 C_o \tau$$

Where k_2 is the second-order rate constant for the decomposition of $RNO_2^{\bullet -}$, C_o is the nitrocompound concentration and $\tau = (E_\lambda - E_{1/2})/\nu$, where E_λ is the switching potential, $E_{1/2}$ is the half wave potential and ν is the scan rate. Consequently we can obtain the second order rate constant for the decomposition of the nitro radical anion from the slope of the straight line ω versus τ. The assumption that the decomposition of $RNO_2^{\bullet -}$ follows second-order kinetics is supported by the obtained linearity between the kinetic parameters ω and τ.

3. Results and Discussion

In order to investigate the influence of electron withdrawing substituents in the nitroimidazole moiety on the electrochemical reduction of the nitro group we have synthesized two iodo derivatives (Figure 1).

3.1. Electrochemical Behavior in Protic Medium

In protic medium (0.1 M Britton-Robinson buffer + 0.3 M KCl / EtOH : 70/30) all compounds were reduced at dropping mercury electrode (DME), producing signals which were dependent of the number of iodo substituents in the molecule. Figure 2 shows the differential pulse polarograms (DPP) at four different pHs for each nitroimidazole derivative. A direct relation between the number of iodo and the complexity of the signals can be observed. In this way, M-NIm (Figure 2A) shows one reduction signal between pHs 2 and 7.5 and two signals above pH 8. This behaviour was previously observed [16] for the 4-nitroimidazole reduction in protic medium wherein the signal I corresponds to the 4-electron and 4-protons nitro reduction to form the hydroxylamine derivative. This mechanism was corroborated by coulometry where at pH 5 the calculated total transferred electrons were 4.02 $\pm$ 0.065. Consequently, the overall mechanism at acid and neutral media is described by:

$$RNO_2 + 4e^- + 4H^+ \rightarrow RNHOH + H_2O \quad (1)$$

When the pH increased a splitting of this signal is produced, being possible to obtain an isolated signal due to the one electron reduction of the nitro group, to produce the nitro

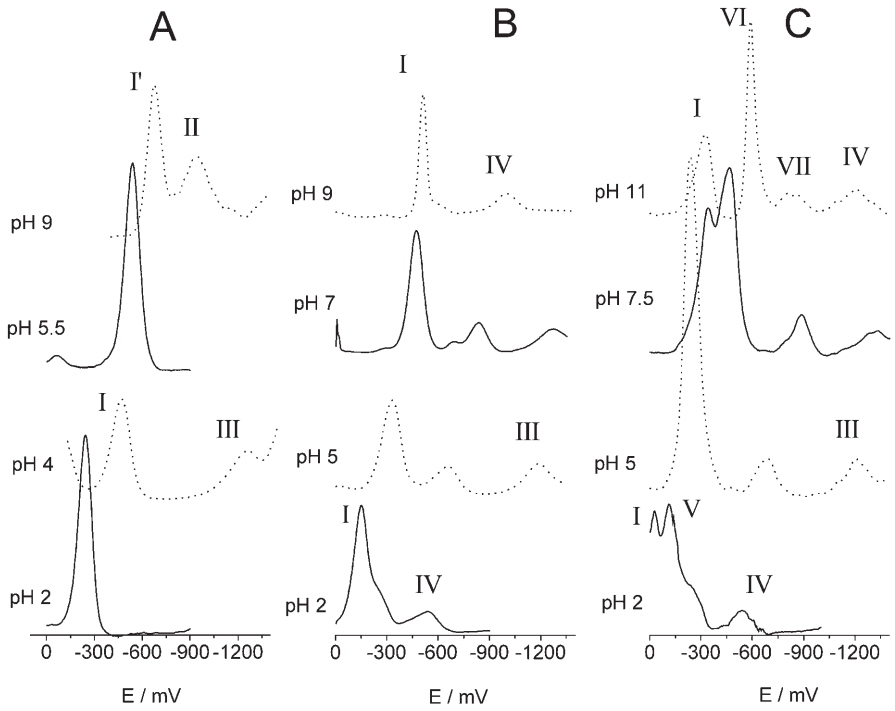

Fig. 2. Differential pulse polarograms of M-NIm (A), M-I-NIm (B) and M-I_2-NIm (C) in ethanol/Britton-Robinson buffer medium at different pHs.

radical anion, which is further reduced to the hydroxylamine derivative (signals I' and II in Fig. 2A):

$$RNO_2 + e^- \rightleftharpoons RNO_2^{\bullet -} \quad (2)$$

$$RNO_2^{\bullet -} + 3e^- + 4H^+ \rightarrow RNHOH + H_2O \quad (3)$$

The above observed behavior was corroborated by cyclic voltammetry at the mercury electrode. At pH 5 (Fig. 3A) we can observe two reduction peaks, peak I due to the four electron reduction of the nitro group to the hydroxylamine derivative, and peak III, at sufficiently higher potentials, due to the C=N reduction of the imidazole ring. In the reverse scan a new peak IIa, due to the hydroxylamine oxidation, is observed according to the following equation:

$$RNHOH \rightleftharpoons RNO + 2e^- + 2\ H^+ \quad (4)$$

Changing the pH to the basic zone (Fig. 3B) a splitting of peak I in the new peaks I′c and IIc is observed, also a new anodic peak I'a appear, which correspond to the nitro radical anion oxidation. In this Figure a short cyclic voltammogram is included (dotted line) showing the isolation of the redox couple $RNO_2/RNO_2^{\bullet -}$. Furthermore, from this Figure we can observe a notorious increase of the oxidation current I'a, which is due to the nitro radical anion oxidation, when short and large scans are compared. This result agree with the fact that in the case of the short scan the radical remains much less time in the immediacy of the electrode before oxidizing in the back scan thus avoiding further reactions.

Selecting appropriately the switching potential is possible to work with the couple in isolation which is characterized by its current ratio values, $I_{p,a}/I_{p,c}$. For M-NIm in basic medium an EC mechanism was determined since the $I_{p,a}/I_{p,c}$ value increases concomitant the sweep rate of the experiment was increased too (Figure 3C).

According to the literature information [17] the chemical reaction coupled to the electron transfer in the EC mechanism in a basic protic medium correspond to a disproportionation reaction (Eq. 5) which can be characterized by its corresponding rate constant, k_2:

$$2\ RNO_2^{\bullet -} + 2H^+ \rightarrow RNO_2 + RNO + H_2O \quad (5)$$

According to the previously informed methodology [14] we have obtained the decay rate constant (k_2) at different pH values. Figure 3D shows the correlation existing between k_2 values and the pH of reaction medium, concluding that the nitro radical anion is more unstable whereas the pH is lower. Moreover, the dependence of the k_2 value with pH obeys the following regression curve: $\log k_2 = 6.36 - 0.27\ pH$ ($r = 0.993$). By extrapolation from this relation the k_2 value at different pHs was obtained. In this way and considering that the physiological aqueous pH is 7.4, the extrapolated rate constant was $2.2 \times 10^4\ M^{-1}s^{-1}$. Comparing this value to that previously obtained using the same procedure for 4-NIm, $7.48 \times 10^5\ M^{-1}s^{-1}$ [16] it is clear that the methyl substitution in position 1 of the imidazole ring produces a more stable nitro radical anion.

When iodo was incorporated in the M-NIm moiety producing both M-I-NIm and M-I_2-NIm compounds, a

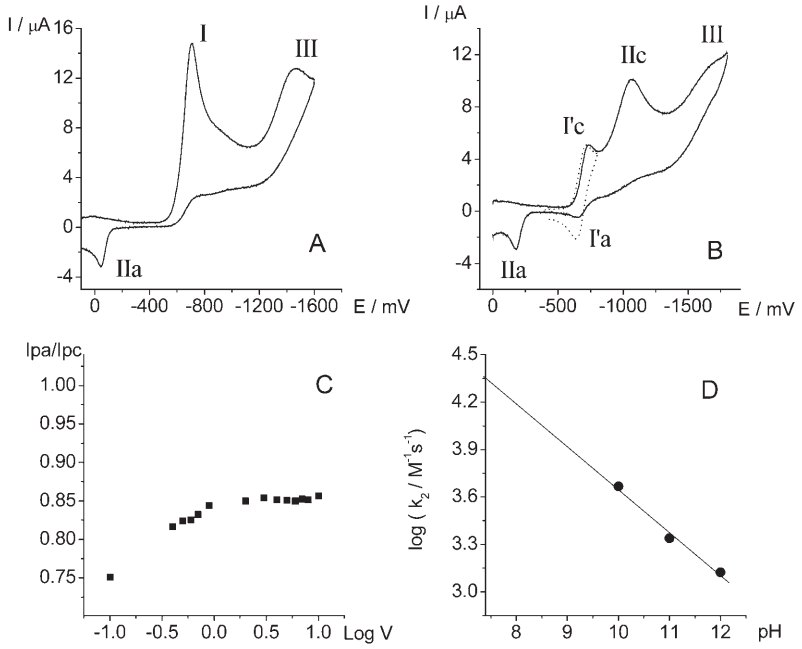

Fig. 3. Cyclic voltammograms on mercury electrode of 1 mM M-NIm in ethanol/Britton-Robinson buffer 0.1 M at pH 5 (A) and pH 10 (B). Sweep rate 1 Vs^{-1} . Dashed line shows a short sweep with the $RNO_2/RNO_2^{\bullet -}$ isolated couple. C) Current ratio dependence on sweep rates of the $RNO_2/RNO_2^{\bullet -}$ couple from cyclic voltammograms of 1mM M-NIm in ethanol/Britton Robinson buffer at pH 10. D) pH dependence of the natural decay, k_2, of the nitro radical anion.

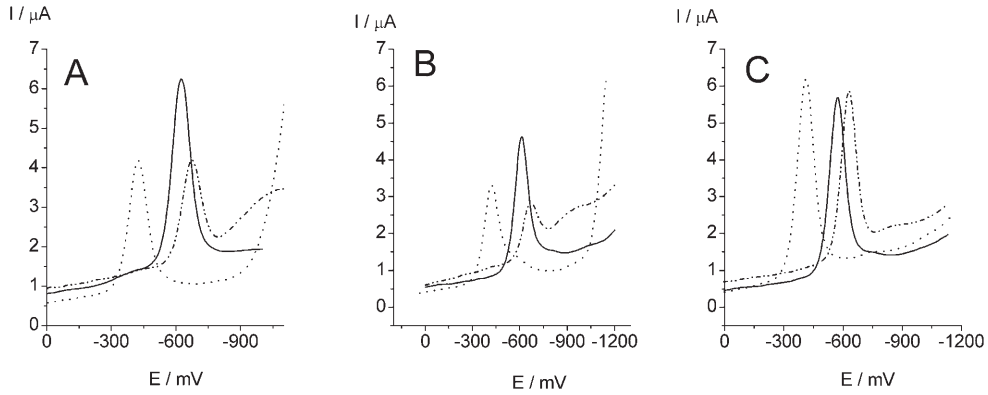

Fig. 4. Differential pulse voltammograms of M-NIm (A), M-I-NIm (B) and M-I_2-NIm (C) in ethanol/Britton-Robinson buffer medium at different pHs obtained using glassy carbon electrode. (·····) pH 3; (—) pH 7 and (·· – ·· – ··) pH 10.

completely different redox behavior was observed in comparison with M-NIm. The presence of iodo in the molecule produced not reliable polarograms with a series of minor peaks probably due to an interference between mercury and iodo (Fig. 2B, C).

With the aim of deepening in the redox mechanism, a series of cyclic voltammetric experiments were conducted. A very sharp peaks were obtained then we can conclude the adsorptive character of the nitro reduction peak (data not shown). Also, the slope of log I_p vs. log V plots, were very close to 1 for both compounds, corroborating the strong adsorption of the molecule over the mercury electrode.

Thinking that the adsorption phenomenon could be due to interactions between mercury and the iodo atoms, we change the electrode material by glassy carbon, to avoid this interaction. Surprisingly the observed voltammogram was modified considerably when carbon was changed by mercury as the electrode material. Figure 4 shows the differential pulse voltammograms at pHs 3, 7 and 10, revealing only one signal, which is due to the 4-electrons and 4-protons nitro reduction. Consequently no distortions and new signals in the voltammograms for M-I-NIm and M-I_2-NIm were observed. Consequently we can confirm the hypothesis that an interaction between mercury and iodo affects considerably the voltammetric response over mercury in aqueous protic medium. With the objective of quantify the effect of the iodo substitutions on the energetic of the nitro reduction process, we have calculated the corresponding peak potential values. The potential peak values for the nitro group reduction at glassy carbon electrode are shown

Table 1. Peak potentials values (mV), obtained from cyclic voltammetric experiments using glassy carbon electrodes at different pH in protic medium.

pH	M-NIm	M-I-NIm	M-I_2-NIm
4	−432	−422	−412
8	−620	−612	−572
12	−672	−667	−630

Table 2. Peak potentials values (mV), obtained from cyclic voltammetric experiments using glassy carbon electrodes, for signal Ic and IIc at different pH in mixed medium.

pH	M-NIm		M-I-NIm		M-I_2-NIm	
	Ic	IIc	Ic	IIc	Ic	IIc
4	751	–	−735	–	−646	–
8	−855	−1329	−836	–	−778	–
12	−839	−1377	−825	−1306	−782	−1189

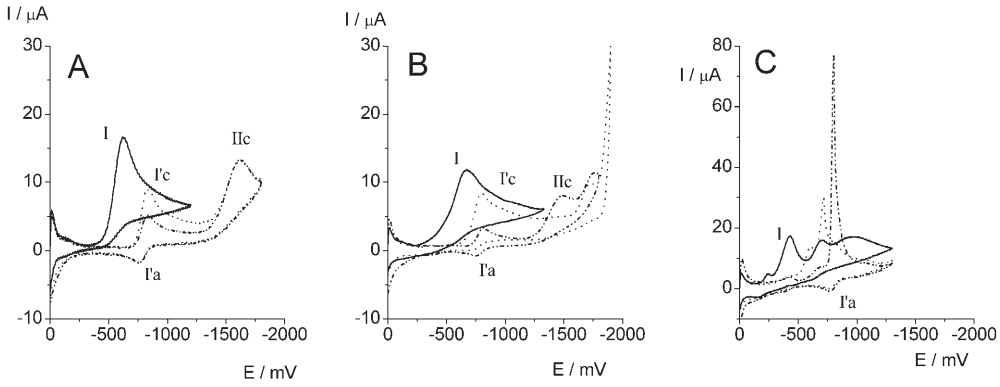

Fig. 5. Cyclic voltammograms of 1 mM of M-Nim (A), M-I-NIm (B) and M-I_2-NIm (C) at pH 3, 7 and 11 in DMF/Citrate + KCl 0.3 M medium at Static mercury drop electrode. Sweep rate 1 V s^{-1}.

in Table 1, being clear that the presence of iodo in the molecules produced a more easy reduction of the nitro group. Certainly, this fact can be explained by the electron withdrawing character of the iodo substitution that acts diminishing the electronic density on the nitro group thus facilitating their reduction.

The most important difference between both electrodes is that only in the case of the mercury electrode is possible to appreciate the splitting of the reduction signal due to the one-electron reduction of M-NIm to produce the corresponding nitro radical anion derivative.

3.2. Electrochemical Behavior in Mixed Medium

In mixed medium (60/40: DMF/Citrate buffer + 0.3 M KCl) the redox behavior of M-NIm, obtained by differential pulse polarography, was very close to that observed in protic medium. In the case of the iodo substituted compounds the observed adsorption interference in the mercury electrode at protic medium was substantially diminished in mixed medium. However exists an important difference between both reaction media, since in mixed medium, i.e., in the presence of an non-aqueous solvent as major component, the splitting of signal I was observed for the three compounds, indicating that the nitro radical anion is more stable in this medium.

By using cyclic voltammetry, the signals for M-NIm and M-I-NIm had a diffusion control, which permit us to identify clearly each electron transfer (Fig. 5A and 5B). At acid medium, the nitro reduction (signal I) occurs via 4-electron and 4-protons according to Equation 1 but when pH was increased, the splitting of this signal in two new signals occurred i.e. a first reversible couple (I′c, I′a) and a second irreversible peak (IIc) (Eqs. 2 and 3). On the other hand, M-I_2-NIm (Fig. 5C) shows a very sharp distortion due to an adsorption phenomenon complicating the cyclic voltammograms. However also is possible to observe some anodic signal due to the nitro radical anion formation (signal I′a). By changing the working electrode from mercury to glassy carbon, a cyclic voltammetric response without adsorption complications was obtained for the three compounds (Figs. 6 A, B and C). In this case, the reduction process of the nitro group shows one signal between pH 2 and 8, and the splitting of this signal over this pH value. Comparing the peak potential values (Fig. 6D) obtained for each cathodic signal, it is clear that the nitro group of M-I_2-NIm is easier to be reduced in all the pH range, and is still more clear the effect of iodo substitution on the nitro radical anion reduction potential (Signal IIc), where the quantity of iodo present in the molecule is proportional to the peak potential values. In Table 2 we can observe a similar behaviour that observed in protic medium, with lower values in the iodo substituted compounds, revealing the withdrawing character of the iodo substituent.

As the nitro radical anion signal was observed using both mercury and glassy carbon electrodes, a detailed study in order to determinate its stability and the effect of substituents in its stability was conducted in both media.

Figure 7 shows the cyclic voltammograms obtained for the redox couple $RNO_2/RNO_2^{\bullet -}$ using mercury electrode for M-NIm and M-I-NIm (Fig. 7A and B) and glassy carbon

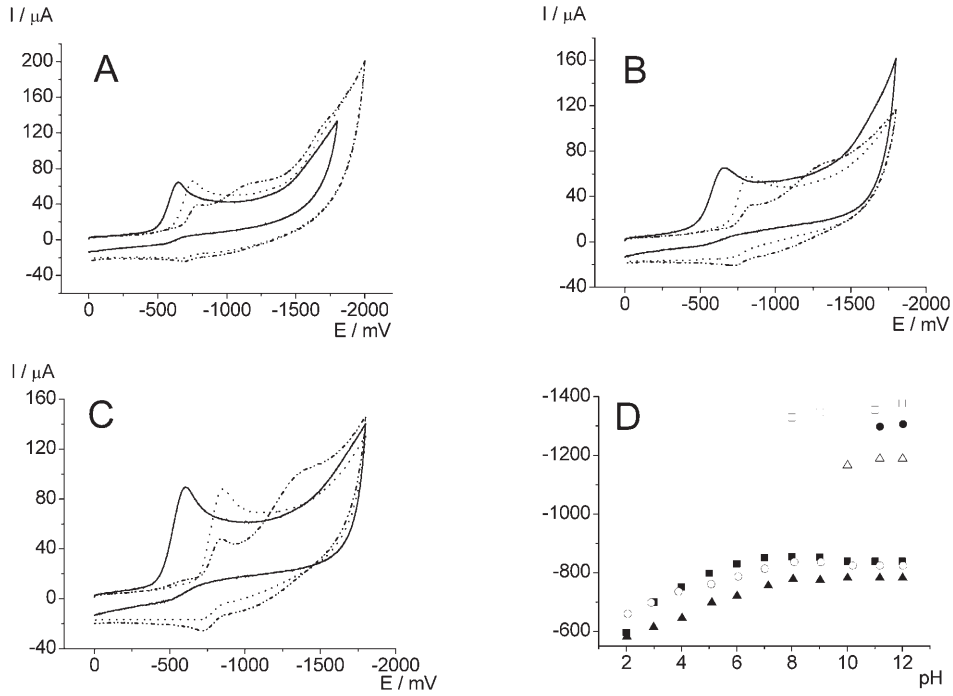

Fig. 6. Cyclic voltammograms of 1 mM of M-Nim (A), M-I-NIm (B) and M-I_2-NIm (C) at pH 3, 7 and 11 in DMF/Citrate + KCl 0.3 M medium at glassy carbon electrode. Sweep rate 1 Vs^{-1}. D) Peak potential dependence with pH for M-NIm (□), M-I-NIm (●) and M-I_2-NIm (△) in DMF/Citrate + KCl 0.3 M medium.

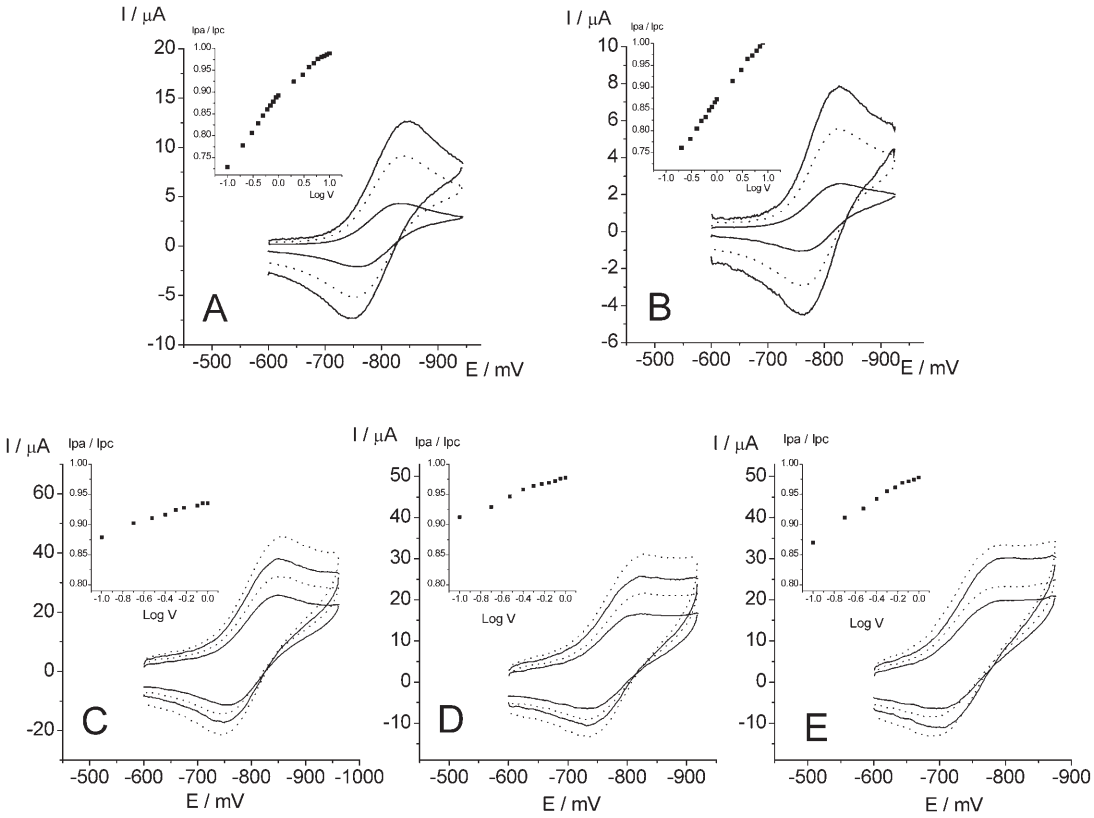

Fig. 7. Cyclic voltammograms showing the reversible couple due to the one-electron reduction of M-NIm (A), M-I-NIm (B) at mercury electrode, pH 10 and M-NIm (C), M-I-NIm (D) and M-I_2-NIm (E) at glassy carbon electrode pH 12 in DMF/Citrate + KCl 0.3 M medium. Inset: Current ratio dependence on sweep rates of the $RNO_2/RNO_2^{\bullet -}$ couple from cyclic voltammograms for each experiment.

Table 3. Decay constant ($k_{2\times}10^{-2}$ $[Ms]^{-1}$) for the nitro radical anion electrochemically formed in mixed medium at different pHs and different electrodes.

	M-NIm	M-I-NIm	M-I_2-NIm
Mercury			
pH 9	175	173	–
pH 10	41	64	–
Glassy carbon			
pH 10	10.4	12.4	10.9
pH 11	7.1	6.5	7.3
pH 12	3.3	3.5	6.6

electrode for all the compounds (Fig. 7C, D, and E), also the corresponding dependence of the current ratio ($I_{p,a}/I_{p,c}$) with the sweep rate are shown (Inset Fig. 7). From these experiments and studying the effect of the nitro compound concentration on the current ratio (data not shown) we concluded that in this medium the nitro radical anion decays according to an *ECi* mechanism, wherein the chemical reaction corresponds to a disproportionation in the same way that in protic medium.

Consequently, in mixed medium, we have calculated the decay constant values, k_2, at different pHs and different electrodes, which are shown in Table 3. From these results we can conclude that the stability of nitro radical anion is not affected by the presence of iodo as substituent in the molecule since the constant values of the three compounds are quite similar when the pH remain constant using both mercury and glassy carbon electrodes. However the stability of the radical is strongly affected with pH changes showing an enhanced stability at alkaline pHs (Table 3).

Finally the electrode material seems to affect also the stability of the radical, although we have only one pH value to compare (pH 10), the decay constant values obtained with mercury are slightly higher than that obtained below the same conditions with glassy carbon electrode.

3.3. Electrochemical Behavior in Non-Aqueous Medium

With the aim of eliminate all adsorption interferences we have also studied a totally non-aqueous medium (100% DMF + TBAP 0.1 M). The stability of the nitro radical anion was studied by cyclic voltammetry using mercury electrode. On these conditions the couple $RNO_2/RNO_2^{\bullet-}$ was detected without any adsorption complications (Fig. 8) for the three compounds. This behavior was confirmed according to the slopes of the $\log I_p$ vs. $\log v$ plots, with values of 0.46, 0.41 and 0.44 for M-NIm, M-I-NIm and M-I_2-NIm respectively.

For M-I_2-NIm, in non-aqueous medium, the behavior was markedly different with the emergence of a prepeak before the nitro reduction couple (Fig. 8C). In a first instant this prepeak was evaluated as a consequence of an acid-base equilibrium, since this phenomenon had been observed previously with other nitro imidazole compound [18]. Thus we added drops of a strong alkaline solution to the nitro

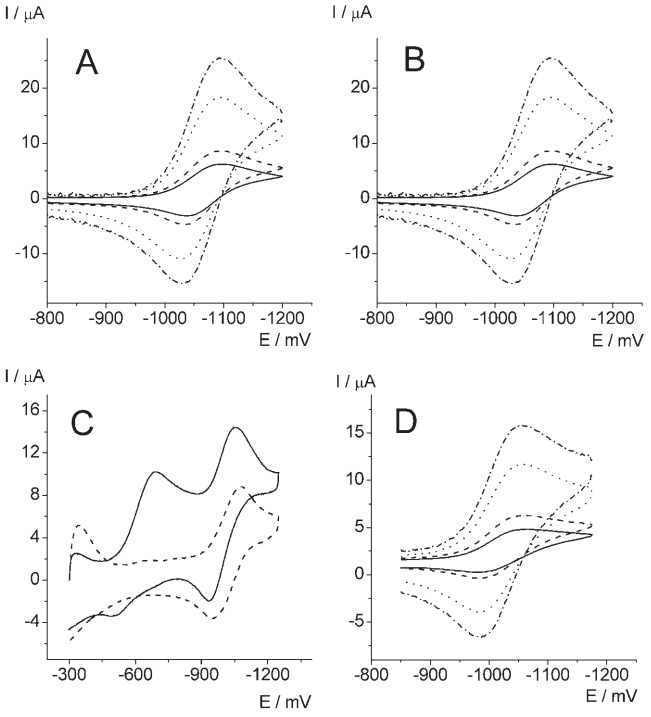

Fig. 8. Cyclic voltammograms at different sweep rates showing the reversible couple due to the one-electron reduction of M-NIm (A), M-I-NIm (B) at mercury electrode, in non-aqueous medium (100% DMF). C) Cyclic voltammograms of M-I_2-NIm without added NaOH (solid lines) and with added NaOH drops (dashed line). D) Cyclic voltammograms at different sweep rates showing the reversible couple due to the one-electron reduction of M-I_2-NIm with added NaOH.

compound solution in order to affect the equilibrium. In fact we saw the complete disappearance of the prepeak after alkalinization of the medium (Fig. 8 D), nevertheless this effect was not reverted with the later addition of acid, as would expected if an acid-base equilibrium was present. Consequently, we discarded the existence of the acid-base equilibrium as the cause of producing the prepeak and probably the observed change in the prepeak is due to the occurrence of an irreversible chemical reaction whose elucidation needs further investigation. In the present study we have evaluated the $RNO_2/ RNO_2^{\bullet-}$ couple, without prepeak, i.e. after the addition of base generating a named OH-M-I_2-NIm compound.

In Figure 8D the cyclic voltammogram of M-I_2-NIm in presence of NaOH is displayed, showing a similar behavior with the sweep rate that M-NIm and M-I-NIm (Figs. 8A and B). From those experiments we calculated the stability of each nitro radical anion (Table 4). A completely different behavior between the compounds was found, being the radical generated from the two iodo substituted nitro-imidazoles considerably more unstable than the M-NIm. Then it is possible to conclude that the iodo substitutions increase the nitro radical anion instability. The difference in the stability of the radicals was observed in this non aqueous medium, but not in mixed medium were the radicals decay with the same rate. This fact could be explained considering

Table 4. Peak potential values (E_p) and decay constant (k_2) for the nitro radical anion electrochemically formed in non-aqueous medium.

	M-NIm	M-I-NIm	OH-M-I_2-NIm
E_p (mV)	−1101	−1071	−1056
E^1_7 (mV) [a]	−458	−428	−413
$k_2 \times 10^{-2}$ [Ms]$^{-1}$	5.81	132	1100

[a] vs. NHE

that the decay reaction in non aqueous medium is the dimerization of the radicals and not the disproportionation as in mixed medium.

Comparing the peak potential of the one electron nitro reduction (E_p values in Table 4) we can observe that the presence of iodo substituents in the molecule produces more easily reducible compounds, in a similar way that in protic and mixed media.

Under biological point of view the difference in the redox potential as function of the medium used to carried out the electrochemical experiments is relevant since that in several cases the redox potential of nitrocompounds, obtained in mixed or non-aqueous media, do not show correlation with biological activity. However, as has been previously described exists a good correlation between the cathodic peak potential, obtained in non-aqueous medium, with the E^1_7 value obtained by pulse radiolysis [19]. The E^1_7 value is a parameter that account for the energy necessary to transfer the first electron to an electroactive group, at pH 7 in aqueous medium, to form a radical anion and it is considered as indicative of nitro radical anion formation in vivo [17]. Consequently, with the experimental obtained values by cyclic voltammetry in non-aqueous medium we can calculate the E^1_7 parameter for all the studied compounds. Table 4 lists the peak potential values obtained by cyclic voltammetry in non-aqueous medium and the calculated E^1_7 values. This result is very significant because the obtained values for the E^1_7 parameter are very closed with the described parameters of other nitroimidazole derivatives of biological significance such as metronidazole, ronidazole and tinidazole [17] meaning that our synthesized derivatives are also candidates to being enzymatically reducible.

4. Conclusions

According to the above results we can conclude that all the studied compounds were reducible in protic, mixed and non-aqueous media at both, mercury and glassy carbon electrodes. However in the case of the iodo substituted derivatives a strong interaction with mercury in protic medium was found. This interaction was only partial in mixed medium and nonexistent in totally non-aqueous medium. According to the measurements on glassy carbon electrode we have found that the inclusion of iodo in the molecule produces a more easy reduction of the nitro group as expected from the electron withdrawing character of the iodo atom.

According to the voltammetrically obtained E^1_7 values we can conclude that the nitro radical anion from all the studied compounds could be biologically formed via enzymatic reduction, because the energy requirements of reduction are similar with that obtained for other well-known enzymatic reducible nitroimidazole drugs.

Related to the formation and stability of the nitro radical anions it is possible to conclude that in protic medium (mercury electrode) only the M-NIm derivative produced radicals in the time schedule of the voltammetric experiment. From this results ($k_2 = 2.2 \times 10^4$ M^{-1}s^{-1}) and comparing the decay constant with that previously reported for 4-NIm ($k_2 = 7.48 \times 10^5$ M^{-1}s^{-1}) [16], using the same procedure, it is possible to conclude that the methyl substitution in position 1 of the imidazole ring produced a substantially more stable nitro radical anion. In mixed medium the radicals decay by a disproportionation reaction and its stability is not affected by the presence of iodo as substituent. However, in non-aqueous medium the nitro radical anion decays by a dimerization reaction and the stability is strongly diminished by the presence of iodo as substituent in the molecule.

5. Acknowledgements

This work was partially supported by Grant from FONDECYT 8000016. Also the support from DID of University of Chile is also acknowledged.

6. References

[1] D. I. Edwards, *Biochem. Pharmacol*. **1986**, *35*, 53
[2] B. Mester, R. M. Claramunt, J. Elguero, J. Atienza, A. Gomez Barrio, J. A. Escario, *Chem. Pharm. Bull*. **1991**, *39*, 1990
[3] C. K. Stover, P. Warrener, D. R. Van Devanter, D. R. Sherman, T. M. Arain, M. H. Langhorne, S. W. Anderson, J. A. Towell, Y. Yuan, D. N. Mc Murray, B. N. Kreiswirth, *Nature* **2000**, *405*, 962.
[4] F. Riché, A. du Molinet, S. Sèpe, L. Riou, D. Fagret, M. Vidal, *Biorg. Med. Chem. Lett.* **2001**, *11*, 71.
[5] S. A. Everett, M. A. Naylor, K. B. Patel, M. R. Stratfordand, P. Wardman, *Biorg. Med. Chem. Lett.* **1999**, *9*, 1267.
[6] J. D. Maya, S. Bollo, L. J. Nuñez-Vergara, J. A. Squella, Y. Repetto, A. Morello, J. Périé, G. Chauvière, *Biochem. Pharmacol.* **2003**, *65*, 999.
[7] S. Bollo, L. J. Núñez-Vergara, M. Bontá, G Chauviere, J. Périé, J. A. Squella, *Electroanalysis* **2001**, *13*, 936
[8] S.Bollo, L. J. Nunez-Vergara, M. Bontá, G. Chauvière, J. Périé, J. A. Squella, *J. Electroanal. Chem.* **2001**, *511*, 46.
[9] S.Bollo, L. J.Núñez-Vergara, C.Martinez, G.Chauviere, J. Périé, J. A.Squella, *Electroanalysis* 2003, *15*, 19.
[10] J. Carbajo, S. Bollo, L. J. Núñez-Vergara, P. Navarrete, J. A. Squella, *J. Electroanal. Chem.* **2000**, *494*, 69.
[11] J. Carbajo, S.Bollo, L. J.Núñez-Vergara, A.Campero, J. A.Squella, *J. Electroanal. Chem*. 2002, 531, 187.
[12] P. L. Olive, *Cancer Res.* **1979**, *39*, 4512.
[13] R. S. Nicholson, *Anal. Chem*. **1966**, *38*, 1406.
[14] M. L.Olmstead, and R. S.Nicholson, *Anal. Chem*. **1969**, *41*, 862.

[15] M. L. Olmstead, R. G. Hamilton, R. S. Nicholson, *Anal. Chem*. **1969**, *41*, 260.
[16] J. Carbajo, S. Bollo, L. J. Nuñez-Vergara, A. Campero, J. A. Squella, *J. Electroanal. Chem*. **2002**, *531*, 187.
[17] P. Wardman, *Environm. Health Perspectives* **1985**, *64*, 309.
[18] M. Bontá, G. Chauviere, J. Périe, L. J. Núñez-Vergara, J. A.Squella, *Electrochim. Acta* **2002**, *47*, 4045.
[19] A. Breccia, G. Berrilli, S. Roffia *Int. J. Radiat. Biol.***1979**, *36*, 85.

Available online at www.sciencedirect.com
ScienceDirect
Electrochimica Acta 52 (2006) 511–518
ELECTROCHIMICA Acta
www.elsevier.com/locate/electacta

Electrochemical reduction of 2-nitroimidazole in aprotic medium: Influence of its dissociation equilibrium on the reduction mechanism

J.A. Squella [a,*], A. Campero [b], J. Maraver [b], J. Carbajo [b]

[a] *Bioelectrochemistry Laboratory, Chemical and Pharmaceutical Sciences Faculty, University of Chile, POB 233, Olivos 1007, Santiago, Chile*
[b] *Departamento de Ingeniería Química, Química Física y Química Orgánica, Facultad de Ciencias Experimentales, Universidad de Huelva, Huelva, Spain*

Received 3 March 2006; received in revised form 20 May 2006; accepted 22 May 2006
Available online 27 June 2006

Abstract

The electrochemical reduction of 2-nitroimidazole in a non-aqueous medium using cyclic voltammetry (CV) at a mercury electrode was carried out.

The 2-nitroimidazole derivative in DMF + 0.1 M tetra(*n*-butyl)ammonium hexafluorophosphate (TBAHFP6) resulted in the following dissociation equilibrium:

$$HNRNO_2 \leftrightarrows {}^{-}NRNO_2 + H^{+}$$

The neutral species ($HNRNO_2$) and the corresponding conjugate base ($^{-}NRNO_2$) are characterized by UV absorption bands at 328 and 370 nm, respectively.

The voltammograms of 2-nitroimidazole produced two well-defined signals, which were determined by the above dissociation equilibrium. The first reduction peak was caused by the reduction of the neutral species according to the following overall mechanism:

$$5HNRNO_2 + 4e^{-} \rightarrow 4^{-}NRNO_2 + HNRNHOH + H_2O$$

The second quasi-reversible couple was caused by the reduction of the conjugate base according to the following equation:

$$^{-}NRNO_2 + e^{-} \rightarrow NRNO_2^{\bullet -}$$

Keywords: 2-Nitroimidazole; Cyclic voltammetry; Electro-reduction

1. Introduction

Nitroimidazolic compounds display a wide range of biological activities, mainly their use as radiosensitizers, antibacterial and antiprotozoans drugs. Their use as radiosensitizers takes advantage of their cytotoxicity in hypoxic mammalian cells, increasing sensitivity to the radiation of cancerigenic tumors [1–4]. Their antimicrobial characteristic takes advantage of their selective toxicity towards anaerobic microorganisms, permitting their extensive use in the treatment of infectious diseases [5–11].

According to the position of the nitro substituent in the imidazolic ring, it is possible to classify the nitroimidazolic derivatives as 2-, 3- and 4-nitroimidazolic derivatives (Fig. 1). In relation to their biological activity, 2-nitroimidazolic derivatives are preferably used as radiosensitizers, while 5-nitroimidazolic derivatives are mainly used because of their toxicity towards microorganisms and 4-nitroimidazolic derivatives are relatively more inert [12]. However, the descriptions of the mutagenic and carcinogenic properties of some 2- and 5-nitroimidazole derivatives have also increased the interest in minor mutagenic 4-nitroimidazoles [13,14]. Although the nitro reduction is crucial for any biological activity, there are still no conclusive results about the incidence of the nitro position in their biological activity.

* Corresponding author. Tel.: +56 2 9782927; fax: +56 2 7371241.
E-mail address: asquella@ciq.uchile.cl (J.A. Squella).

0013-4686/$ – see front matter © 2006 Elsevier Ltd. All rights reserved.
doi:10.1016/j.electacta.2006.05.032

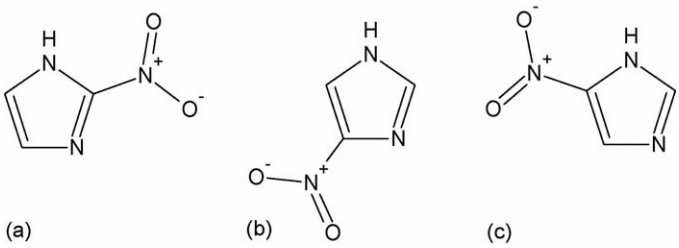

Fig. 1. Molecular structure of the isomers: (a) 2-nitroimidazole; (b) 4-nitroimidazole (tautomer); (c) 5-nitroimidazole (tautomer).

There are numerous studies aiming at the electrochemical aspects of nitroimidazolic compounds. Nevertheless, those works are mostly focused on the electroanalytical determination of some 5-nitroimidazoles of importance in medicine such as: metronidazol [15], ornidazol [16], secnidazol [17], tinidazol [18] and megazol [19]. In addition, cyclic voltammetry has been used in the study of nitro radical anions generated by 5-nitroimidazoles such as misonidazol, metronidazol and megazol [20–24]. These studies demonstrated the utility of cyclic voltammetry (CV) for the study of the formation and stability of nitro radical anions.

The studies of 4-nitroimidazole derivatives are restricted to a couple of works. The first report in the 1980s was done by Roffia et al. [25]. In that study, the voltammetric behavior of 4-nitroimidazole in an aprotic medium was presented. Two reduction peaks were displayed using CV. The first peak was irreversible, whereas the second was reversible. The first irreversible peak was attributed to the following global reaction:

$$5HRNO_2 + 4e^- \rightarrow HRNHOH + 4RNO_2{}^- + H_2O \quad (1)$$

The second reversible peak was attributed to Eq. (2):

$$RNO_2{}^- + e^- \leftrightarrows RNO_2{}^{2-} \quad (2)$$

From that study, it was concluded that the nitro radical anion decays fast because of a protonation reaction by the proton acid of the initial 4-nitroimidazole (father–son reaction).

Furthermore, the electrochemical behavior of 4-nitroimidazole was also exhaustively studied in a protic medium using a wide pH scale [26]. The results in a protic medium were substantially different from those previously described for aprotic medium, since they showed that the reduction of 4-nitroimidazole produced stable nitro radical anion within the time scale of the CV, which had not been possible in the aprotic medium. The nitro radical anion decayed according to a disproportionation reaction wherein the disproportionation constants (k_2) were calculated according to a CV approach. The disproportionation constants relied strongly on both pH and co-solvent content.

The electrochemical studies about the 2-nitroimidazole derivative are scarce and are restricted almost exclusively to a study where its electrocatalytic reduction on gold and modified gold electrodes is described [27]. The mechanism described in that report involved two different routes in acid medium, an electrocatalytic and an electronic interchange. There were no references in that study to the formation of radical intermediates. Moreover, it does not exist studies in the literature that demonstrate the reduction mechanism of 2-nitroimidazole.

Thus, the lack of electrochemical investigation in relation to 2-nitroimidazole and the importance of its reduction in medical applications have prompted us to carry out a study with the purpose of contributing to its basic REDOX understanding.

2. Experimental

2.1. Reagents and solutions

2-Nitroimidazole and 4-nitroimidazole (Fig. 1a), 97% pure, were obtained from Aldrich Chem. Co., and were used without prior purification. All the other reagents employed were of analytical grade. Nitrogen gas was obtained from ALPHAGAZ-AIR LIQUIDE with maximum impurities of $H_2O < 3$ ppm; $O_2 < 2$ ppm; $C_nH_m < 0.5$ ppm.

All the voltammetric experiments were obtained after bubbling with N_2 for 10 min in the cell before each run. Temperature was kept constant at 25 ± 0.1 °C in all experiments.

Solutions for cyclic voltammetry were prepared starting from a 0.2 M stock solution of the nitroimidazole derivative in DMF daily prepared. Final solutions in the voltammetric cell were prepared by diluting an appropriate quantity of the stock solution in order to obtain a final concentration of 1 mM.

Experiments in aprotic medium were made in DMF with 0.1 M tetra(*n*-butyl)ammonium hexafluorophosphate (TBAHFP6) as supporting electrolyte.

2.2. Apparatus and methods

Voltammetric curves were recorded on an Electrochemical Analyzer type BAS 100B/W (Bioanalytical System) attached to a PC computer with appropriate software (BAS 100W 2.3 for Windows) for total control of the experiments and data acquisition and treatment. A static mercury drop electrode (SMDE) (BASi EF-1400) with mercury drop area of 0.43 mm^2 was used as the working electrode and a platinum wire (BASi MW-1032) as the counter electrode. All potentials were measured against Ag|AgCl|NaCl (3 M) (BASi MF-2052).

Controlled potential electrolysis (CPE) was carried out at constant electrode potential (−1.1 or 2.0 V) on a mercury pool electrode. Oxygen was removed with pure and dry pre-saturated nitrogen. A three-electrode circuit with an Ag|AgCl|NaCl (3 M) electrode was used as reference and platinum wire as a counter electrode. A BAS-CV 50 assembly was used to electrolyze the 2-nitroimidazole solutions.

UV–vis spectra were recorded in the 200–600 nm range, using an UNICAM UV-3 spectrophotometer.

Temperature was controlled with a Thermostat/cryostat SELECTA Frigiterm-10, resolution of 0.1 °C.

3. Results and discussion

2-Nitroimidazole was reduced in a non-aqueous medium containing 0.1 M TBAHFP6 in DMF when it is subjected to a cyclic voltammetric (CV) experiment on Hg surface. As observed in

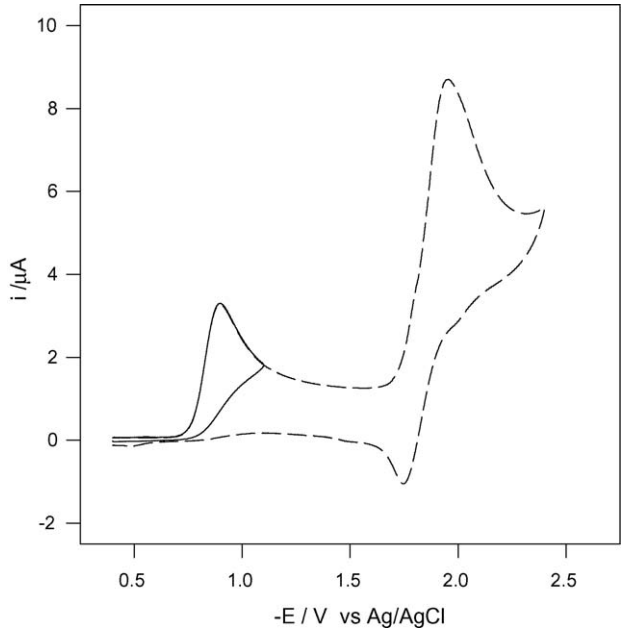

Fig. 2. Cyclic voltammograms (dotted line = large sweep and whole line = short sweep) of 1 mM 2-nitroimidazole in DMF, 0.1 M TBAHFP6. $v = 0.5$ V/s.

Fig. 2, two cathodic peaks are displayed. The first peak has a cathodic peak potential, E_{pc}, of −0.9 V and the second one an E_{pc} of −1.96 V, at a sweep rate of 0.5 V/s. The last of these peaks shows an apparently reversible behavior, since the corresponding anodic peak is observed in the anodic sweep with an E_{pa} of −1.76 V. With the aim to study the voltammetric behavior at different time scales of the experiment, measurements were made at different sweep rates (Fig. 3). From the voltammograms shown in Fig. 3, the difference between cathodic and anodic peak potentials, ΔE_p, for the apparently reversible couple exceeds the theoretical value of 0.060 V for a one-electron reversible

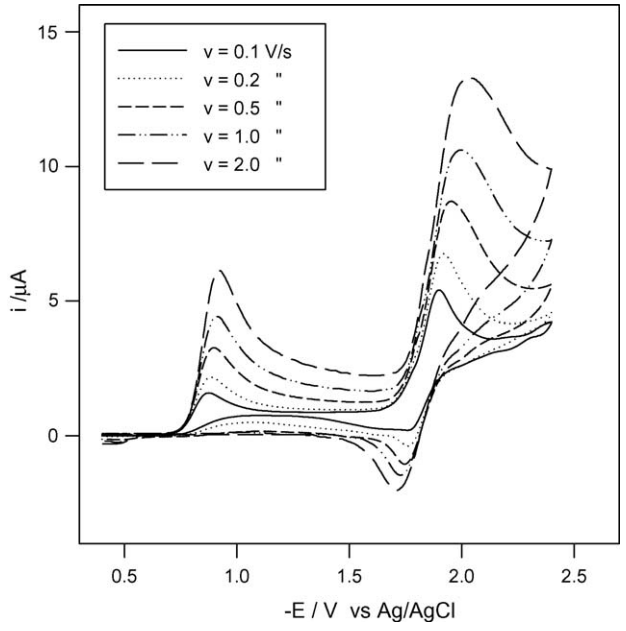

Fig. 3. Cyclic voltammograms of 1 mM 2-nitroimidazole in DMF, 0.1 M TBAHFP6 at different sweep rates.

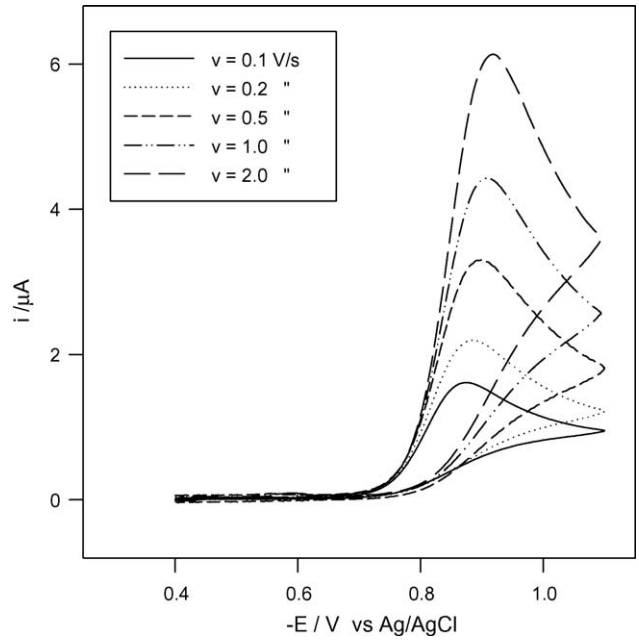

Fig. 4. First peak cyclic voltammograms of 1 mM 2-nitroimidazole in DMF, 0.1 M TBAHFP6 at different sweep rates.

process. This difference increases considerably with the sweep rate changing from approximately 0.12 V at the slowest rate to approximately 0.38 V at the fastest rate. This result led us to discard the reversibility of this wave since in fact the involved electron transfer would obey to a quasi-reversible process.

Cyclic voltammograms of the isolated first peak at different sweep rates are shown in Fig. 4. In addition, the data corresponding to the current intensities and the peak potentials of the first cathodic peak are shown in Table 1. From these data we obtained a linear relation between the cathodic peak current and the logarithm of the sweep rate with a slope of 0.45 as shown in the plot of Fig. 5a. This slope value is indicative of a diffusion-controlled process since it is near the theoretical value of 0.5 for this type of process. In Fig. 5a, on the other hand, a linear dependence between the peak potentials of the first cathodic peak and the logarithm of the sweep rate with a slope of 0.033 V is shown. From both plots in Fig. 5 we conclude that the first peak would obey to a diffusion controlled process wherein a slow one-electron process is followed by a first fast chemical reaction according to the following reaction scheme:

$$HNRNO_2 + e^- \rightarrow HNRNO_2^{\bullet -} \quad (3)$$

$$HNRNO_2^{\bullet -} \rightarrow \text{product} \quad (4)$$

Table 1
Current and potential values from the first peak obtained from CV of 1 mM 2-nitroimidazole in DMF, 0.1 M TBAHFP6 at different sweep rates

v (V/s)	$\log(v)$ (V/s)	i_{pc} (μA)	$-E_{pc}$ (V)	$\log(i_{pc})$ (μA)
0.1	−1.00000	1.563	0.875	0.19396
0.2	−0.69897	2.13	0.885	0.32838
0.5	−0.30103	3.196	0.901	0.50461
1.0	0.00000	4.332	0.909	0.63669
2.0	0.30103	6.034	0.918	0.78061

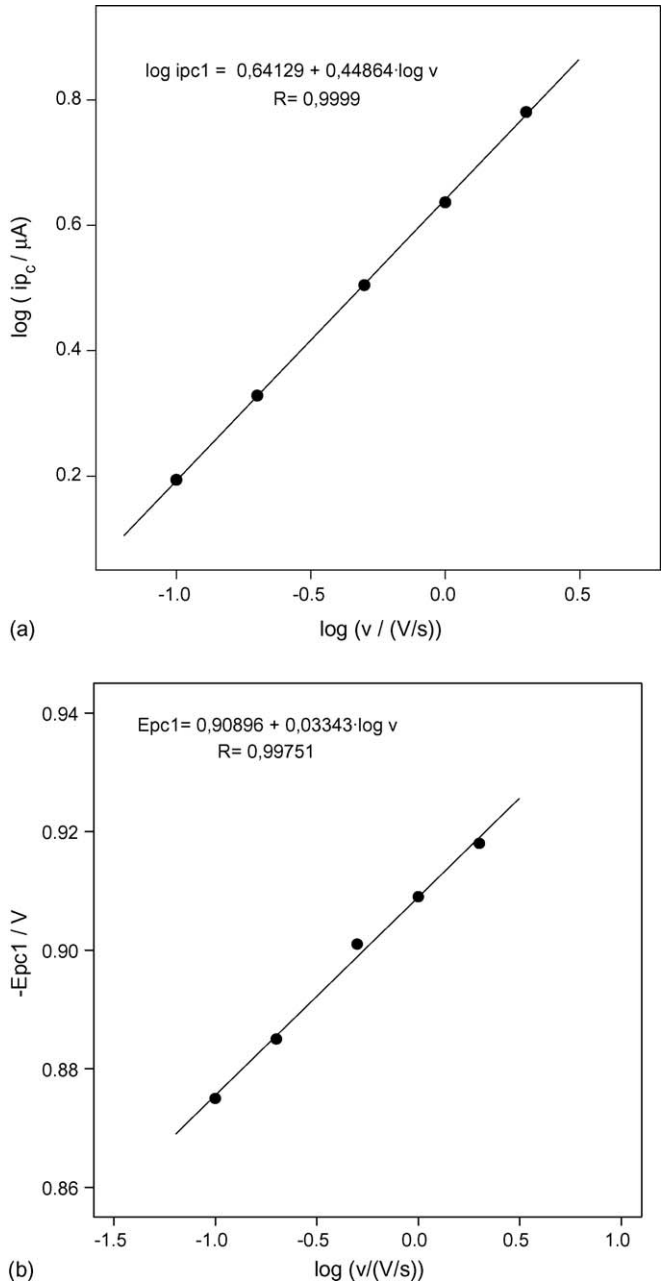

Fig. 5. (a) log i_{pc} vs. log v and (b) E_{pc} vs. log v, of the first peak of the reduction of 2-nitroimidazole in DMF with 0.1 M TBAHFP6. $C^0 = 1$ mm.

wherein $HNRNO_2$ represents the neutral species of 2-nitroimidazole and $HNRNO_2^{\bullet -}$ represents its radical anion.

This reaction scheme corresponds to a coupled process wherein the radical anion produced in the first step (Eq. (3)) decays chemically in a second step (Eq. (4)). As the chemical step is fast compared with the one-electron transfer, no back oxidation of the radical anion will be possible, thus the shape of the first peak will be irreversible (no anodic peak). However, there are several possibilities for the chemical decay of the radical anion, i.e. protonation, dimerization, dismutation or father–son reactions. Consequently, our next step will be to find the nature of the decay reaction.

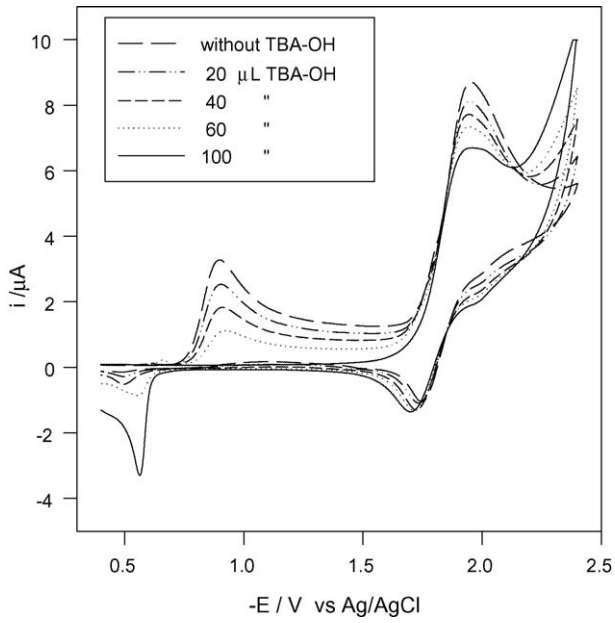

Fig. 6. Cyclic voltammograms of 1 mM 2-nitroimidazole in DMF, 0.1 M TBAHFP6 with different quantities of 0.1 M TBA-OH added. $v = 0.5$ V/s.

2-Nitroimidazole is a heterocyclic ring with two N atoms wherein one of them (N1) is linked to an H atom, which can act as a proton donor. On the other hand, the other N (N3) can act as a proton acceptor. Consequently, the molecule can act as acid or base, in such way that a dissociation equilibrium can affect its voltammetric behavior. Fig. 6 shows the effect of adding different quantities of a base as tetrabutyl ammonium hydroxide (TBA-OH) on a solution containing 1 mM of 2-nitroimidazole. From this figure, we observe that the addition of a base produces a decrease in the first cathodic peak, which means a decrease in the concentration of the initial reactant. Obviously, this result supports the existence of a dissociation equilibrium wherein probably the H linked to the N1 shows an acid behavior. If the hypothesis of a dissociation equilibrium is correct, the subsequent addition of an acid, to the previously alkalinized solution, would produce the reversion of the equilibrium to the initial condition. As observed in Fig. 7, the addition of an acid as $HClO_4$ (in ethanol) over the previous alkalinized solution produced the reversion of the reaction toward the regeneration of the electroactive species responsible for the first cathodic peak thus confirming the existence of dissociation equilibrium. The equilibrium can be represented by the following equation:

$$HNRNO_2 \leftrightarrows {}^{-}NRNO_2 + H^{+} \quad (5)$$

wherein the nitranion species $^{-}NRNO_2$ represents the conjugate base formed as a consequence of the loss of the weakly acid proton on the N1 of the neutral $HNRNO_2$ species in the alkalinized solution. The pK_a for 2-nitroimidazole in DMF have not been described but a value of 7.15 was informed for the pK_a of 2-nitroimidazol in a mixture CH_3OH–water, 1:1 [28]. So, considering this equilibrium we can explain both peaks for the reduction of 2-nitroimidazole. The electroactive species producing the first cathodic peak corresponds to the neutral

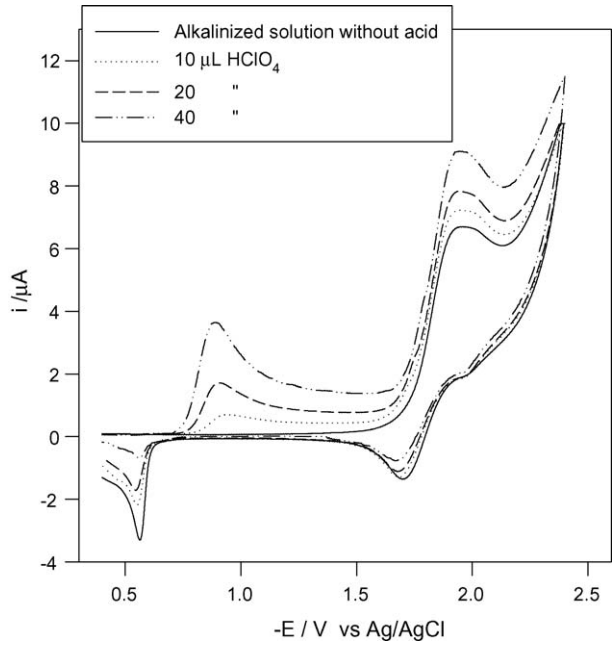

Fig. 7. Cyclic voltammograms of an alkalinized solution (100 μl of 0.1 M TBA-OH) of 1 mM 2-nitroimidazole in DMF, 0.1 M TBAHFP6 with different quantities of 0.2 M $HCLO_4$ (in ethanol) added. $v = 0.5$ V/s.

species $HNRNO_2$ and the electroactive species producing the second quasi-reversible couple corresponds to the conjugate base $^{-}NRNO_2$. The generation of this type of stable nitranion species has been also described for other nitrogen heterocycles in aprotic medium [29].

As can be appreciated from the voltammograms of Figs. 2, 3, 6 or 7 there are big differences between the reduction potential of both peaks (approximately, 1.0 V), meaning that the $HNRNO_2$ species is substantially more easily reducible than its corresponding nitranion. In the case of the nitranion, this difference can be explained by its negative center of charge that is localized very near the site of entrance of the electron, thus hindering its reduction.

According to the above experimental evidences, we can summarize that the first reduction peak is due to the above-mentioned Eqs. (3) and (4) and the second one by the following equation:

$$^{-}NRNO_2 + e^{-} \rightarrow NRNO_2^{\bullet -} \quad (6)$$

where the nitranion species of the 2-nitroimidazole is reduced to the corresponding dianion radical (radical anion of the nitranion), which is oxidized in the reverse sweep in a quasi-reversible process. The heterogeneous electron transfer rate constant was calculated by CV from the variation of the ΔE_p values at different sweep rates according to the theoretical curve described by Nicholson [30]. We have obtained a heterogeneous electron transfer rate constant, k_{het}, of $(1.24 \pm 0.013) \times 10^{-3}$ cm/s for the quasi-reversible reduction of the nitranion.

On the other hand, in the case of the radical anion generated in the first reduction peak (according to the above Eq. (3)) it has a sufficiently basic character to interact with the initial reactant, $HNRNO_2$, generating the following father–son reaction:

$$HNRNO_2 + HNRNO_2^{\bullet -} \rightarrow HNRNO_2H^{\bullet} + {}^{-}NRNO_2 \quad (7)$$

where the sufficiently basic radical anion species ($HNRNO_2^{\bullet -}$) deprotonates the initial reactive ($HNRNO_2$), generating the protonated radical ($HNRNO_2H^{\bullet}$) and the nitranion species ($^{-}NRNO_2$). Obviously, the occurrence of the above reaction (7) explains the irreversible character of peak 1 because the formed radical anion reacts more easily with the parent compound than its possible oxidation in the reverse sweep, thus not producing the corresponding anodic peak.

Furthermore in order to prove the existence of the above Eq. (7) we have carried out experiments of controlled potential electrolysis (CPE) and then track both the consumption of the parent compound $HNRNO_2$ and the formation of the nitranion. In Fig. 8a, we show the cyclic voltammograms recorded before and after the CPE carried out at a controlled potential of −1.1 V. From this experiment, it is clear that the electrolytic process consumed all the electroactive specie responsible for the first cathodic peak. Moreover we have compared the UV spectra maxima of 2-nitroimidazole in DMF solution in order to show the similarity between the effect of both to alkalinize or to electrolyze the solution. According to the UV spectra in Fig. 8b, it is possible to distinguish two different absorption maxima for the initial solution of 2-nitroimidazole in DMF. The neutral species ($HNRNO_2$ according to Eq. (5)) shows a maximum at 328 nm and the conjugate base (the nitranion according to Eq. (5)) shows a shoulder at 370 nm. This result is in accord with the previously reported by Gallo et al. [28] wherein absorption bands at 372 nm (conjugate base) and 325 nm (neutral molecule) were informed for 2-nitroimidazole solutions. Furthermore, Fig. 8 shows the comparative spectra of both alkalinized and electrolyzed solutions of 2-nitroimidazole. The comparison shows that both procedures, addition of a base and electrolysis, produced the same effect i.e. the vanishing of absorption at 328 nm and the enhanced absorption at 370 nm. In the case of the electrolysis the explanation for this fact is that electrolysis produced the reduction of the initial $HNRNO_2$ (vanishing of 328 nm band), generating the radical anion, which is sufficiently basic to deprotonate the parent compound generating the nitranion derivative (increase of the 370 nm band) according to the above Eq. (7). Consequently, the above experiments support the occurrence of a father–son type reaction as the chemical reaction following the electron transfer, obeying the following scheme:

$$HNRNO_2 + e^{-} \rightarrow HNRNO_2^{\bullet -} \quad (3)$$

$$HNRNO_2 + HNRNO_2^{\bullet -} \rightarrow HNRNO_2H^{\bullet} + {}^{-}NRNO_2 \quad (7)$$

In order to obtain only stable products in the overall reaction and also based on previous evidences [31], where nitroso and hydroxylamine derivatives are intermediates or products in the reduction of nitro compounds, it is possible to postulate the following steps (8) and (9) and thus originate the following mechanism to explain the cathodic peak 1:

$$HNRNO_2 + e^{-} \rightarrow HNRNO_2^{\bullet -} \quad (3)$$

$$HNRNO_2 + HNRNO_2^{\bullet -} \rightarrow HNRNO_2H^{\bullet} + {}^{-}NRNO_2 \quad (7)$$

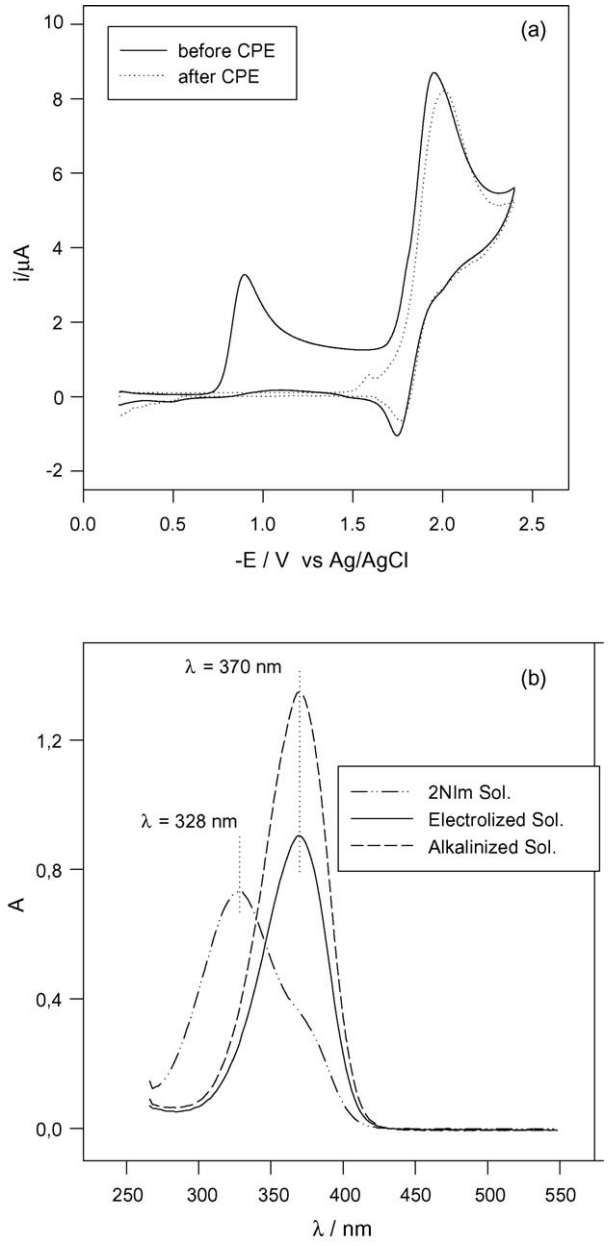

Fig. 8. (a) Cyclic voltammograms of 1 mM 2-nitroimidazole in DMF, 0.1 M TBAHFP6 before (whole line) and after (dotted line) controlled potential electrolysis at −1.1 V. $v = 0.5$ V/s. (b) Comparative UV spectra of 1 mM 2-nitroimidazole in DMF, 0.1 M TBAHFP6 solution and the corresponding alkalinized and electrolyzed solutions.

$$HRNO_2H^{\bullet} + HNRNO_2 + e^- \rightarrow HNRNO + {}^-NRNO_2 + H_2O \quad (8)$$

$$HNRNO + 2HNRNO_2 + 2e^- \rightarrow HNRNHOH + 2^-NRNO_2 \quad (9)$$

the overall reaction being the following Eq. (10):

$$5HNRNO_2 + 4e^- \rightarrow 4^-NRNO_2 + HNRNHOH + H_2O \quad (10)$$

The above overall reaction is in accord with the experimental evidences showing the consumption of the initial reactant ($HNRNO_2$) and the generation of the nitranion derivative ($^-NRNO_2$), furthermore, the proposed mechanism turns out to be analogous to the previously proposed for 4-nitroimidazole by Vianello and co-workers [25].

Moreover, according to the above proposed mechanism, the overall reaction would imply the consumption of 4 electrons for each five molecules of 2-nitroimidazole, consequently, the number of electrons per mol would be a value of (4 e)/(5 mol) = 0.8. In Fig. 9, we show the results of electrolysis at a controlled potential of −1.1 V for concentrations of 1 mM (Fig. 9a) and 4 mM (Fig. 9b) of 2-nitroimidazole in DMF. From Fig. 9a the charge accumulated during the electrolysis was 0.852 C. As we added 10 ml of 1 mM 2-nitroimidazole solution to the electrol-

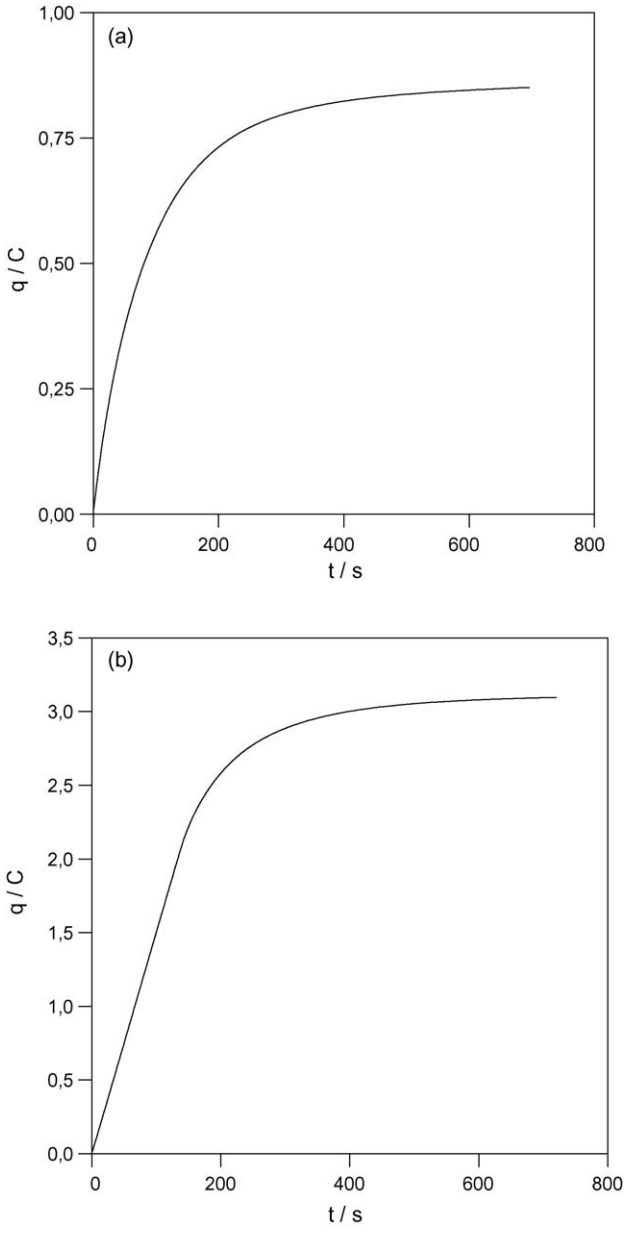

Fig. 9. Controlled potencial electrolysis of: (a) 1 mM and (b) 4 mM, of 2-nitroimidazole in DMF, 0.1 M TBAHFP6. $E = -1.1$ V.

ysis vessel, a value of 0.880 e mol^{-1} was obtained. Similarly, from the results of Fig. 9b, we obtained 0.801 e mol^{-1} of 2-nitroimidazole. Both results reveal a tendency to a value near 0.8, as theoretically predicted for the proposed mechanism, thus confirming this proposal.

On the other hand, CPE carried out at −2.0 V potential causes the disappearance of the first cathodic peak without appreciable modification of the second peak. After disappearance of the first peak, i.e. for $Q > 0.8$ e mol^{-1}, the second peak continues even if electrolysis is continued for long times and the electrolysis current reached a steady-state value, significantly higher than the background. Furthermore we have detected tri-*n*-butyl amine and 1-butene in the electrolyzed solution. All of these aspects suggest that protons would have come from the electrolyte through a Hoffmann degradation.

According to our results, although 2-nitroimidazole differs structurally from 4-nitroimidazole, both molecules follow exactly the same reduction mechanism in non-aqueous medium. However, the energetics of both reduction reactions is different. In Fig. 10 shows comparative CV of equimolar solutions of 2-nitroimidazole and 4-nitroimidazole in DMF plus 0.1 M TBAHFP6. From these voltammograms, it is clear that there is a great difference in the reduction potential of the first cathodic peak, wherein the $HNRNO_2$ species in the 2-nitroimidazole derivative is more easily reduced (approximate difference, 0.3 V) than the corresponding species in the 4-nitroimidazole derivative. This difference is explained because the nitro group in 2-position possesses two electronegative N atoms adjacent, thus diminishing the electronic density on the nitro group. On the other hand, in the case of the second cathodic peak, the reduction peak potential for both 2-nitroimidazole and 4-nitroimidazole are similar, which means that the nitranion species on both derivatives are reduced with similar energy requirements. This fact can be explained if we consider that in the case of the nitranion species there is a ionic negative charge on the N(1) whose effect is predominant over the effect caused by the charge densities that accounted for the first peak differences.

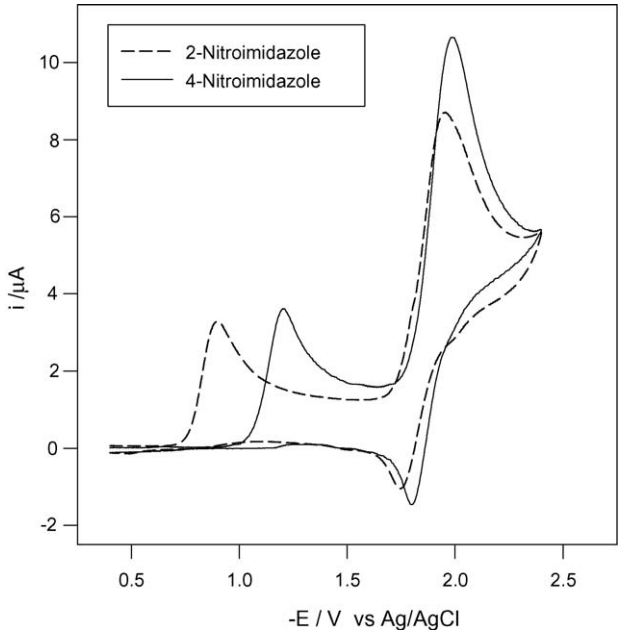

Fig. 10. Cyclic voltammograms of 1 mM 2-nitroimidazole (dotted line) and 4-nitroimidazole (whole line) in DMF, 0.1 M TBAHFP6. $v = 0.5$ V/s.

4. Conclusions

In the studied medium containing DMF + 0.1 M tetra(*n*-butyl)ammonium hexafluorophosphate (TBAHFP6) the 2-nitroimidazole derivative originates an equilibrium between the neutral species ($HNRNO_2$) and the corresponding conjugate base ($^{-}NRNO_2$) according to the following equation:

$$HNRNO_2 \leftrightarrows {}^{-}NRNO_2 + H^{+}$$

This equilibrium is caused by the ionization of the imino-nitrogen N(1) and determined the electro-reduction mechanism. Furthermore, the $HNRNO_2$ (neutral species) showed an UV absorption maximum at 328 nm and the nitranion $^{-}NRNO_2$ (conjugate base) showed a maximum at 370 nm. The reduction CV of the $HNRNO_2$ species produced an irreversible reduction peak with a cathodic peak potential of −0.9 V versus Ag|AgCl. On the other hand, the CV of the nitranion species ($^{-}NRNO_2$) produced a quasi-reversible couple with a cathodic reduction peak of −1.96 V versus Ag|AgCl and a heterogeneous electron transfer rate constant, k_{het}, of $(1.24 \pm 0.013) \times 10^{-3}$ cm/s.

According to the above results we demonstrated that 2-nitroimidazole follows a similar reduction mechanism that the previously described by Roffia et al. [25] for the 4-nitroimidazole derivative. This is a non-obvious matter because both isomers are structurally different with nitro groups suffering different electronic influences from its neighborhood, aspects that could affect its mechanism. In fact there is not information in the state of the art revealing that 2- and 4-isomers would share a similar mechanism. However, in spite of sharing the same mechanism, both derivatives differ strongly in the energetic of the reaction, being 2-nitroimidazole far more easily reduced than the 4-nitroimidazole derivative, thus confirming that 2-nitroimidazole derivatives are better radiopotentiators than 4-nitroimidazole derivatives.

Acknowledgement

The authors are grateful to FONDECYT (project number 1050767) for support this work.

References

[1] D. Thall, G. Rosner, C. Azuma, M. Mc Entee, J. Raleigh, Radiother. Oncol. 44 (1997) 171.
[2] F. Riché, A. du Molinet, S. Sèpe, L. Riou, D. Fagret, M. Vidal, Biorg. Med. Chem. Lett. 11 (2001) 71.
[3] S.A. Everett, M.A. Naylor, K.B. Patel, M.R. Stratfordand, P. Wardman, Biorg. Med. Chem. Lett. 9 (1999) 1267.
[4] G.E. Adams, I.J. Stratford, Int. J. Radiat. Oncol. Biol. Phys. 29 (1994) 231.
[5] D.I. Edwards, Prog. Med. Chem. 18 (1981) 87.
[6] D.I. Edwards, J. Antimicrobiol. Chemother. 31 (1993) 9.
[7] D.I. Edwards, Biochem. Pharmacol. 35 (1986) 53.
[8] P. Wardman, Environ. Health Perfect. 64 (1985) 309.
[9] M. Muller, Scand. J. Infect. Dis. (Suppl.) 26 (1981) 31.

[10] H. Van den Bassche, Nature 273 (1978) 626.
[11] D.I. Edwards, J. Antimicrob. Chemother. 31 (1993) 9.
[12] D. Church, H. Rabin, E. Laishley, J. Antimicrob. Chemother. 25 (1990) 15.
[13] S. Gómez-Arroyo, S. Melchor-Castro, R. Villalobos-Pietrini, E. Melendez-Camargo, H. Salgado-Zamora, M. Campos-Aldrete, Toxicol. In Vitro 18 (2004) 319.
[14] S. Khabnadideh, Z. Rezaei, A. Khalafi, R. Bahrinajafi, R. Mohamadi, A. Farrokhroz, Biorg. Med. Chem. Lett. 13 (17) (2003) 2863.
[15] D. Dumanovic, J. Volke, V. Vajgand, J. Pharm. Pharmacol. 18 (1966) 507.
[16] S.A. Ozcan, Z. Senturk, I. Biryol, Int. J. Pharm. 157 (1997) 137.
[17] A. Radi, S. El-Laban, A.-G. El-Kourashy, Electroanalysis 9 (1997) 625.
[18] S.A. Okzan, Analysis 25 (1997) 130.
[19] S. Bollo, L.J. Núñez-Vergara, M. Bontá, G. Chauviere, J. Perie, J.A. Squella, Electroanalysis 13 (2001) 936.
[20] J.H. Tocher, D.I. Edwards, Free Radic. Res. Commun. 16 (1992) 19.
[21] J.H. Tocher, D.I. Edwards, Free Radic. Res. Commun. 9 (1990) 49.
[22] D. Barety, B. Resibois, G. Vegoten, Y. Moschetto, J. Electroanal. Chem. 162 (1984) 335.
[23] S. Bollo, L.J. Núñez-Vergara, M. Bontá, G. Chauviere, J. Perie, J.A. Squella, J. Electroanal. Chem. 511 (2001) 46.
[24] M.L. Arguelho, G. Silva, N. Stradiotto, J. Electrochem. Soc. 148 (2) (2001) D1.
[25] S. Roffia, C. Gottardi, E. Vianello, J. Electroanal. Chem. 142 (1982) 263.
[26] J. Carbajo, S. Bollo, L.J. Núñez-Vergara, A. Campero, J.A. Squella, J. Electroanal. Chem. 531 (2002) 187.
[27] A. Papoutsis, G. Kokkinidis, J. Electroanal. Chem. 371 (1994) 231.
[28] G.G. Gallo, C.R. Pasqualucci, P. Radaelli, G.C. Lancini, J. Org. Chem. 29 (1964) 862.
[29] J. Arguello, L.J. Núñez-Vergara, J.A. Squella, Electrochem. Commun. 7 (2005) 53.
[30] R.S. Nicholson, Anal. Chem. 37 (1965) 1351.
[31] J.A. Squella, S. Bollo, L.J. Núñez-Vergara, Curr. Org. Chem. 9 (6) (2005) 565.

Journal of The Electrochemical Society, **154** (4) F77-F81 (2007)
0013-4651/2007/154(4)/F77/5/$20.00 © The Electrochemical Society

Electrochemical Reduction of 2-Nitroimidazole in Aqueous Mixed Medium

J. A. Squella,[a,*,z] L. J. Núñez-Vergara,[a,*] A. Campero,[b] J. Maraver,[b] P. Jara-Ulloa,[a] and J. Carbajo[b]

[a]*Bioelectrochemistry Laboratory, Chemical and Pharmaceutical Sciences Faculty, University of Chile, Olivos 1007, Santiago, Chile*
[b]*Departamento de Química Física y Química Orgánica, Facultad de Ciencias Experimentales, Universidad de Huelva, Huelva, Spain*

A detailed investigation of the electrochemical reduction of 2-nitroimidazole (2-NIm) in a mixed aqueous medium was carried out by means of cyclic voltammetry (CV) at a mercury electrode. The voltammetric behavior of 2-NIm in 60% dimethylformamide (DMF) (0.1 M tetrabutyl ammonium perchlorate, TBAP)/40% aqueous buffer (0.3 M KCl + 0.015 M citric acid + 0.03 M boric acid) is pH-dependent, changing from one irreversible reduction peak at acid pHs to two reduction peaks at alkaline pHs. At pH 2.5 it is possible to obtain a voltammetric pK which is due to the protonation-deprotonation equilibrium produced by the hydroxylamine derivative formed from the reduction of 2-NIm. This indicates that 2-NIm is reduced to the unprotonated hydroxylamine derivative above pH 2.5 and to its protonated form below it. At pH $>$ 7 it is possible to observe a cyclic voltammetric couple due to the one-electron reduction of 2-NIm to produce the corresponding nitro radical anion. Furthermore, the nitro radical anion disproportionates with a rate constant, k_2, of 6.78×10^5 M s^{-1} and a half-life, $t_{1/2}$, of 1.5 ms for the first half-life. The voltammetric behavior of 2-NIm in aqueous mixed medium is substantially different from that described in nonaqueous medium; in fact, only in the aqueous medium is it possible to study in isolation the nitro radical anion.
 [DOI: 10.1149/1.2472553]

Manuscript submitted October 23, 2006; revised manuscript received December 13, 2006.
Available electronically February 22, 2007.

It is possible to distinguish 2-, 4-, and 5-nitroimidazole derivatives (Fig. 1) according to the position of the nitro substituent in the imidazole ring. From the point of view of biological activity, 2-nitroimidazolic derivatives are used preferably as radiosensitizers and as cytotoxins in hypoxic cells, whereas 5-nitroimidazole derivatives are mainly used for their toxicity towards microorganisms and 4-nitroimidazole derivatives are relatively more inert biologically.[1] The 2-nitroimidazoles have been used clinically to radiosensitize resistant hypoxic cells. Their use as radiosensitizers takes advantage of their cytotoxicity in hypoxic mammalian cells that allows the sensitivity to the radiation of cancerigenic tumors to be increased.[2-4] The mechanism of action usually involves the reduction of the nitro group via single or multiple reduction steps with one, two, four, or six electrons.[5] The nitro group is "electron-attractive" and thus may interact with damages on DNA induced by radiation in a manner analogous to oxygen; hence, they are called oxygen mimetic radiosensitizers or classic radiosensitizers.[6] Electron transfer from a damaged DNA site to the NO_2 group prevents charge recombination and produces the radical anion (RNO_2^-). As a consequence, the subsequent irreversible reactions may lead to a DNA strand breakage and cause the fixation of the damages.[7] The selective toxicity of nitroaromatics toward hypoxic cells is due to the production of reactive intermediates, such as nitroso and hydroxylamine derivatives. Their reactivities, and thus cytotoxicities, are modulated by aromatic ring substituents as well as by the pH of the medium.[8]

Although nitro reduction and redox behavior are crucial for all biological activity, there are still no conclusive studies about the electrochemistry of 2-nitroimidazole. In fact, electrochemical studies about 2-nitroimidazole derivatives are restricted almost exclusively to work where electrocatalytic reduction on gold and modified gold electrodes is described.[9] The mechanism described in that work involved two different routes in an acid medium, one of an electrocatalytic type and the other of an electronic interchange. No reference in that work refers to the formation of radical intermediates. Moreover, no previous studies devoted to elucidating the reduction mechanism of 2-nitroimidazole have been published. In a recent paper,[10] we have discussed the electrochemical reduction of 2-nitroimidazole in a nonaqueous medium. In an aprotic medium the voltammogram of 2-nitroimidazole is strongly influenced by the existence of a dissociation equilibrium between the neutral species ($HNRNO_2$) and the corresponding conjugate base ($^-NRNO_2$). Consequently, the voltammograms of 2-nitroimidazole produce two well-defined reduction peaks. The first is caused by the reduction of the neutral species according to the following overall mechanism

$$5HNRNO_2 + 4e^- \rightarrow 4\,^-NRNO_2 + HNRNHOH + H_2O \quad [1]$$

The second peak is caused by the reduction of the conjugate base to form the corresponding dianion radical according to the following equation

$$^-NRNO_2 + e^- \rightarrow {}^-NRNO_2^-$$

Curiously, in the nonaqueous medium, it was not possible to isolate and characterize the nitro radical anion intermediate of the monoelectronic reduction process.

According to the above results we hypothesize that the behavior in the aqueous medium will vary because the mentioned equilibrium in nonaqueous medium will not exist. Consequently, our current interest is to elucidate the voltammetric behavior in an aqueous mixed medium and to investigate the possible stabilization of the nitro radical anion derivative in this medium.

Experimental

Reagents and solutions.— 2-nitroimidazole (2-NIm) and 4-nitroimidazole (4-NIm) (Fig. 1a), 97% pure, were obtained from Aldrich Chemical Co. and were used without prior purification. All other reagents employed were of analytical grade. Nitrogen gas was

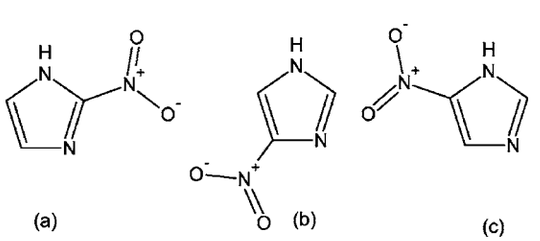

Figure 1. Molecular structures of (a) 2-NIm, (b) 4-NIm, and (c) 5-NIm.

* Electrochemical Society Active Member.
z E-mail: asquella@ciq.uchile.cl

obtained from Alphagaz-Air Liquide with maximum impurities of $H_2O < 3$ ppm, $O_2 < 2$ ppm, and $C_nH_m < 0.5$ ppm.

All voltammetric experiments were conducted after bubbling with N_2 for 10 min in the cell before each run. Temperature was kept constant at 25 ± 0.1°C in all experiments.

Solutions for cyclic voltammetry (CV) were prepared starting from a 0.2 M stock solution of the nitroimidazole derivative in dimethylformamide (DMF) prepared daily. Final solutions in the voltammetric cell were prepared by diluting an appropriate quantity of the stock solution to obtain a final concentration of 1 mM.

Experiments for the pH study were made in a buffer containing 0.05 M boric acid + 0.015 M citric acid (anhydrous) + 0.3 M KCl//DMF [0.2 M tetrabutyl ammonium perchlorate (TBAP)] (40:60). For comparative studies we also used a different aqueous organic medium containing 0.1 M Brittton–Robinson buffer + 0.3 M KCl//EtOH (70:30) at pH 8.0. The pH was adjusted by the addition of concentrated solutions of NaOH or HCl, depending on the desired final pH.

All pH measurements were carried out with a Crison model Basic 20 pH meter equipped with a glass electrode Crison 52-01 (resolution 0.01, precision ±0.01). The standard solutions used for calibration were Crison 4.00 and 7.02 and Probus 10.00. Measurements of pH were corrected according to the following equation:[11] $pH^* - B = \log U_H^o$, where pH^* equals $-\log a_H$ in the mixed solvent, B is the pH meter reading, and the term $\log U_H^o$ is the correction factor for the glass electrode, which was calculated for the different mixtures of DMF or EtOH and aqueous solvent, according to a procedure previously described.[12]

Apparatus and methods.— Voltammetric curves were recorded on an electrochemical analyzer type BAS 100B/W (Bioanalytical System) attached to a PC computer with appropriate software (BAS 100W 2.3 for Windows) for total control of the experiments, data acquisition, and treatment. A static mercury drop electrode (SMDE) (BASi EF-1400) with a mercury drop area of 0.43 mm^2 was used as the working electrode and a platinum wire (BASi MW-1032) served as the counter electrode. All potentials were measured against Ag|AgCl|NaCl (3 M) (BASi MF-2052); $E = -0.045$ V vs saturated calomel electrode (SCE).

The peak current ratio, $i_{p,a}/i_{p,c}$, for the reversible first electron transfer (RNO_2/RNO_2^- couple) was measured for each cyclic voltammogram, according to the procedure described by Nicholson.[13] A reproducibility study involving 10 independent runs at different sweep rates (5 and 40 V s^{-1}) produced variation coefficients of 0.5 and 1.1% for peak potential and current-ratio measurements, respectively.

Using the theoretical approach of Olmstead and Nicholson,[14] the $i_{p,a}/i_{p,c}$ values experimentally measured at each scan rate were inserted into a working curve to determine the parameter ω, which incorporates the effects of the rate constant, 2-NIm concentration, and scan rate. A plot of ω vs τ resulted in a linear relationship described by the equation $\omega = k_2 C^\circ \tau$, where k_2 is the second-order rate constant for the decomposition of RNO_2^-, C° is the 2-NIm concentration, and $\tau = (E\lambda - E_{1/2})/\upsilon$. Consequently, we can obtain the second-order rate constant for the decomposition of the nitro radical anion from the slope of the ω vs τ straight line.

Spectrophotometric measurements were recorded in the 250–450 nm range, using an ATI Unicam model UV-2 spectrophotometer in a 1 cm quartz cell and equipped with Vision 2.1 acquisition and treatment software.

Temperature was controlled with a Thermostat/cryostat Selecta Frigiterm-10 with a precision of 0.1°C.

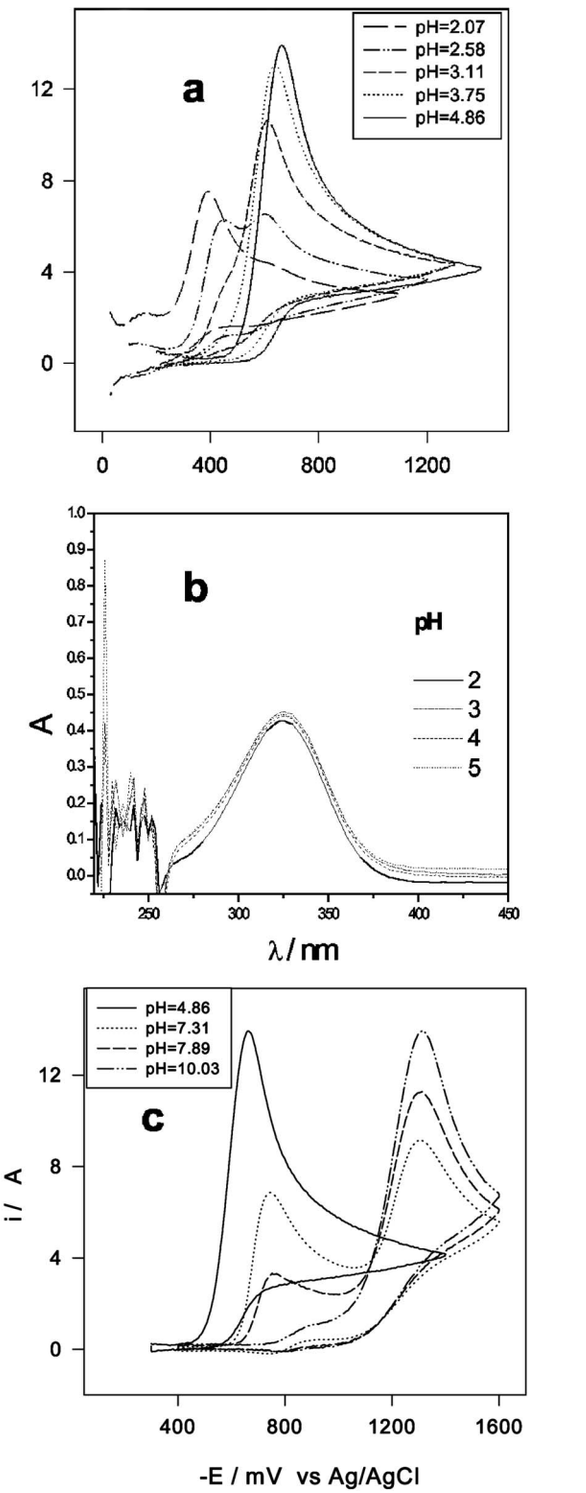

Figure 2. CVs of 1 mM 2-NIm in 60% DMF (0.1 M TBAP)/40% H_2O (0.3 M KCl + 0.015 M citric acid + 0.03 M boric acid) at pH (a) 2–5 and (c) 5–10 (υ = 1 V/s). (b) UV spectra of 0.05 mM 2-NIm in the same pH conditions of a.

Results and Discussion

2-NIm was electrochemically reduced in a mixed medium containing an aqueous buffer of boric acid 0.05 M + anhydrous citric acid 0.015 M + 0.3 M KCl//DMF (0.2 M TBAP 40:60 by means of CV with a Hg electrode. The voltammetric behavior was found to be pH-dependent, changing from one irreversible reduction peak at acid pH to two peaks at alkaline pH. Figure 2a shows the voltammetric reduction peak in acidic medium. At pH between 2–3 (approx. 2.5) it is possible to observe a splitting of the peak, which is

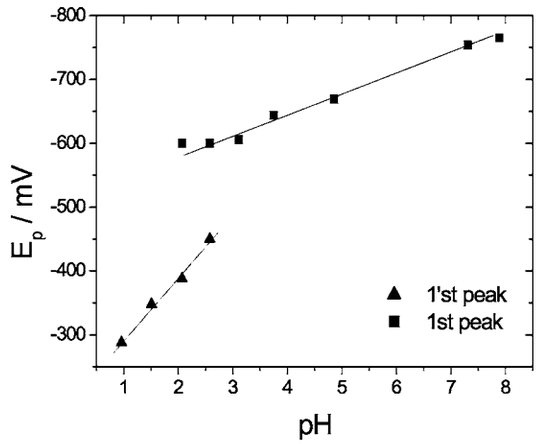

Figure 3. Peak–potential dependence on pH of both peaks for the reduction of 2-NIm in 60% DMF (0.1 M TBAP)/40% H_2O (0.3 M KCl + 0.015 M citric acid + 0.03 M boric acid) in acidic and neutral medium.

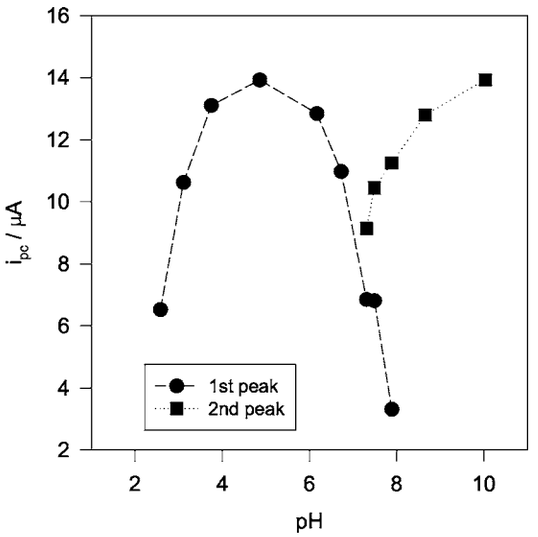

Figure 4. Peak–current dependence on pH of the (circles) first and (squares) second peaks for the reduction of 2-NIm in 60% DMF (0.1 M TBAP)/40% H_2O (0.3 M KCl + 0.015 M citric acid + 0.03 M boric acid) in acidic and alkaline medium (v = 1 V/s).

also observed in the E_P vs pH plot in Fig. 3. The change of the slope in the E_P vs pH plot means a change in the overall reaction, probably provoked by the existence of a voltammetric pKa at approximately 2.5 in 2-NIm compound. No change was observed in the UV spectra of 2-NIm in the same pH range (Fig. 2b).

Our first hypothesis for explaining the voltammetric pK implied the existence of a protonation–deprotonation equilibrium on the acidic N of the imidazole moiety. However, this hypothesis was discarded because the pKa value of −0.8 described for 2-NIm[15] is very different. Furthermore, in the same previous paper, UV-absorption bands with λ_{max} at 298, 325, and 372 nm for conjugate base, neutral molecule, and conjugate acid, respectively, were described. In our case the UV spectra with an absorption band at 325 nm at pHs between 1 and 5 (Fig. 2b) proved that the only species is the neutral molecule of 2-NIm. A second hypothesis was the possible protonation of the nitro group, but this protonation is very difficult according to the described values of −11 for the case of nitrobenzene.[16] A third hypothesis assumed that the change in the mechanism is due to the pKa of the product of the electrode reaction, i.e., the hydroxylamine derivative. This hypothesis was supported by a previous work of Laviron et al.[17] In that paper, a pKa of 2.5 for the equilibrium between protonated and deprotonated hydroxylamine derivatives from nitrosobenzene was reported. In our case the pKa of 2.5 corresponds to the protonation–deprotonation equilibrium of the hydroxylamine derivative from 2-NIm. This indicates that 2-NIm is reduced to the unprotonated hydroxylamine derivative above pH 2.5 and to its protonated form below it. Consequently, the reduction peaks in acidic medium are due to the well-known[18] four-electron reduction of the nitro group to produce the hydroxylamine derivative according to

$$\text{pH} < \text{pKa} \quad RNO_2 + 5H^+ + 4e^- \rightarrow RNHOH_2^+ + H_2O$$

$$\text{pH} > \text{pKa} \quad RNO_2 + 4H^+ + 4e^- \rightarrow RNHOH + H_2O \qquad [2]$$

At pH > 7 the voltammetric behavior changes, revealing two other cathodic peaks as shown in Fig. 2c. The single peak observed in acidic medium splits into two new peaks as the pH increases. This behavior follows the well-known general pattern, previously described[19] for nitro compounds in an aprotic medium or in the presence of inhibitors. Consequently, at pH > 7, the equations describing the two new cathodic peaks correspond to

$$RNO_2 + e^- \leftrightarrows RNO_2^- \qquad [3]$$

$$RNO_2^- + 3e^- + 4H^+ \rightarrow RNHOH + H_2O \qquad [4]$$

In Fig. 4 we have summarized the pH effect on cathodic peak current. As can be seen, the peak current is strongly pH dependent, showing the decrease in peak current at acidic pH due to the protonation of the hydroxylamine derivative. Furthermore, at pH near 7 the presence of a new peak and the diminution of the first peak show the change of the mechanism passing from an overall reaction according to Eq. 2 to a new one according to Eq. 3 and 4.

In the voltammograms at pH > 7 it is possible to observe an anodic peak associated with the first cathodic peak. However, the current of this anodic peak is considerably enhanced when the sweep range is narrowed. In fact, if the width of the sweep is restricted to involve only the first peak, it is possible to observe a very-well-defined couple, as seen in Fig. 5. From this couple we have measured a ΔE_p value of approximately 60 mV, confirming

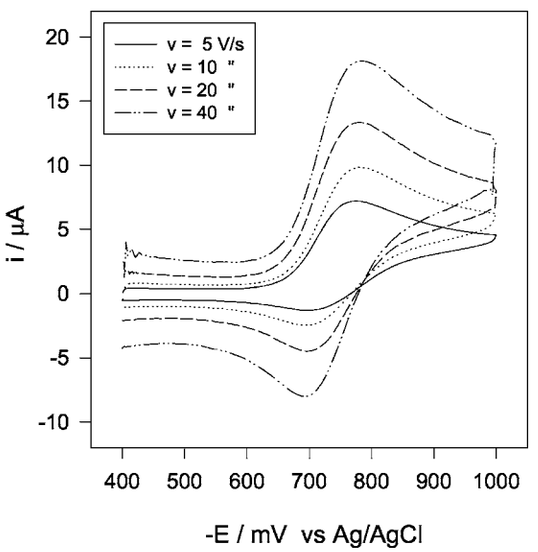

Figure 5. CVs showing the RNO_2/RNO_2^- couple from 1 mM 2-NIm in 60% DMF (0.1 M TBAP)/40% H_2O (0.3 M KCl + 0.015 M citric acid + 0.03 M boric acid) at different sweep rates (pH 8).

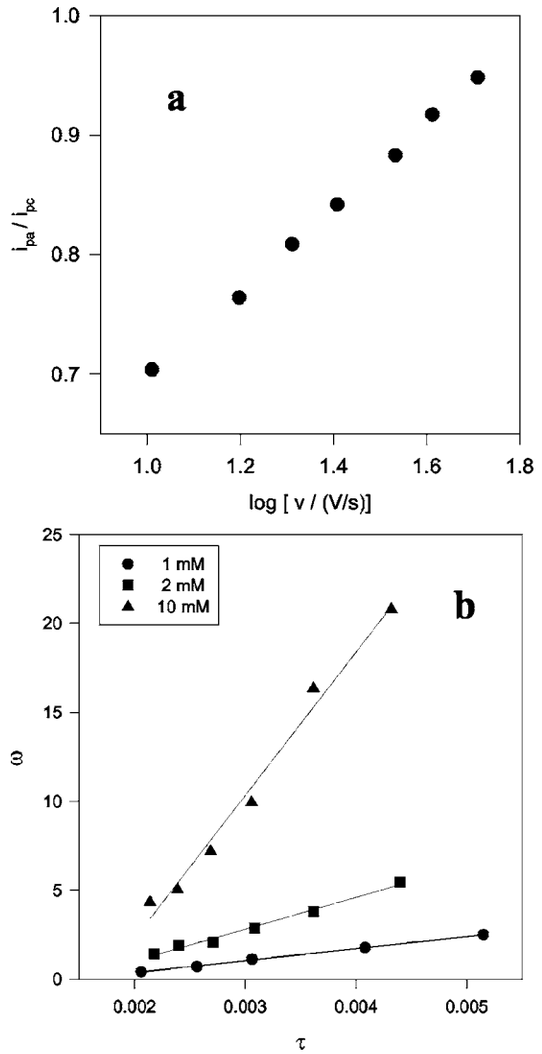

Figure 6. (a) Current-ratio dependence on sweep rates of the RNO_2/RNO_2^- couple from CVs of 1 mM 2-NIm in 60% DMF (0.1 M TBAP)/40% H_2O (0.3 M KCl + 0.015 M citric acid + 0.03 M boric acid) at different sweep rates at pH 8 and (b) plot of the kinetic parameter, ω, with the time constant, τ, for 1, 2, and 10 mM 2-NIm in 60% DMF (0.1 M TBAP)/40% H_2O (0.3 M KCl + 0.015 M citric acid + 0.03 M boric acid) at pH 8.

the one-electron character of the couple. Consequently, the observed couple is the one-electron reduction of 2-NIm to form the corresponding nitro radical anion, according to Eq. 3. From the CVs it is possible to calculate the current ratio, $i_{p,a}/i_{p,c}$, and the variation of the current ratio with the sweep rate as shown in Fig. 6a. From this figure we observe an increase of the current ratio with an increase of the sweep rate, reaching a value of 1 at sufficiently high rates. These results imply that the monoelectronic reduction does not correspond to a simple reversible process (i.e., $i_{p,a}/i_{p,c} = 1$); on the contrary, the above results are indicative of a coupled chemical reaction. In fact, the results indicate that the nitro radical anion generated in the cathodic sweep is not totally oxidized in the back anodic sweep, producing a current ratio lower than 1. This means that part of the nitro radical anion is consumed by the coupled chemical reaction. In the case of nitro radical anions in mixed medium, the coupled chemical reaction probably is a disproportionation reaction.[20] Consequently, the process that better defines the monoelectronic couple should be represented by the following reactions

$$RNO_2 + e^- \leftrightarrows RNO_2^-$$

Table I. Disproportionation rate constants: half-lives (first half-live) for the nitro radical anion and cathodic peak potentials for the RNO_2/RNO_2^- couple for 2- and 4-NIm derivatives in mixed aquo-organic media at pH 8.

Compound	$k_2 \times 10^{-3}$ (1 mol^{-1} s^{-1})	$t_{1/2}$ (ms)	$-E_{p,c}$ (V)
2-NIm[a]	678	1.5	780
2-NIm[b]	610	1.6	660
4-NIm[c]	145	6.8	830

[a] Values obtained in 0.05 M boric acid + 0.015 M citric acid (anhydrous) + 0.3 M KCl//DMF (0.2 M TBAP) (40:60) at pH 8.
[b] Values obtained in 0.1 M Britton–Robinson buffer + 0.3 M KCl// EtOH (70:30) at pH 8.0.
[c] Values obtained from Ref. 21.

$$2RNO_2^- + 2H^+ \rightarrow RNO_2 + RNO + H_2O \quad [5]$$

In order to confirm the proposed mechanism, we applied the CV theory for the disproportionation reaction described by Olmstead and Nicholson.[14] By applying this theory we obtained straight lines for plots of the kinetic parameter ω vs τ at different concentrations of 2-NIm, in perfect accordance with that anticipated by the theory (Fig. 6b). Furthermore, according to the theory, for $a\tau = 4$, it should be noted that $\omega = k_2 C^\circ \tau$; consequently, we can obtain the disproportionation rate constant (k_2) from the slope of the straight lines between ω and τ. We have calculated the k_2 values and the corresponding half-lives ($t_{1/2}$) for the nitro radical anion of 2-NIm. For comparative purposes we have also calculated the k_2 and $t_{1/2}$ values for two different aqueous media at the same pH. These results and a comparison with analogous parameters obtained for the 4-NIm isomer[21] are shown in Table I. From these results is clear that 2-NIm is more easily reducible than 4-Nim. This difference is explained because the nitro group in the 2-position possesses two adjacent electronegative N atoms, thus diminishing the electron density on the nitro group. Exactly the same effect was found in an aprotic medium.[10] From the results in Table I it is possible to deduce that the k_2 and $t_{1/2}$ values for the nitro radical anion from 2-NIm are very similar in both mixed aqueous organic mediums. However, the cathodic-peak potential is strongly affected by the nature of the medium. According to these results, the stability of the nitro radical anion appears to be independent of the nature of the aqueous-organic medium, but the ease of formation of the nitro radical anion, expressed in the $E_{P,C}$ values, is strongly dependent on the medium. When a more aqueous medium is used, but at the same pH, the reduction of 2-NIm is easier by 120 mV.

Furthermore, in Table I, we see that the disproportionation rate constant, k_2, is almost five times larger for the 2-NIm derivative than for the 4-NIm derivative. This result is in accord with the fact that 2-NIm derivatives are used as radiosensitizers and as cytotoxins in hypoxic cells. The highest values of k_2 imply more production of the nitroso intermediate and consequently improved conditions for acting as a cytotoxic agent against hypoxic mammalian cells. Thus, the k_2 parameter can be considered as an index to account for production of the nitroso derivative.

Conclusions

Although 2-NIm is a relatively simple heterocyclic molecule, its complex behavior is strongly determined by the existence of two N atoms with different characteristics in the molecule. One of them (N1) is linked to an H atom, which can act as an ionizable proton; the other N (N3) can act as a proton acceptor. Consequently, the molecule is very sensitive to the nature of the media. In the previous study in a nonaqueous medium,[10] we reported the existence of an equilibrium between the neutral species ($HNRNO_2$) and the corresponding conjugate base ($^-NRNO_2$) arising from loss of a proton from the imino nitrogen (N1). In the present study in aqueous mixed medium, we have detected that the only present species was the

neutral molecule. However, the overall electrodic reaction was influenced with the protonation of the hydroxylamine derivative generated in the reduction of 2-NIm.

According to the above results the voltammetric reduction of 2-NIm in a mixed aqueous medium is substantially different from that seen previously in totally nonaqueous medium.[10] The most important difference is related to the formation and stability of the nitro radical anion. In spite of what seems to be a contradiction, the nitro radical anion is stabilized only in the mixed aqueous medium. This result is rather paradoxical considering that free radicals are normally better stabilized in nonaqueous media. In this paper we have studied the couple in isolation, showing the formation of the nitro radical anion. According to this study we have postulated that a coupled disproportionation reaction follows the one-electron transfer and we have calculated the rate constant, k_2, for this disproportionation reaction. Considering that the disproportionation reaction produces the toxic nitroso species, which is responsible for the selective toxicity of 2-NIm derivatives toward hypoxic cells, we propose the k_2 parameter as an index to account for production of the nitroso derivative.

Acknowledgments

The authors are grateful to FONDECYT (project no. 1050767) for support of this work.

University of Chile assisted in meeting the publication costs of this article.

References

1. D. Church, H. Rabin, and E. Laishley, *J. Antimicrob. Chemother.*, **25**, 15 (1990).
2. D. Thall, G. Rosner, C. Azuma, M. Mc Entee, and J. Raleigh, *Radiother. Oncol.*, **44**, 171 (1997).
3. F. Riché, A. du Molinet, S. Sèpe, L. Riou, D. Fagret, and M. Vidal, *Bioorg. Med. Chem. Lett.*, **11**, 71 (2001).
4. S. A. Everett, M. A. Naylor, K. B. Patel, M. R. Stratfordand, and P. Wardman, *Bioorg. Med. Chem. Lett.*, **9**, 1267 (1999).
5. M. I. Walton and P. Workman, *Biochem. Pharmacol.*, **36**, 887 (1987).
6. N. Farrell, *Inorg. Chim. Acta*, **92**, 61 (1984).
7. F. D. Rochon, P. C. Kong, R. Melanson, K. A. Skov, and N. P. Farrell, *Inorg. Chim. Acta*, **30**, 4531 (1991).
8. R. A. McClelland, R. Panicucci, and A. M. Rauth, *J. Am. Chem. Soc.*, **109**, 4308 (1987).
9. A. Papoutsis and G. Kokkinidis, *J. Electroanal. Chem.*, **371**, 231 (1994).
10. J. A. Squella, A. Campero, J. Maraver, and J. Carbajo, *Electrochim. Acta*, **52**, 511 (2006).
11. A. G. Gonzalez, F. Pablos, and A. Asuero, *Talanta*, **39**, 91 (1992).
12. A. Asuero, M. A. Herrador, and A. G. Gonzalez, *Talanta*, **40**, 479 (1993).
13. R. S. Nicholson, *Anal. Chem.*, **36**, 1406 (1964).
14. M. L. Olmstead and R. S. Nicholson, *Anal. Chem.*, **41**, 862 (1969).
15. G. G. Gallo, C. R. Pasqualucci, P. Radaelli, and G. C. Lancini, *J. Org. Chem.*, **29**, 862 (1964).
16. E. Laviron and L. Roullier, *J. Electroanal. Chem. Interfacial Electrochem.*, **288**, 165 (1990).
17. E. Laviron, A. Vallat, and R. Meunier-Prest, *J. Electroanal. Chem.*, **379**, 427 (1994).
18. H. Lund, in *Organic Electrochemistry*, 4th ed., H. Lund and O. Hammerich, Editors, p. 379, Marcel Dekker, New York (2001); D. I. Edwards, *Prog. Med. Chem.*, **18**, 87 (1981).
19. B. Kastening, *Progress in Polarography*, Vol. 3, P. Zuman and L. Meites, Editors, p. 259 Wiley-Interscience, New York (1972).
20. J. A. Squella, S. Bollo, and L. J. Núñez-Vergara, *Curr. Org. Chem.*, **9**, 565 (2005).
21. J. Carbajo, S. Bollo, L. J. Núñez-Vergara, A. Campero, and J. A. Squella, *J. Electroanal. Chem.*, **531**, 187 (2002).

Full Paper

Micellar Effects on the Reduction of 4-Nitroimidazole Derivative: Detection and Quantification of the Nitroradical Anion

*P. Jara-Ulloa, L. J. Núñez-Vergara, J. A. Squella**

Bioelectrochemistry laboratory, Chemical and Pharmaceutical Sciences Faculty, University of Chile, POB 233, Olivos 1007, Santiago, Chile
*e-mail: asquella@ciq.uchile.cl

Received: January 19, 2007
Accepted: March 27, 2007

Abstract
The reductive electrochemistry of 1-methyl-4-nitro-2-hydroxymethylimidazole, a 4-nitroimidazole derivative, was examined in the presence of surfactants anionic as sodium dodecyl sulfate (SDS), nonionic, Triton-X, Cationic, Hyamine and Cetyl Trimethyl Ammonium Bromide (CTAB). The reductive mechanism of the nitroimidazole derivative was found to be dependent of both, nature and concentration of the surfactants.
By using appropriately the wide versatility of the cyclic voltammetric technique it was possible to study the generation of the nitroradical anion and their stability in different micellar media. The experimental scheme involved the measurement of the current ratio, $i_{p,a}/i_{p,c}$, from the cyclic voltammograms and its interpolation into theoretical working curves to determine the ω parameter. A plot of ω versus τ resulted in a linear relation described by $\omega = k_2 C \tau$ where k_2 is the second order rate constant for the decomposition of the nitroradical anion.
Cyclic voltammetric experiments demonstrated that the reduction of the 4-nitroimidazole derivative in presence of cationic micelles generated a sufficiently well stabilized nitroradical anion in aqueous medium at pH 7.4.
The aim of this study is to investigate the electrochemistry of 4-MNImOH in a micellar medium with the objective to obtain a better approach to the in-vivo conditions and to improve the detection and quantification of the nitroradical anion species.

Keywords: 4-Nitroimidazole, Micelles, Cyclic voltammetry, Nitroradical anion

DOI: 10.1002/elan.200703863

1. Introduction

Nitroimidazoles have been the source of many investigations because of their properties as antibiotics, radiosensitizers and antiprotozoans. Its use as radiosensitizers takes advantage of its cytotoxicity in hypoxic mammalian cells what allows to increase sensitivity to the radiation of tumors [1–4]. Its antimicrobial characteristic takes advantage of its selective toxicity towards anaerobic microorganisms and allows that these compounds are used extensively in the treatment of infectious diseases in human and animal therapeutic [5–10]. Furthermore, is very well-known that nitroradical anion is a key intermediate in the biological activity of nitroimidazole derivatives [11]. Consequently, the understanding of the nitroradical behavior is a permanent challenge for this type of compounds and the electrochemistry can play an important role in its study.

The unique properties of surfactants, in particular their adsorption at interfaces and ability to form a variety of organized assemblies in solutions has been exploited in several fields of chemistry such as the electrochemistry. Saveant et al. [12] have reported a remarkable stabilization of the electrogenerated anion radical of phthalonitrile in the presence of cationic micelles and suggested that the observed 250-fold decrease in the rate of protonation of the anion radical was due to its association with the positively charged micelles. On the other hand, McIntire et al. [13], examined the electrochemistry of nitrobenzene in anionic, cationic and nonionic micelles. Results indicate that only anionic micelles stabilized the nitrobenzene anion radical due to a strong surface interaction.

In the scope of our current investigations to find new pharmacological important compounds that use the nitroradical anion as the active specie, we synthesized 1-methyl-4-nitro-2-hydroxymethylimidazole (4-MNImOH) a new 4-nitroimidazole derivative 1, 2- substituted. In a previous study [14], we studied the nitroradical anion formation in aqueous, mixed and nonaqueous media, but the nitroradical anion was detected only in mixed and nonaqueous media.

Taking into account that the micellar environment is considered to be a primitive, although simple, model for biological membranes [15], the present cyclic voltammetric study would be a very useful tool to quantify the stability and reactivity of the nitroradical anion in conditions that resembling the cell environmental.

2. Experimental

2.1. Reagents and Solutions

1-Methyl-4-nitro-2-hydroxymethylimidazole (4-MNImOH) (Fig. 1) was synthesized and characterized in our laboratory according to the procedure previously described [15]. The surfactants employed: sodium dodecyl sulfate (SDS) anionic; Triton-X, nonionic; Hyamine, Cationic and Cetyl Trimethyl Ammonium Bromide (CTAB) cationic were obtained from Sigma-Aldrich. All the other reagents employed were of analytical grade and were used without prior purification. Nitrogen gas was obtained from AGA Chile S. A. with maximum impurities of $H_2O < 3$ ppm; $O_2 <$ 2 ppm; $C_nH_m < 0.5$ ppm.

All the voltammetric experiments were obtained after bubbling with N_2 for 10 min in the cell before each run. Temperature was kept constant at $25 \pm 0.1\,^{\circ}C$ in all experiments.

0.1 M Britton – Robinson buffer was prepared dissolving 6.18 g of boric acid, 5.7 mL of glacial acetic acid, 6.7 mL of phosphoric acid and completing up to 1000 mL with water, and then the desired pH was adjusted with concentrate solutions of NaOH. The water used was purified with Milli-Q Ultra-Pure Water System.

Solutions containing surfactants were prepared with concentrations higher than the critical micelle concentration (CMC) in 0.1 M Britton – Robinson buffer.

4-MNImOH stock drug solution was prepared dissolving 7.85 mg and diluted up to 5 mL with 0.1 M Britton – Robinson buffer, to obtain a final concentration of 0.01 M.

Work solution was prepared taken an aliquot of the stock solution and diluted to 10 mL with 0.1 M Britton – Robinson buffer with and without surfactants.

2.2. Apparatus and Methods

Voltammetric curves were recorded on an Electrochemical Analyzer BAS CV-50W (Bioanalytical System) attached to a PC computer with appropriate software (BAS 100 W 2.3 for Windows) for total control of the experiments and data acquisition and treatment. A static mercury drop electrode with mercury drop area of 0.43 mm^2 (SMDE) (BASi EF-1400) for CV and a controlled growth mercury electrode (CGME) for polarography was used as the working electrode and a platinum wire (BASi MW-1032) as the counter electrode. All the potential measurements were carried out using an Ag | AgCl | NaCl (3 M) (BASi MF-2052) as the reference electrode.

For the kinetic analysis the return-to-forward peak current ratio $i_{p,a}/i_{p,c}$ for the one-electron couple (RNO_2/$RNO_2^{\bullet -}$) was measured for each cyclic voltammogram followed by a data treatment procedure detailed previously [14].

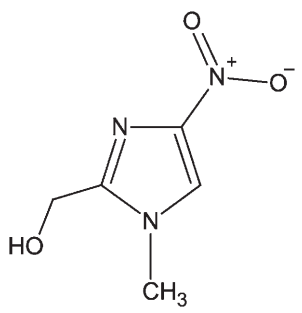

Fig. 1. Molecular structure of 1-methyl-4-nitro-2-hydroxymethylimidazole (4-MNImOH).

3. Results and Discussion

4-MNImOH was electrochemically reduced in aqueous medium containing 0.1 M Britton – Robinson buffer when it is submitted to differential pulse polarography (DPP) and Tast polarography (TP) between pH 2 – 12. As can be observed in Figure 2, only one cathodic peak in all the pH range is observed. The peak has a cathodic peak potential, $E_{p,c}$, of -470 mV at pH 7 but the peak is strongly pH-dependent. In order to study the pH influence on the nitroreduction we have evaluated the behavior of the peak potential, (E_p) obtained by DPP, and the limiting current (I_{lim}) obtained by TP, at different pH between 2 and 12. In the insert of Figure 2, the E_p vs. pH plot shows that the peak potential is pH-dependent shifting to more negative potentials when pH increased up to pH 9.5, but upon pH 9.5 the peak potential remained constant. The limiting currents

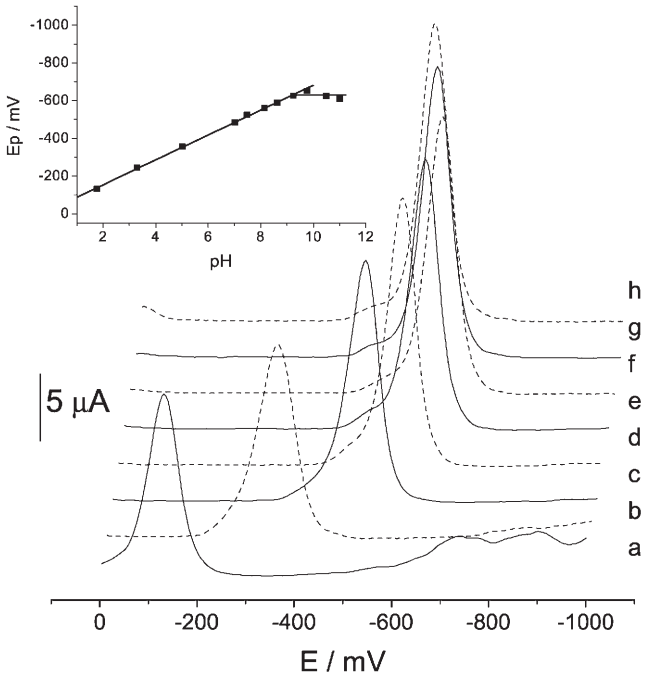

Fig. 2. Differential pulse polarograms of 0.1 mM 4-MNImOH in 0.1 M Britton – Robinson buffer at different pHs between 2 – 11. Insert: The corresponding peak potential dependence with pH: 1.8 (a), 5.0 (b), 7.5 (c), 8.6 (d), 9.2 (e), 9.7 (f), 10.5 (g), 11.0 (h).

remain practically pH independent between pH 2 – 9.5, according to a diffusion controlled process (Fig. 3). As can be proved in a previous paper [14] the reduction of 4-MNImOH produces the hydroxylamine derivative according to the well-known Equation 1:

$$RNO_2 + 4e^- + 4\,H^+ \rightarrow RNHOH + H_2O \quad (1)$$

The cyclic voltammogram of 4-MNImOH in aqueous medium containing 0.1 M Britton – Robinson buffer also shows a single peak with not any signal in the anodic sweep, which indicates that this peak corresponds to an irreversible process.

As can be observed from the above experiments it was not possible to stabilize the nitroradical anion in the aqueous medium. Considering that micelles could produce changes in the stability of the nitroradical anion we have added different types of surfactants to the aqueous solution to study the reduction of the nitroderivative.

The cathodic behavior of 4-MNImOH in aqueous medium was altered when surfactants were added to the solutions. We have tested anionic (SDS), nonionic (Triton X-100) and cationic (Hyamine and CTAB) surfactants but the observed modifications were dependent of the type of used surfactants. In the case of cationic surfactants the changes were more significant. The DPP of 4-MNImOH in CTAB and Hyamine micelles at different pHs are reflected in Figures 4A and B, respectively. From these figures is clear that the polarographic behavior was different from the situation without micelles (Fig. 2). Specifically the morphology of the polarographic peak changed i.e., the only peak observed in all the solutions without micelles is changed by two peaks in the new situation with micelles. In fact the change in the morphology of the polarographic response represents a change in the mechanism of the electrodic process changing from one overall step described in Equation 1 to two steps mechanism described by the well-known [15] following Equations 2 and 3:

$$RNO_2 + e^- \rightarrow RNO_2^{\bullet -} \quad (2)$$

$$RNO_2^{\bullet -} + 3\,H^+ + 4\,H^+ \rightarrow RNHOH + H_2O \quad (3)$$

Also, both potential peaks and current peaks for the reduction of 4-MNImOH changed with the addition of surfactants in all the pH range. The change of the potential peak (ΔE_p) for the nitroreduction resulting of the addition of CTAB and Hyamine in all the pH scale is shown in Figures 5A, B. As is noted from this Figure the ΔE_p is strongly pH-dependent exhibiting decreasing values when pH increased. The E_p values changed from about 400 mV at pH 2 to about 100 mV at pH > 10 meaning that in any pH condition the reduction of the nitrocompound in the micelles environment is more difficult than the situation without micelles. The E_p shift is consistent with the association of 4-MNImOH to the micellar aggregates showing that the NO_2 group is inserted into the CTAB or Hyamine micelles and hence more difficult electron-transfer associated with the reduction of the nitrogroup would be expected.

In the case of the anionic (SDS) and nonionic (Triton-X) surfactants the situation was totally different because the

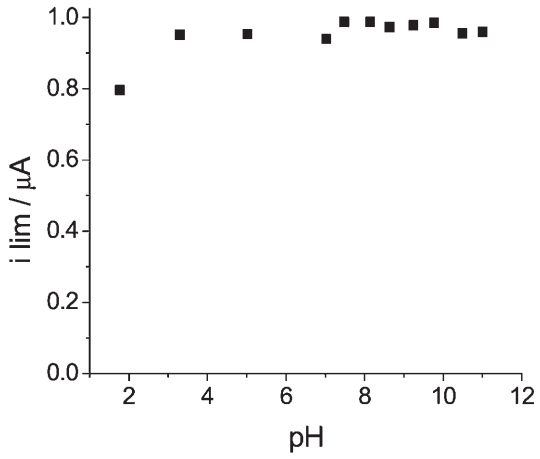

Fig. 3. Limiting current versus pH dependence obtained from Tast polarograms of 0.1 mM 4-MNImOH in 0.1 M Britton – Robinson buffer at different pHs between 2 and 11.

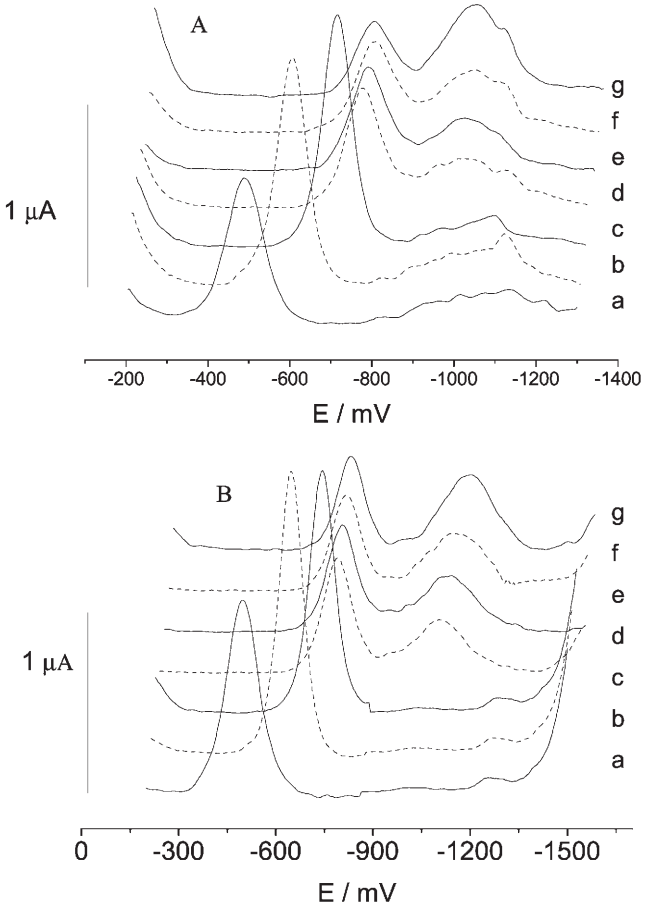

Fig. 4. DPP curves obtained 0.1 mM 4-MNImOH in 0.1 M Britton – Robinson buffer at different pHs between 2 and 11 with: A) 15 mM CTAB; B) 15 mM Hyamine. pH: 1.8 (a), 5.0 (b), 7.5 (c), 8.6 (d), 9.2 (e), 9.7 (f), 10.5 (g), 11.0 (h).

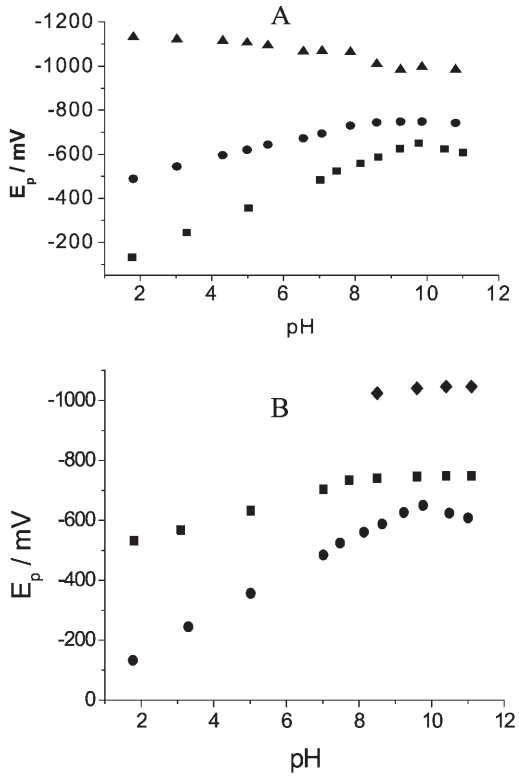

Fig. 5. Comparative E_p vs. pH plots obtained from 0.1 mM 4-MNImOH in 0.1 M Britton–Robinson buffer at different pHs between 2–11 with different surfactants: A) ■ = without surfactants, ● = peak I and ▲ = peak II with 15 mM CTAB; B) ● = without surfactants, ■ = peak I and ◆ = peak II with 15 mM Hyamine.

presence of the surfactants did not change the characteristics of the electrochemical processes, consequently only one DPP peak due to the 4-electron reduction of the nitrogroup was observed with and without surfactants added.

The observed splitting when cationic surfactants were added it was also confirmed by cyclic voltammetry (CV). Figure 6 displays CVs at the same pH by using different surfactants but only in the case wherein cationic surfactants (CTAB and Hyamine) were used it was possible to observe the splitting of the nitroreduction peak according to the above Equations 2 and 3. Notice that in the presence of SDS and Triton, the morphology of the nitroreduction peak is essentially the same as that in its absence, indicating that SDS or Triton-X micelles do not modify the characteristics of the electrochemical processes. According to these results we found the possibility of stabilizing the nitroradical anion at the interfaces of cationic micelles meaning a very good alternative to study this free radical in an aqueous medium. Our results are in accord with the previous results of Saveant et al. [12], which have reported a remarkable stabilization of the anion radical of phthalonitrile in the presence of cationic micelles and suggested that the observed 250-fold decrease in the rate of protonation of the anion radical was due to its association with the positively charged micelles. However, our results are contradictory with the previously reported by Mc Intire et al. [13] which examined the reductive electrochemistry of nitrobenzene in anionic, cationic and nonionic micelles, and found that the only medium capable of stabilizing the nitroradical anion to the point where it became detectable by cyclic voltammetry was not the cationic, but rather the anionic micelles. The combined results suggest that the influence of micellar systems on the electrochemistry of a particular substrate cannot be predicted only on the basis of simple electrostatic considerations and that micellar effects are strongly dependent upon the substrate and surfactants structures [16]. However, considering that our results show that the nitroradical anion is more persistent in the presence of cationic micelles (Hyamine and CTAB) that in either isotropic aqueous solution or nonionic (Triton-X) or anionic (SDS) micelles an explanation based in electrostatic considerations appear to be more important. Consequently the effect of cationic micelles on the stabilization of the nitroradical anions is: (a) the nitroradical anions are more strongly bound to the cationic micelle than the parent compound due to favorable coulombic interaction; (b) the cationic micelles do protect the anion radical against protonation by water.

Using the preceding cyclic voltammetric response, we can study the kinetic stability of the nitroradical species from 4-MNImOH in a micellar medium. As can be observed from Figure 6 (whole line), in the case of Hyamine and CTAB micelles a very well resolved CV for the nitro/nitroradical anion couple ($RNO_2/RNO_2^{\bullet -}$) can be obtained by adjusting the switching potential appropriately. In Figure 7, we can observe the isolated CV for the $RNO_2/RNO_2^{\bullet -}$ couple from 4-MNImOH solutions containing Hyamine as surfactant at different sweep rates. Furthermore, in the insert of Figure 7, the effect of different sweep rates on the current ratio for solutions having Hyamine as surfactant at three different pHs is shown. A similar general trend in all cationic surfactants was observed, i.e., the $i_{p,a}/i_{p,c}$ current ratio increases as the scan rate is increased. These results fulfill the requirements for an irreversible chemical reaction following a reversible charge-transfer step according to the Nicholson–Shain criteria [17]. Furthermore the current ratio was dependent on the 4-MNImOH concentration implying a second-order chemical step. According to the previously observed for the same compound in a mixed medium [14], the second-order chemical reaction is the disproportionation of the nitroradical anion, consequently, we have used the theoretical approach of Olmstead et al. [18] for disproportionation, to calculate the kinetic second-order rate constant, k_2, and the corresponding half-lifetime for the first half-life. The obtained kinetic second-order rate constant, k_2, and the corresponding half-lifetime values for the nitroradical anion from 4-MNImOH in aqueous medium with micellas at different pHs are shown in Table 1. Furthermore we have included the comparison of solutions containing different micellar concentration and solutions in mixed media without micelles. From these results we can state that the use of micellas is the only condition capable to stabilizing the nitroradical anion from 4-MNImOH to the

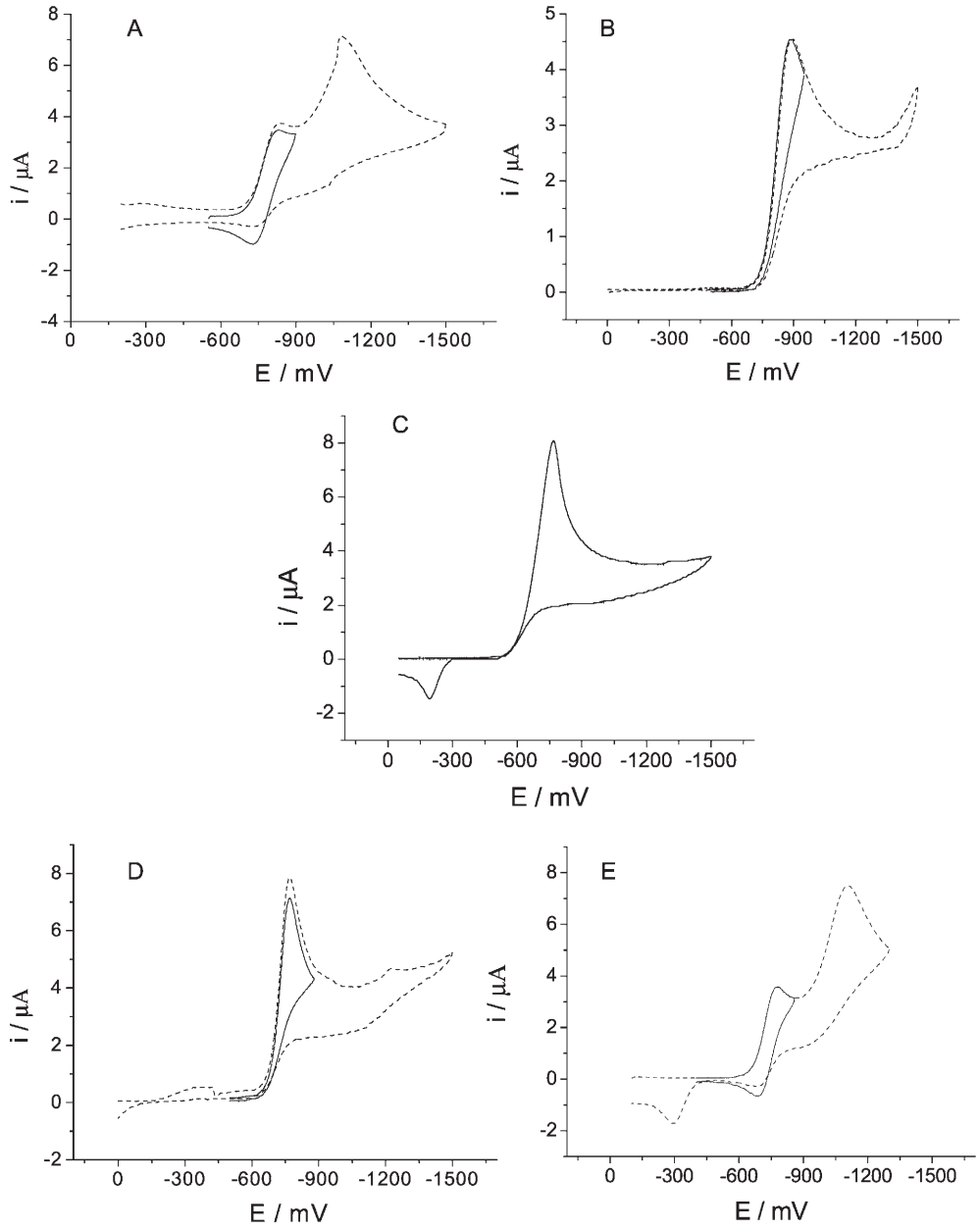

Fig. 6. CVs of 1 mM 4-MNImOH in 0.1 M Britton – Robinson buffer at pH 8.4 containing 15 mM of different surfactants: A) CTAB, B) Triton-X, C) without surfactant, D) SDS and E) Hyamine. Sweep rate = 1 V/s. Whole lines in A), E) shows a short sweep with RNO_2/ $RNO_2^{\bullet -}$ couple isolated.

point where it became detectable by CV, in aqueous solution in the pHs 7 – 9 zone. In mixed media without surfactants the CV study it was possible only since pH 10. Probably this fact is due to the decrease in the rate of protonation of the anion radical. On the other hand, when the concentration of Hyamine diminished from 15 to 5 mM the k_2 values shows a six-fold increase and the cathodic peak potential diminishing about 20 mV. Both facts can be rationalized by the adsorption of the surfactants at the electrode surface which may alter the overvoltage of the electrode and by the formation of micellar aggregates which influences the disproportionation reaction. Furthermore, in all the cases, when micelles were incorporated in the aqueous solution the cathodic peak potentials were cathodically shifting making the reduction of the nitroderivative more difficult. Also, if we compare the results obtained with the same concentrations of micelles but at different pHs we found that the pH affected strongly the stability of the nitroradical anion (k_2 values) however did not affect the energetic of the reduction of the nitrogroup ($E_{p,c}$ values). These results confirmed the pH-dependence of the disproportionation reaction and the pH-independence of the one-electron reduction of the nitroderivative to form the corresponding nitroradical anion according to the above Equation 2.

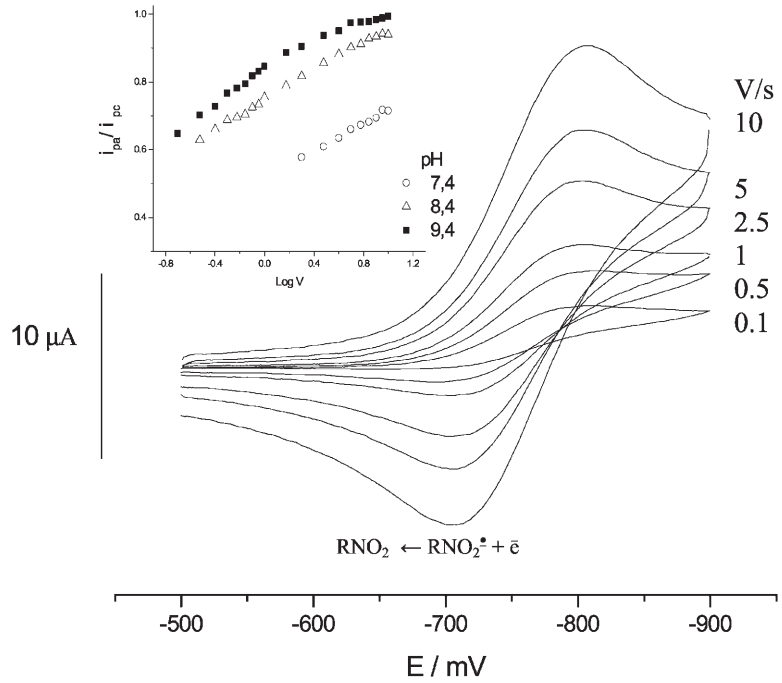

Fig. 7. Cyclic voltammograms showing the $RNO_2/RNO_2^{\bullet-}$ couple of 1 mM 4-MNImOH in 0.1 M Britton – Robinson buffer at pH 8.4 containing 15 mM Hyamine at different sweep rates. Insert: Current ratio dependence on sweep rates of $RNO_2/RNO_2^{\bullet-}$ couple of 1 mM 4-MNImOH in 0.1 M Britton – Robinson buffer containing 15 mM Hyamine at pHs 7.4, 8,4 and 9.4

Table 1. Disproportionation rate constants, half-lifetime for the nitroradical anion, and cathodic peak potentials for the $RNO_2/RNO_2^{\bullet-}$ couple from 4-MNImOH aqueous solutions in 15 mM Hyamine micelles at different pH.

pH	$k_2 \times 10^{-4}$ (L mol^{-1}s^{-1})	$t_{1/2}$ (ms)	$-E_{p,c}$ (mV)
7.4	104 ± 2.11	0.96	804
8.4	4.30 ± 0.43	23.25	802
9.4	1.37 ± 0.21	72.99	796
9.4[a]	8.77 ± 0.62	11.40	774
10[b]	0.59 ± 0.03	169.49	760
10[c]	1.36 ± 0.21	73.52	727

[a] Aqueous solution in 5 mM Hyamine micelles. Data obtained [15] from solutions containing a mixed medium. [b] 30/70: Ethanol/ Britton – Robinson buffer without micelles. [c] 60/40: DMF/citrate buffer, KCl without micelles.

4. Conclusions

We have found that reduction of 4-nitroimidazole derivative in aqueous medium in presence of cationic micelles generated a nitroradical anion sufficiently stable to be detected in the time scale of the cyclic voltammetric technique. This finding provides a very useful tool to quantify the formation, stability and reactivity of the nitroradical anion in conditions that resembling the cell environmental in biological membranes.

5. Acknowledgements

The authors are grateful to FONDECYT (Project number 1050767) for support this work.

6. References

[1] D.Thall, G. Rosner, C. Azuma, M. Mc Entee, J. Raleigh, *Radiotherapy Oncol.* **1997**, *44*, 171.
[2] F. Riché, A. du Molinet, S. Sèpe, L. Riou, D. Fagret and M. Vidal. Biorg, *Med. Chem. Lett.* **2001**, *11*, 71.
[3] S. A. Everett, M. A. Naylor, K. B. Patel, M. R. Stratfordand, P. Wardman. Biorg, *Med. Chem. Lett.* **1999**, *9*, 1267.
[4] G. E. Adams, I. J. Stratford, R. G. Wallace, P. Wardman, M. E. Watts, *Int. J. Radiat. Oncol. Biol. Phys.* **1994**, *29*, 231.
[5] D. I. Edwards, *Progress Med. Chem.* **1981**, *18*, 87.
[6] D. I. Edwards, *Biochem. Pharmacol.* **1986**, *35*, 53.
[7] P. Wardman, *Environ. Health Perfect.* **1985**, *64*, 309.
[8] M. Muller, Scand, *J. Infect. Dis. (Suppl.)* **1981**, *26*, 31.
[9] H. Van den Bassche, *Nature* **1978**, *273*, 626.
[10] D. I. Edwards, *J. Antimicrobiol. Chemother.* **1993**, *31*, 9.
[11] D. Church, H. Rabin, E. Laishley, *J. Antimicrobiol. Chemother.* **1990**, *25*, 15.
[12] G. Meyer, L. Nadjo, J. M. Saveant, *J. Electroanal. Chem.* **1981**, *119*, 417.
[13] G. L. McIntire, D. M. Chiappardi, R. Cassalberry, H. N. Blount, *J. Phys. Chem.* **1982**, *86*, 2632.
[14] C. Yañez, J. Pezoa, M. Rodriguez, L. J. Núñez-Vergara, J. A. Squella, *J. Electrochem. Soc.* **2005**, *152*, J46.
[15] J. H. Fendler. *Membranes Mimetic Chemistry*, Wiley, New-York **1982**, ch. 2.
[16] E. Gonzalez-Romero, M. B. Fernandez-Calvar, C. Bravo-Díaz, *Langmuir* **2002**, *18*, 10311.
[17] R. S. Nicholson, I. Shain, *Anal. Chem.* **1964**, *36*, 706.
[18] M. L. Olmstead and R. S. Nicholson, *Anal. Chem.* **1969**, *41*, 862.

